

STRUCTURE/FUNCTION ANALYSES OF *MYCOPLASMA PNEUMONIAE*
CYTADHERENCE PROTEINS HMW1 AND HMW3

by

MELISA JOHNSON WILLBY

(Under the direction of Duncan Charles Krause)

ABSTRACT

Mycoplasma pneumoniae is a pathogen of the human respiratory tract. *M. pneumoniae* adheres to respiratory epithelial cells via a sophisticated structure, the attachment organelle. The attachment organelle is composed of cytodherence-accessory proteins including HMW1, HMW2, HMW3 and P65. P1, the primary adhesin, and P30 a candidate adhesin are prominently displayed on this structure. Biochemical analysis has demonstrated that many cytodherence-accessory proteins are components of a Triton X-100 insoluble complex. Recent studies have illuminated a circuit of interactions among these proteins.

Mutations in cytodherence-accessory proteins result in a reduced or nonadherent phenotype. Evaluation of additional effects of such mutations has advanced our understanding of the contribution of each cytodherence-accessory protein to a functional attachment organelle. I describe here the isolation of the first HMW3 mutant. This transposon insertion derived mutant had an altered cellular morphology, at times with an

aberrant electron-dense core, reduced levels of P65, and failed to localize P1 and P65 properly.

Cytadherence mutant M6, lacks HMW1 and produces a truncated P30 protein (Layh-Schmitt *et al.*, 1995). I describe an aberrant morphology and altered P1 distribution in this mutant. Additionally, I showed that the C-terminus of HMW1 is required for these activities. I used mutant M6 to demonstrate a reciprocal dependency between HMW1 and HMW2, whereby the entire C-terminus of HMW1 was needed for HMW2 stabilization. The C-terminus of HMW1 was previously implicated in the rapid turnover of HMW1, in the absence of HMW2 (Hahn *et al.*, 1996; Popham *et al.*, 1997). Potential proteolytic target sequences were identified within this section of HMW1 and I constructed truncation/deletion mutants based on these sequences. I assessed the stability of each mutant. Amino acids 906-926 destabilized HMW1, while amino acids 927-1018, especially 978-1018 stabilized HMW1, particularly in the presence of HMW2. I also assessed the contribution of regions of the C-terminus of HMW1 to morphology revealing that the entire C-terminus of HMW1 influences morphology. Finally, I observed that fusion of the C-terminus of HMW1 to mouse dihydrofolate reductase destabilized DHFR in *Escherichia coli* in a manner dependent on ClpP and Lon.

INDEX WORDS: *Mycoplasma pneumoniae*, cytoskeleton, attachment organelle, post-transcriptional regulation, *hmw3*, HMW3, *hmw1*, HMW1, *hmw2*, HMW2, *hmw3::Tn4001mod*

STRUCTURE/FUNCTION ANALYSES OF *MYCOPLASMA PNEUMONIAE*
CYTADHERENCE PROTEINS HMW1 AND HMW3

by

MELISA JOHNSON WILLBY

B.S., The University of Georgia, 1995

A Dissertation Submitted to the Graduate Faculty of The University of Georgia in Partial
Fulfillment of the Requirements for the Degree

DOCTOR OF PHILOSOPHY

ATHENS, GEORGIA

2002

© 2002

Melisa Johnson Willby

All Rights Reserved

STRUCTURE/FUNCTION ANALYSES OF *MYCOPLASMA PNEUMONIAE*
CYTADHERENCE PROTEINS HMW1 AND HMW3

by

MELISA JOHNSON WILLBY

Approved:

Major Professor: Duncan C. Krause

Committee: Mark Farmer
Margie Lee
Kojo Mensa-Wilmot
Lawrence J. Shimkets

Electronic Version Approved:

Gordhan L. Patel
Dean of the Graduate School
The University of Georgia
December 2002

DEDICATION

I dedicate this work to my wonderful husband, Keith.

Without your love, your belief in me, and your shoulder to lean on I would never
have made it. I love you baby!

ACKNOWLEDGMENTS

I would like to thank my major professor, Dr. Duncan C. Krause for inviting me into his lab, encouraging me to get a Ph.D., and supporting me throughout my time in graduate school. I am especially grateful for his advice and help over the last few months as I prepared to graduate and embark on my career. I learned a great deal from his example.

I also owe a huge debt of gratitude to my past and present labmates especially, Mitch, Stephanie, Jarrat, Rob, Kyung, Ryan, Makda, Karen, Philip and Hahn. There are not words to express how fortunate I feel to have had such a wonderful and diverse group of individuals to work with. I learned so much from each of you personally and professionally. Your enthusiasm for science and zest for life made coming to work every day (...OK, most days) a joy. I love you all and wish you much happiness and success in life.

I would also like to thank my extended lab family over at the EM lab for being so generous with their time and knowledge and for lots of laughs.

Last but not least, I would like to thank Mom, Dad, Pam, Erin, Francyne, Cliff, Kelli, Christy and the rest of my family and friends for helping me get where I am today. I love you guys.

Thanks again to all of you!

TABLE OF CONTENTS

ACKNOWLEDGMENTS.....	v
LIST OF TABLES	ix
LIST OF FIGURES.....	x
INTRODUCTION.....	1
CHAPTER I	
REVIEW OF THE LITERATURE.....	7
History.....	7
Taxonomy and Phylogeny.....	9
Physiology and Growth.....	13
Molecular Biology.....	16
Pathogenesis of <i>M. pneumoniae</i> Infection	19
Clinical Aspects of <i>M. pneumoniae</i> Infection.....	25
Morphology and Ultrastructure.....	29
P1 Adhesin	32
Cytadherence-Accessory Proteins.....	36
CHAPTER II	
MATERIALS AND METHODS.....	49
Bacterial strains and Culture Conditions.....	49
Plasmid Construction	50
Polymerase Chain Reaction	58

Isolation of an <i>hmw3</i> Insertion Mutant	58
Isolation of <i>hmw3::Tn4001</i> mod Excision Revertants	59
SDS-PAGE and Western Immunoblot Analysis	60
DHFR- Δ HMW1 Turnover Assays in <i>E. coli</i>	60
Triton X-100 Extraction	61
Pulse-Chase Analysis of Recombinant HMW1 Derivatives	62
Hemadsorption Analysis	62
Microscopy	63

CHAPTER III

FUNCTIONAL ANALYSIS OF HMW3

RESULTS AND DISCUSSION	66
Identification of an <i>hmw3</i> Insertion Mutant	66
Only the Steady State Level of P65 is Reduced in the Absence of HMW3	72
Morphology and Ultrastructure are Aberrant in HMW3-Deficient Cells	77
Loss of HMW3 Results in an Intermediate Cytadherence Phenotype	84
P1 and P65 have Altered Localization Patterns in the Absence of HMW3	84
Isolation and Characterization of <i>hmw3::Tn4001</i> mod Excision Revertants	93
Summary	94

CHAPTER IV

STRUCTURE-FUNCTION ANALYSIS OF HMW1

RESULTS AND DISCUSSION	96
Altered Morphology and P1 Localization in the Absence of HMW1	96

C-terminally Truncated HMW1 fails to Restore Morphology or P1 Localization.....	104
Loss of HMW1 Leads to Decreased Stability of HMW2	107
Stability of Recombinant HMW1 Derivatives is Affected by Elements of its C-terminal Domain.....	110
The C-terminal Domain of HMW1 Influences its Association with the Cytoskeleton.....	120
The C-terminal Domain of HMW1 is Required for Wild-type Morphology.....	123
Functional ClpP and Lon Proteases are Required for Turnover of DHFR- Δ HMW1 in <i>E. coli</i>	126
CHAPTER V	
CONCLUSIONS.....	131
REFERENCES.....	138

LIST OF TABLES

1. Protein profiles of mutant <i>M. pneumoniae</i>	10
2. Construction of HMW1 truncation/deletion derivatives.....	51
3. Conditions for PCR amplification of plasmid inserts	52

LIST OF FIGURES

1. Construction of pKV204 encoding DHFR-ΔHMW1	53
2. Schematic of HMW1 and recombinant HMW1 constructs, pKV74 and pKV37	55
3. Anti-HMW3 Western immunoblot of the <i>hmw3::Tn4001</i> mod transformant	67
4. Schematic of the HMW operon illustrating the point of transposon insertion in the <i>hmw3::Tn4001</i> mod transformant	70
5. Western immunoblot of the <i>hmw3::Tn4001</i> mod transformant to assess steady- state levels of cytoadherence-associated proteins	73
6. Western immunoblot of the <i>hmw3::Tn4001</i> mod transformant to assess levels of P43	75
7. Morphological comparison of wild-type <i>M. pneumoniae</i> and the <i>hmw3::Tn4001</i> mod transformant	79
8. Transmission electron micrographs of wild-type <i>M. pneumoniae</i> and the <i>hmw3::Tn4001</i> mod transformant for comparison of electron-dense cores.....	81
9. Qualitative hemadsorption analysis of the <i>hmw3::Tn4001</i> mod transformant	85
10. P1 localization in the <i>hmw3::Tn4001</i> mod transformant	87
11. P65 localization in the <i>hmw3::Tn4001</i> mod transformant	90
12. P1 localization in <i>M. pneumoniae</i> P30 mutants (II-3 and II-7).....	97
13. P1 localization in <i>M. pneumoniae</i> mutant M6, M6 + HMW1, and M6 + P30.....	100

14. Morphological analysis of mutant M6, M6 + HMW1, and M6 + P60	102
15. P1 localization in and morphological analysis of mutant M6 + HMW1'	105
16. Western immunoblot demonstrating HMW2 levels in M6 and M6 transformed with HMW1 truncation/deletion alleles.....	108
17. Analysis of steady-state levels and stability of HMW1 truncation/deletion constructs in mutant M6 <i>M. pneumoniae</i>	112
18. Analysis of steady-state levels and stability of HMW1 truncation/deletion constructs in wild-type <i>M. pneumoniae</i>	114
19. Analysis of steady-state levels and stability of HMW1 truncation/deletion constructs in mutant I-2 <i>M. pneumoniae</i>	117
20. Triton X-100 solubility of HMW1 truncation/deletion constructs.....	121
21. Morphological analysis of mutant M6 producing HMW1 truncation/ deletion constructs.....	124
22. Stability of DHFR- Δ HMW1 in <i>E. coli</i> strains deficient in ClpP, Lon or FtsH.....	128
23. Proposed model of assembly of a functional attachment organelle.....	133

INTRODUCTION

Mycoplasma pneumoniae is a bacterial pathogen of the human respiratory tract. In general, infections are mild, target children and young adults, and manifest as tracheobronchitis or primary atypical pneumonia (Collier 1972). *M. pneumoniae* cells have no cell wall and therefore exhibit pleomorphic cellular morphology. Nevertheless, a single morphology is predominant, characterized by spindle-shaped cells with a distinct asymmetry due to the presence of a polar terminal structure, the attachment organelle (Boatman 1979b). Examination of thin sections of the attachment organelle by electron microscopy reveals a membrane-bound, laterally oriented, electron-dense core that ends distally in a bulbous knob (terminal button). The electron-dense core is a significant component of the Triton X-100-insoluble *M. pneumoniae* cytoskeleton (Gobel, *et al.* 1981; Krause and Balish 2001).

The major adhesin protein P1 is densely clustered in the membrane of wild-type *M. pneumoniae* cells at the attachment organelle (Baseman *et al.*, 1982b; Feldner *et al.*, 1982; Hu *et al.*, 1982). As its name suggests, this structure mediates adherence of mycoplasmas to host epithelium (cytadherence), an activity that is essential for successful infection of the respiratory tract (Razin and Jacobs 1992). In addition, the attachment organelle is the leading pole as *Mycoplasma* cells travel by gliding motility (Bredt 1979). Moreover, *M. pneumoniae* cells divide by binary fission, and bifurcation of the

attachment organelle is thought to be an early step in the process of division (Boatman 1979a; Seto *et al.*, 2001).

Since correct assembly of the attachment organelle is paramount for attachment, considerable research has focused on the isolation and characterization of non-cytadhering mutants (Hansen *et al.*, 1979b; Krause *et al.*, 1982), resulting in identification of several cytoadherence-accessory proteins, including HMW1, HMW2, HMW3, and P65 (Hansen *et al.*, 1979b; Krause *et al.*, 1982; Morrison-Plummer *et al.*, 1986; Proft and Herrmann 1994). Each is associated with the attachment organelle (Jordan *et al.*, 2001; Stevens and Krause 1991; Stevens and Krause 1992) and is at least partially insoluble in the detergent Triton X-100 (Proft and Herrmann 1994; Stevens and Krause 1990; Stevens and Krause 1991). Mounting evidence reveals a complex circuit of interactions among these proteins. Mutants lacking one or more cytoadherence-accessory proteins fail to localize P1 properly, exhibit atypical morphologies, and are defective in cytoadherence (Baseman *et al.*, 1982b; Hahn *et al.*, 1998; Krause *et al.*, 1982; Willby and Krause 2002). Additionally, attachment organelle proteins stabilize one another for example, loss of P30 results in reduced levels of P65 (Jordan *et al.*, 2001), while loss of HMW2 leads to a decrease in HMW1, HMW3, and P65 due to accelerated turnover (Jordan *et al.*, 2001; Ogle *et al.*, 1992). Ideally, in order to assign function and to determine the chronology of their incorporation into the attachment organelle mutants containing knockouts of each protein individually and in combination would be generated. However, the lack of genetic tools available for use in *M. pneumoniae* makes these studies impossible at present. Homologous recombination has not been described in *M. pneumoniae*, preventing targeted mutations in proteins of interest. Instead, the

generation of new strains must rely on identifiable spontaneous mutations, serendipitous transposition events into genes of interest, or transposon delivery of recombinant DNA into existing strains.

In Chapter III, I describe an *hmw3* transposon-insertion mutant; the first reported *hmw3* mutant. While steady-state levels of HMW3 (along with HMW1 and P65) are reduced in *hmw2* mutants due to accelerated protein turnover (Jordan *et al.*, 2001; Popham *et al.*, 1997), until now no defined *hmw3* mutant had been isolated. HMW3 is a cytoskeletal protein that is thought to be peripherally associated with the inner surface of the *M. pneumoniae* membrane (Proft and Herrmann 1994; Stevens and Krause 1992). Analysis by immunoelectron microscopy suggests that polymers of HMW3 wrap around the electron-dense core and terminal button of the attachment organelle in a helical pattern (Stevens and Krause 1992). This protein has a deduced mass of 73,725 Da but a relative mobility by sodium dodecyl sulfate-polyacrylamide gel electrophoresis (SDS-PAGE) of 140,000 (Ogle *et al.*, 1992). The major structural feature of HMW3 is an acidic, proline-rich (APR) domain (residues 88 to 488), which probably contributes to the anomalous migration by SDS-PAGE (Ogle *et al.*, 1992). Loss of HMW3 due to a transposon insertion resulted in alterations in (i) Mycoplasma cellular morphology, (ii) localization of P1 and P65, (iii) stability of P65, (iv) hemadsorption capacity, and (v) the ultrastructure of the electron-dense core, suggesting a role for HMW3 in its stabilization.

M. pneumoniae cytoadherence mutant M6 lacks protein HMW1 and produces a truncated adherence-associated protein P30 (Layh-Schmitt *et al.*, 1995). HMW1 has a predicted mass of 112 kDa and no known homologs outside of the mycoplasmas (Dirksen *et al.*, 1996). Its relative mobility by SDS-PAGE (sodium dodecyl sulfate-

polyacrylamide gel electrophoresis) is 210,000, probably due to a disproportionately high percentage of proline residues within the central region of the protein (Dirksen *et al.*, 1996). This structural feature and aberrant electrophoretic mobility are shared by HMW3, P65, and P200 (Dirksen *et al.*, 1996; Ogle *et al.*, 1992; Proft *et al.*, 1995; Proft *et al.*, 1996). HMW1 is a peripheral membrane protein on the *Mycoplasma* surface (Balish, *et al.* 2001) at the attachment organelle (Seto *et al.*, 2001; Stevens and Krause 1991) and the trailing filament (Stevens and Krause 1991), but lacks typical secretion signal or transmembrane sequences (Dirksen *et al.*, 1996).

M. pneumoniae cytoadherence mutant I-2 lacks protein HMW2, resulting in decreased levels of HMW1, HMW3, and P65, failure to localize P1 to the attachment organelle, and an abnormal morphology (Baseman *et al.*, 1982b; Fisseha *et al.*, 1999; Jordan *et al.*, 2001; Krause *et al.*, 1982). HMW1 and HMW3 are synthesized initially at wild-type levels in this mutant but diminish with time, apparently due to accelerated proteolytic turnover (Popham *et al.*, 1997). HMW1 stability is associated with efficient incorporation into the cytoskeleton and localization to the cell surface (Balish *et al.*, 2001). Transformation of mutant I-2 with recombinant wild-type *hmw2* by transposon delivery restores HMW1 at levels proportional to the amount of HMW2 produced, demonstrating the importance of proper stoichiometry in the interplay between these two proteins (Fisseha *et al.*, 1999). Significantly, recombinant HMW1 lacking the C-terminal 112 amino acids appeared to be more stable than full-length HMW1 in mutant I-2 (Hahn *et al.*, 1996; Popham *et al.*, 1997). A paired serine motif occurs four times within the C-terminal domain of HMW1, four times in the C-terminal domain of HMW3, and immediately downstream of a known *M. pneumoniae* processing site in the polypeptide

precursor to the cytoadherence-accessory proteins B and C (Popham *et al.*, 1997; Sperker *et al.*, 1991), raising the possibility that one or more of these motifs might be targeted for accelerated turnover (Popham *et al.*, 1997). Thus, the C-terminal domain of HMW1 appears to be necessary for both accelerated turnover in the absence of HMW2 and for normal function.

In Chapter IV I report that HMW1 is required for clustering of the adhesin P1 at the attachment organelle. Complete loss of HMW1 results in morphologically irregular cells lacking the tapered appearance normally associated with the attachment organelle. Complementation of mutant M6 with recombinant wild-type HMW1, but not a derivative thereof lacking the C-terminal 112 amino acids, restored a tapered appearance and P1 clustering to this mutant. Additionally, loss of HMW1 resulted in a decline in the level of HMW2. However, recombinant full-length HMW1 restored wild-type levels of HMW2. Thus, a reciprocal dependency exists between these two cytoskeletal components. I constructed C-terminal deletion derivatives of HMW1 lacking one or more of the double serine motifs and assessed each for stability, association with the mycoplasma cytoskeleton, capacity to stabilize HMW2, and ability to confer a normal cellular morphology. This approach revealed regions that (i) destabilized HMW1 significantly in all *Mycoplasma* backgrounds tested, (ii) contributed to its association with the cytoskeleton, and (iii) were required to confer a wild-type morphology. All HMW1 deletion derivatives conferred higher steady-state levels of resident HMW1 in mutant I-2, suggesting titration of an element responsible for HMW1 turnover. Finally, I explored the ability of several *Escherichia coli* proteases to recognize and act on the C-terminus of HMW1 fused to a carrier protein.

The aim of this dissertation project was to further our knowledge regarding interactions among components of the *M. pneumoniae* attachment organelle. I accomplished this goal by isolating and characterizing the first mutant exclusively deficient in the protein HMW3. In addition, I described a mutually stabilizing relationship between cytoadherence-accessory proteins HMW1 and HMW2 and undertook structure-function analysis of the C-terminus of HMW1.

CHAPTER I

REVIEW OF THE LITERATURE

History.

Eaton *et al.* isolated an infectious agent associated with lower respiratory tract illness in man, including atypical pneumonia (Eaton *et al.*, 1944). The biological nature of Eaton's agent was the source of great debate in the medical community for a number of years, as it was unclear whether this infectious agent, which could not be cultivated in pure culture, was resistant to penicillin, and was not readily visible by light microscopy, was viral or bacterial. In 1961 Marmion and Goodburn demonstrated that Eaton's agent was inhibited by organic gold salt and sensitive to tetracyclines. They also visualized small cocco-bacillary bodies on the mucous layer covering the bronchial epithelium of chick embryos infected with Eaton's agent consistent with fluorescence patterns visualized when fluorescent-antisera to Eaton's agent was applied to infected chick embryos. Additionally, similarities were noted between Eaton's agent and pleuropneumonia-like organisms (PPLO) from cattle, and Marmion suggested that Eaton's agent might be a member of the bacterial genus *Mycoplasma* (Marmion and Goodburn 1961). This finding was further substantiated and expanded upon when Clyde observed round, granular structures composed of "forms near the limit of resolution" by light microscopy in Rhesus monkey kidney cell cultures inoculated with chick embryo-passaged Eaton's agent (Clyde 1961). These structures were always in direct association

with the simian cells and grew larger over the course of the study. Furthermore, they were brightly fluorescent when stained with antisera generated against Eaton's agent. Clyde also observed the similarities between Eaton's agent and the bovine PPLO (Carson *et al.*, 1979).

However, the organism was not successfully cultured in cell-free media until 1962, when Chanock *et al.* described growth of Eaton's agent on agar plates, thereby proving that Eaton's agent was bacterial and not viral (Chanock *et al.*, 1962). The plates were formulated with a PPLO agar base supplemented with 20% horse serum and 2.5% fresh yeast extract. Colonies reacted with convalescent serum from patients with confirmed Eaton pneumonia, but not with serum from patients with respiratory disease associated with adenovirus, parainfluenza virus or Q fever. Additionally, the colonies were reactive with antiserum prepared in a rabbit immunized with Eaton's agent. Chanock *et al.* also demonstrated that Eaton's agent was distinct from three human oral and four human genital PPLO strains, in addition to rat, bird, and sewage-associated PPLOs, by using an immunologic assay with convalescent serum from an individual infected with Eaton's agent. Therefore, staining patterns and the requirement for serum, as well as the small size, and antibiotic and gold salt sensitivities classified this organism to the genus *Mycoplasma*. In 1963 Eaton's agent was officially renamed *Mycoplasma pneumoniae* to reflect its relationship to atypical pneumonia (Chanock *et al.*, 1963).

The ability to maintain *M. pneumoniae* in pure culture opened the door to a world of research. The organism was characterized in terms of its morphology, physiology, motility, interactions with host cells, and pathogenesis in experimentally infected animals and human subjects over the next four decades. A breakthrough in the cell biology and

pathogenesis of *M. pneumoniae* occurred in 1982 with the isolation and characterization of four classes of *M. pneumoniae* cytoadherence mutants (Table 1) (Krause *et al.*, 1982). Each class was characterized by the absence of one or more proteins, based upon analysis of their one- and two-dimensional protein profiles. Additional cytoadherence mutants have since been isolated (Table 1) (Layh-Schmitt *et al.*, 1995; Willby and Krause 2002). Characterization of these mutants has enabled us to learn a great deal about *M. pneumoniae* cell biology. In 1993, *M. pneumoniae* was brought into the era of molecular biology with the first published transformation with a transposon-containing plasmid (Hedreyda *et al.*, 1993), making it possible to introduce new genetic material into the organism by transposon delivery. Finally, the complete sequence of the *M. pneumoniae* genome was published in 1996 (Himmelreich *et al.*, 1996) providing a powerful resource to guide *M. pneumoniae* research into the next millennium.

Taxonomy and Phylogeny.

Members of the class *Mollicutes* are often simply referred to as mycoplasmas. The term *Mollicutes* comes from the greek *mollis*, meaning soft, and *cutis*, meaning skin. The orders *Mycoplasmatales*, *Acholeplasmatales*, and *Anaeroplasmatales* comprise the class *Mollicutes*. Two families fall in the order *Mycoplasmatales*: *Mycoplasmataceae* containing the genera *Mycoplasma* and *Ureaplasma*, and *Spiroplasmataceae* containing the genus *Spiroplasma*. The *Acholeplasmatales* order contains a single family, *Acholeplasmataceae* with a single genus, *Acholeplasma*. The order *Anaeroplasmatales* houses the family *Anaeroplasmataceae* including the genera *Anaeroplasma* and *Asteroleplasma*. Finally, the thus-far uncultivated phytoplasmas (formerly the

TABLE 1. Protein profiles of mutant *M. pneumoniae*

<i>M. pneumoniae</i>	Proteins						
	HMW1	HMW2	HMW3	A, B, C	P1	P30	P65
I-2^a	+/-	-	+/-	++	++	++	+/-
II-3^{a,b,c}	++	++	++	++	++	-	+/-
II-7^{a,c}	++	++	++	++	++	Δ	+/-
III-4^a	++	++	++	-	-	NT	NT
IV-22^a	++	++	++	++	-	NT	NT
M6^{d,e,f}	-	+/-	+/-	++	++	Δ	+/-
<i>hmw3::Tn4001^g</i>	++	++	+/-	++	++	++	+/-

Key: ++, protein present at wild-type levels; -, protein absent; +/-, protein present at significantly reduced levels; Δ, deletion in 3' end of gene; NT, not tested.

^aKrause, et al.1982; ^bDallo, et al.1996; ^cJordan, et al.2001; ^dLayh-Schmitt, et al.1995;

^eWillby, et al.In preparation; ^fKrause and Balish, 2001; ^gWillby and Krause2002

mycoplasma-like organisms) are also included in the class *Mollicutes*. This taxonomic system was based on a number of traits including genome size, although recent studies have shown that this is not a reliable predictor (Chambaud *et al.*, 2001; Cocks *et al.*, 1989; Fraser *et al.*, 1995; Himmelreich *et al.*, 1996; Ladefoged and Christiansen 1992; Pyle and Finch 1988; Pyle *et al.*, 1990), mole percent G + C, DNA modification, DNA-DNA and DNA-RNA hybridization, restriction fragment length polymorphism, nutritional requirements, and cell protein maps generated by two-dimensional gel electrophoresis.

Today, phylogenetic relationships among bacteria are primarily determined by comparison of 16S rRNA sequences (Fox *et al.*, 1980). 16S rRNA sequences are ideal tools for this task since they are found in all bacteria, have a conserved function in every organism studied, and are generally not laterally transferred among bacteria. Additionally, these sequences contain two “phylogenetic clocks”—some parts of the 16S rRNA sequence evolve slowly allowing for comparisons among distantly related organisms, while other parts evolve at a more accelerated pace facilitating analysis of more recently diverged organisms. Prior to the advent of 16S rRNA, two models were proposed to explain mycoplasmal evolution. Neimark proposed that mycoplasmas are polyphyletic and individual mycoplasma species arose by degenerate evolution from different ancestral bacteria (Neimark and Tung 1973; Neimark 1979; Neimark and London 1982). Conversely, Morowitz and Wallace theorized that mycoplasmas are the ancestors of all bacteria (Morowitz and Wallace 1973; Wallace and Morowitz 1973). Mycoplasmal 16S rRNA comparisons compiled by Woese *et al.* (Woese *et al.*, 1980) proved that neither of these theories was accurate. Based on sequence data the

mycoplasmas are monophyletic and arose at a node on a branch of the low mole percent G + C gram-positive bacteria within the *Lactobacillus* group (Woese *et al.*, 1980). The *Lactobacillus* group contains *Lactobacillus*, *Bacillus*, and *Streptococcus* species as well as *Clostridium ramosum* and *C. innocuum*, two clostridial species not closely related phylogenetically to other clostridial species (Woese *et al.*, 1980). This phylogenetic assignment based on 16S rRNA sequences has been substantiated numerous times when different research laboratories proved that a certain mycoplasma property was more similar to the same property from a gram positive organism than from a gram negative organism. Another interesting trait of the mycoplasmas revealed by analysis of 16S rRNA sequences is that the mycoplasma branches of the phylogenetic tree evolved about 50% more rapidly than the *Lactobacillus* group (Maniloff 1992), perhaps explaining their evolution from an ancestor with a predicted genome of 2,200-2,500 kb (Maniloff, unpublished), to their much smaller present day genomes.

The first mycoplasma is believed to have belonged to the obligate anaerobic species *Asteroleplasma*. From this non-sterol-requiring species arose the sterol-requiring, obligate anaerobic *Anaeroplasma* group and the sterol-nonrequiring, facultative anaerobic *Acholeplasma* group. It is impossible to tell at present which of these arose first. The sterol-requiring, facultative anaerobic genera *Spiroplasma*, *Mycoplasma*, and *Ureaplasma* evolved from one of these ancestral organisms. The *Mycoplasma* phylogenetic group includes *M. pneumoniae* and its closest identified relative, *M. genitalium*, as well as *M. gallisepticum* and *M. pirum*.

Physiology and Growth.

As a result of its fastidious nature, successful cultivation of *M. pneumoniae* in cell-free media took many years of trial and error. Eventually, a complex medium containing horse serum and yeast dialysate in PPLO broth base was developed and proved effective. Both the horse serum and the yeast extract were essential for growth of the organism (Chanock *et al.*, 1962). Horse serum is thought to provide lipids in a nontoxic form, including cholesterol, a required component of the cell membrane, inorganic ions, sugars and urea (Rodwell and Mitchell 1979). Yeast dialysate provides NADH, nucleic acids and nucleic acid precursors among other things (Rodwell and Mitchell 1979). *M. pneumoniae* can also be cultivated on solid medium with a similar formulation. Colonies are granular with embedded centers. The dense centers and less dense peripheral areas are often described as resembling the appearance of a fried-egg. Colonies were first visible by light microscopy at about 10 μm in diameter and grew to a diameter of 50 to 100 μm (Chanock *et al.*, 1962). *M. pneumoniae* grows optimally at 36-38°C (Freundt and Razin 1984).

The *M. pneumoniae* genome sequence and annotation were published in 1996 (Himmelreich *et al.*). The chromosome is 816,394 bp; analysis of the completed sequence affords an explanation for *M. pneumoniae*'s complex growth requirements. During its evolution from a more genetically robust ancestor, *M. pneumoniae* lost complete metabolic pathways, including those for amino acid biosynthesis (Himmelreich *et al.*, 1996). *M. pneumoniae* is a facultative anaerobe and metabolizes glucose fermentatively via the Embden-Meyerhoff-Parnas pathway to produce two moles each of pyruvate, ATP, and NADH per mole of glucose (Freundt and Razin 1984). All of the

enzymes required for the Embden-Meyerhoff-Parnas pathway have been identified in the genome (Himmelreich *et al.*, 1996). Pyruvate is further degraded by one of two pathways. It is converted to lactate by lactate dehydrogenase or to acetyl-CoA and then acetate via the pyruvate dehydrogenase complex, phosphotransacetylase and acetate kinase (Himmelreich *et al.*, 1996). Due to their lack of lipoquinones and cytochromes, *M. pneumoniae* cells make use of flavin-terminated respiration (FTR). NADH is oxidized by means of NADH oxidase mediated transfer of electrons directly from NADH to molecular oxygen through a flavoprotein (Pollack 1992). Arginine can serve as an energy source for some mycoplasmas. *M. pneumoniae* appears to encode the three enzymes involved in arginine hydrolysis but arginine utilization has not been demonstrated in this species (Himmelreich *et al.*, 1996). *M. pneumoniae* does not appear to have a complete pentose phosphate pathway or tricarboxylic acid cycle.

Glucose, fructose and mannitol are transported into the *M. pneumoniae* cell via the phosphoenolpyruvate:carbohydrate phosphotransferase system. Sequencing revealed additional transporters in the form of ABC transporters and facilitated diffusion systems with transmembrane proteins functioning as specific carriers (Himmelreich *et al.*, 1996). Due to its nutritional fastidiousness, *M. pneumoniae* is expected to import a wide array of compounds. Therefore, *M. pneumoniae* was hypothesized to contain a large number of transport systems. The current annotation of the genome does not support this hypothesis. *M. pneumoniae* has approximately the same percentage of genes encoding transport related proteins as *Haemophilus influenzae* and less than *Escherichia coli* or *Bacillus subtilis* (Himmelreich *et al.*, 1996). This suggests that the transporters that are encoded by *M. pneumoniae* may exhibit a low degree of substrate specificity, or perhaps

M. pneumoniae requires less sophisticated transport systems due to the absence of a cell wall.

Bredt (1968) suggested that *M. pneumoniae* divides by binary fission. He constructed a morphological timeline for *M. pneumoniae* cell division based on cells that he observed by electron microscopy. He proposed that prior to cell division the attachment organelle was duplicated, then one of the attachment organelles migrates to the opposite pole of the cell, and finally the cell divides into two individual cells moving in opposite directions. In 2001, Seto *et al.* correlated these observations with DNA content. They used fluorescently labeled P1 as a marker for attachment organelles and stained DNA with DAPI. Cells were divided into four categories: (1) cells with a P1 focus at a single pole; (2) cells with two P1 foci at a single pole (i.e. two attachment organelles); (3) cells with two P1 foci, only one of which was polar; and (4) cells with P1 foci at opposite poles. Based on their calculations, the first two cell types had approximately equal DNA content with 0.84 times the average total DNA content. Cells in category 3 and 4 had 1.04 and 1.48 times the average total DNA content respectively. In addition, Seto *et al.* observed that cells in categories 1, 2 and 3 contained a single nucleoid, while two nucleoids were visible in the majority of category 4 cells. Thus, DNA content and the condensation state of the nucleoid correlated with the external manifestations of cell division observed by Bredt (Bredt 1968; Seto *et al.*, 2001).

The molecular basis for cell division is well-studied in the walled bacteria *E. coli* and *B. subtilis*, but the wall-less mycoplasmas present a unique opportunity to learn more about the function of cell division proteins in an organism with a less complex cell envelope. Thus far, of the proteins implicated in cell division in other bacteria, only

homologs for FtsZ and FtsY have been conclusively identified in *M. pneumoniae* (Himmelreich *et al.*, 1996). However, recent data suggest that FtsA is also present (Balish, unpublished data). The limited number of proteins typically associated with cell division in walled bacteria that have homologs in *M. pneumoniae* suggests that many of these proteins have functions associated with septation of the cell wall. It is also possible that *M. pneumoniae* has a unique collection of cell division proteins.

M. pneumoniae moves by gliding motility at an average speed of 0.3-0.4 $\mu\text{m/s}$ and a maximum speed of 1.5-2.0 $\mu\text{m/s}$ (Bredt 1968; Kirchhoff 1992). Movement is always oriented in the direction of the attachment organelle; *M. pneumoniae* never reverses directions (Radestock and Bredt 1977). Both positive rheotaxis (movement against a current) and chemotaxis toward chemoattractants including D-fructose, D-lactose, D-maltose, D-saccharose and mucus have been shown in *M. mobile*, the fastest of the motile mycoplasmas (Kirchhoff 1992). Furthermore, a chemotactic response to glucose has been described in *M. pneumoniae* (Radestock and Bredt 1977; Rosenbusch *et al.*, 1990). Cells require a solid-liquid interface (Kirchhoff 1992) and energy (Radestock and Bredt 1977) for motility. Very little is known about the mechanism of gliding motility in bacteria in general and in mycoplasmas in particular and it is possible that individual species glide via different mechanisms.

Molecular Biology.

M. pneumoniae has a single circular 816,394 bp chromosome, the sequence of which was completed and published in 1996 (Himmelreich *et al.*, 1996) and reannotated in 2000 (Dandekar *et al.*, 2000). It has an average G + C content of 40.0 mol%.

Although this is currently a hot area of research, only 458 of the 688 open reading frames have published predicted functions, leaving approximately one-third of the predicted genes without functional assignment. The majority of the expected replication and transcription machinery was identified. There is a greatly reduced number of genes expected to function in SOS repair as compared with *E. coli*. Interestingly, a homolog for the SOS regulatory protein LexA was not identified. Based on comparison with tRNA's from prokaryotic and eukaryotic species, 35 tRNA genes were reported in the genome (Dandekar *et al.*, 2000). Nearly 15% of the *M. pneumoniae* genome is dedicated to translation. In spite of this, the ribosomal protein S1, predicted to function in binding mRNA to the 30S small ribosomal subunit, is absent. Also absent is peptide chain release factor 2, which recognizes the UGA codon as a stop codon and unlike other organisms where the codon UGA signals a stop, in *M. pneumoniae* UGA encodes tryptophan. The paucity of transcriptional and translational regulatory mechanisms encoded by *M. pneumoniae* is noteworthy. No two-component signal transduction systems were found, and a single sigma factor was identified (Himmelreich *et al.*, 1996). However, *M. pneumoniae* does encode several GTP-binding proteins, and its heat shock proteins are preceded by regulatory *cis*-acting conserved palindromic repeated sequences (CIRCE), and a proposed CIRCE repressor was identified. It is possible that the lack of a cell wall has also resulted in simplified protein secretion. Several of the cytosolic chaperones and regulatory components of the *E. coli* secretion machinery were not identified in the *M. pneumoniae* genome. However, prospective homologs for all the channel forming proteins of the Sec secretion system with the exception of SecF were identified. Additionally, signal peptidase I, the peptidase responsible for removal of the

signal sequence from secreted proteins was not identified (Himmelreich *et al.*, 1996). This finding was somewhat surprising due to the identification of predicted signal sequences at the 5' end of several genes (Su *et al.*, 1987; Inamine *et al.*, 1988).

Molecular manipulation of *M. pneumoniae* has been challenging. Viruses have been identified only in *Acholeplasma*, *Spiroplasma*, *M. pulmonis*, and *M. arthritidis* (Dybvig and Cassell 1987; Razin 1985). A plasmid has yet to be identified that is capable of replication in *M. pneumoniae*, though plasmids have been identified that successfully replicate in *M. mycoides*, *M. capricolum*, *A. laidlawii*, and *S. citri* (Razin *et al.*, 1998). Although homologs for RecA and enough other recombination proteins have been identified to suggest that homologous recombination is possible in *M. pneumoniae* (Himmelreich *et al.*, 1996), we have not been able to define conditions for homologous recombination *in vitro*. A recent publication, however, does describe homologous recombination in *M. genitalium*, the closest relative to *M. pneumoniae* (Dhandayuthapani *et al.*, 2002).

Mycoplasma research took a giant leap forward in 1987 with the first published report of transposition in these organisms. Dybvig and Cassell reported successful polyethylene glycol (PEG) mediated transformation of *M. pulmonis* and *A. laidlawii* with a plasmid containing streptococcal transposon Tn916 (Dybvig and Cassell 1987). Tn916 encodes tetracycline resistance, and tetracycline-resistant colonies were isolated. Analysis by Southern blot revealed sequences from the transposon, but not the host plasmid on the chromosome of tetracycline-resistant transformants confirming transposition (Dybvig and Cassell 1987). Successful transposition into *M. pulmonis* of the *Staphylococcus aureus* transposon Tn4001 encoding gentamicin resistance followed

in 1989 (Mahairas and Minion 1989). Hedreyda *et al.* (1993) reported transformation of *M. pneumoniae* with Tn4001 via electroporation. Analysis of individual transformants revealed that the transposon inserted only once in each *M. pneumoniae* isolate, and that the insertion site was apparently random (Hedreyda *et al.*, 1993). Since this first report of transposition of Tn4001 into the *M. pneumoniae* chromosome, two modified derivatives of Tn4001 have been generated. In the first, the IS256L of Tn4001 was altered to encode a *Sma*I and a *Bam*HI restriction site (Knutdson and Minion 1993). In the second, the previous construct was modified such that the *Sma*I site was replaced with an *Eco*RI site (Hahn *et al.*, 1998). Genetic material cloned into any of these restriction sites can be expressed in *M. pneumoniae* (Hahn *et al.*, 1996) either from mycoplasmal promoters included on the cloned material or by either of the promoters (P_{IN} or P_{OUT}) encoded on IS256, providing a means for complementation of *M. pneumoniae* mutants for studies of protein function. Subsequently, a Tn4001 composite was constructed conferring chloramphenicol resistance (Hahn *et al.*, 1999).

Pathogenesis of *M. pneumoniae* Infection.

The pathogenic nature of *M. pneumoniae* is attributed to both bacterial and host mediated factors, including *M. pneumoniae* adherence, localized damage to host cells, and the host immune response. *M. pneumoniae* disease begins when a host inhales a bacteria-laden droplet aspirated by an infected individual. Once in the airway, *M. pneumoniae* presumably travels by gliding motility toward the tracheal epithelial cells at the base of the ciliary shafts with attachment organelles leading (Kirchhoff 1992). The primary *M. pneumoniae* adhesin, protein P1, has an asymmetrical distribution on the

mycoplasma cell surface, with a dense concentration at the attachment organelle (Baseman *et al.*, 1982b; Feldner *et al.*, 1982; Hu *et al.*, 1982). Thus, by moving in the direction of the attachment organelle *M. pneumoniae* is effectively presenting the P1 adhesin to host cells as they are encountered. *M. pneumoniae* attaches to sialoglycoproteins and sulfated glycolipids (Krivan *et al.*, 1989; Roberts *et al.*, 1989), moieties that exist on cell surfaces associated with *M. pneumoniae* infection such as bronchial epithelium, the apical microvillar border, and cilia, as well as on erythrocytes, which are used as models for cytoadherence (Razin and Jacobs 1992). Adherence is an essential element of *M. pneumoniae* infection preventing mucociliary clearance of the bacterium and maintaining the mycoplasma in close proximity to host cells from which it obtains metabolic precursors. Nonadherent mutants are unable to cause disease in experimentally infected animals (Baseman and Tully 1997).

Host cells are dramatically changed by *M. pneumoniae* parasitism. Decreased cellular ATP, cyclic AMP, carbohydrate utilization, amino acid transport, macromolecular synthesis, and oxygen consumption have been documented (Gabridge 1975; Gabridge 1976; Gabridge *et al.*, 1977a; Gabridge *et al.*, 1977b; Gabridge and Dee Barden Stahl 1978; Hu *et al.*, 1975; Hu *et al.*, 1976; Upchurch and Gabridge 1981; Wolffing and Gabridge 1979). Furthermore, loss of ciliary motion, morphologic changes and desquamation have been observed microscopically (Collier *et al.*, 1969; Collier and Clyde 1971; Collier and Baseman 1973). Inspection of hamster tracheal rings 24 hours following infection with *M. pneumoniae* revealed alterations in the ciliary necklace with frequent loss of ciliary necklace particles (Carson *et al.*, 1980).

M. pneumoniae damage to host cells is thought to be multifactorial. Glucose metabolism results in hydrogen peroxide and superoxide radical production (Cohen and Somerson 1967; Lynch and Cole 1980; Meier and Habermehl 1990) associated with decreased host catalase activity (Almagor *et al.*, 1983; Almagor *et al.*, 1984; Almagor *et al.*, 1985). It has been demonstrated experimentally that peroxide in amounts similar to those generated by *M. pneumoniae* induces ciliostasis of chicken tracheal rings and that addition of exogenous catalase delays *M. pneumoniae*-induced ciliostasis (Cherry and Taylor-Robinson 1970). It is possible that accumulated reactive oxygen species originating from attached *M. pneumoniae* and from host cells contribute to the localized tissue disruption and disorganization associated with *M. pneumoniae* infection (Tryon and Baseman 1992). *M. pneumoniae* likely competes with host cells for metabolic precursors. *M. pneumoniae* possesses RNA and DNA exonuclease activities and may target host nucleic acid (Himmelreich *et al.*, 1996). A 1978 study reported that addition of 0.01 mM adenine sulfate to infected hamster tracheal explants resulted in noteworthy protection of cellular function during *M. pneumoniae* infection (Gabridge and Stahl 1978). Infected explants maintained for 7 days in the presence of adenine sulfate had nearly identical ciliary activity as uninfected explants, whereas ciliary activity of infected explants maintained for 7 days in the absence of adenine sulfate was half that of uninfected controls (Gabridge and Stahl 1978). This same study also showed uptake of radiolabeled adenine from tracheal explants by *M. pneumoniae*, and the authors proposed that *M. pneumoniae* infection might deplete host adenine, resulting in loss of energy for ciliary motion, and metabolism (Gabridge and Stahl 1978). Additionally, *M. pneumoniae* binds lactoferrin, the glycoprotein responsible for sequestration and transport of iron in

mucosal secretions. Although it has not been correlated with virulence, binding lactoferrin could drain host stores of iron, thus reducing the activity of host iron-requiring enzyme systems (Krause and Taylor-Robinson 1992).

M. pneumoniae infection results in cellular and humoral immune response. Infections are characterized by an influx of polymorphonuclear leukocytes, macrophages and lymphocytes into the lungs (Chambaud *et al.*, 1999). Infected mice exhibit enhanced expression of TNF α , INF γ , IL-1 β , and IL-6 genes (Pietsch *et al.*, 1994). However, *M. pneumoniae* resists phagocytosis in the absence of specific antibodies (Kist *et al.*, 1982). Major antigens include lipids (Razin *et al.*, 1970), polysaccharide (Allen and Prescott 1978), protein P1 and a 116-kDa surface protein (Duffy *et al.*, 1997).

M. pneumoniae can activate complement via both the classical and the alternate pathways. Approximately 99% of the organisms were killed *in vitro* following activation of complement by the classical pathway (Cassell *et al.*, 1985) with rounding of cells observed microscopically prior to death (Bredt and Bitter-Suermann 1975). In another set of experiments, *M. pneumoniae* was incubated with sera depleted of components of the complement specific for the classical pathway assuring complement activation via the alternate pathway. While cell rounding was observed under these circumstances, the rounding was reversible and only 10-50% of cells were killed (Bredt and Bitter-Suermann 1975). The classical pathway is activated by antigen-antibody complexes, thus it is very specific. The alternate pathway is activated by a number of substances that bacteria either produce or induce the host to produce. Therefore, activation by the alternative pathway is much less specific, possibly explaining its inefficient killing of Mycoplasmas *in vitro*. However, the alternate pathway may be more successful *in vivo*

since it results opsonization of cells with C3b, making them more susceptible to phagocytosis by macrophages. Additionally, rounding affects adherence to erythrocytes and may affect attachment to host cells thus, adherence may be temporally compromised in rounded cells possibly leading to enhanced clearance. It is likely that another effect of complement activation is host cell damage due to the resulting inflammation (Bredt and Bitter-Suermann, 1975).

The antibody response to the P1 protein has been studied extensively. Sera collected from humans with acute *M. pneumoniae* infection failed to inhibit attachment of *M. pneumoniae* cells (Jacobs *et al.*, 1985). This suggests that antibodies are not produced against receptor-binding regions of the protein. IgM antibodies appear within the first two weeks following infection in infection, while IgG antibodies appear three to eight weeks after infection (Biberfeld 1968; Fernald 1979). IgA, the major antibody class found in respiratory secretions, is detected following the appearance IgG (Biberfeld and Sterner 1971; Hu *et al.*, 1983). However, the humoral response does not protect individuals from reinfection (Razin and Jacobs 1992).

M. pneumoniae is capable of nonspecific lymphocyte activation (Biberfeld *et al.*, 1983), interferon production, generation of circulating immune complexes, depression of cell-mediated immune reactions to unrelated antigens, and induction of autoantibodies against lymphocytes, lung, heart, liver, kidney, smooth muscle, and brain (Cassell and Cole 1981). However, immunocompromised individuals infected with *M. pneumoniae* develop clinical symptoms but not radiographic changes, indicating that host response is not solely responsible for disease (Clyde 1979).

Mycoplasmas employ a number of tactics to evade the host immune response. Several mycoplasma proteins resemble host proteins (Dallo *et al.*, 1989a; Dallo *et al.*, 1996). There is also some similarity between human and *M. pneumoniae* glycerophospholipids, possibly leading the host immune system to attack itself (Clyde 1979). Several different forms of the adhesin P1 have been identified in strains isolated from infected individuals (Baseman *et al.*, 1988; Dorigo-Zetsma *et al.*, 2000; Dorigo-Zetsma *et al.*, 2001; Kenri *et al.*, 1999). The genome sequence revealed the presence of sequences corresponding to regions of the P1 protein in several places on the *M. pneumoniae* chromosome (Himmelreich *et al.*, 1996), further suggesting that *M. pneumoniae* might use antigenic variation of P1 to evade the hosts immune response. Some Mycoplasmas including the human pathogen *M. penetrans* have been shown to invade host cells (Andreev *et al.*, 1995; Lo *et al.*, 1993). Studies using confocal microscopy and both DiIC₁₈-labeled and anti-Mycoplasma-FITC-labeled *M. penetrans* and *M. pneumoniae* revealed fluorescent particles of a size consistent with that of Mycoplasma within the cytoplasm of human WI-38 lung cells monolayers. Additionally, *M. pneumoniae* infected mammalian cells were treated with gentamicin to kill extracellular *M. pneumoniae* cells, fractionated into nuclear and cytoplasmic components by hypotonic swelling, gradient centrifugation and flow cytometry, and fractions were plated on SP-4 media. After incubation at the appropriate temperature colonies were visible on the plates suggesting that intracellular *M. pneumoniae* remained viable. However, it is not clear whether *M. pneumoniae* was capable of replication within mammalian cells (Baseman *et al.*, 1995). Host cell invasion has, however, never been conclusively demonstrated for *M. pneumoniae in vivo*.

Clinical Aspects of *M. pneumoniae* Infection.

M. pneumoniae has been acknowledged as a causative agent of tracheobronchitis and primary atypical pneumoniae in humans since 1944 (Eaton *et al.*), with Koch's postulates having been fulfilled twice for this organism (Chanock and Riftkind 1961; Riftkind and Chanock 1962). Primary atypical pneumonia was so named because it represents a primary form of lung disease, and unlike typical bacterial pneumonia, organisms associated with it do not respond to penicillin (Clyde 1979). Atypical pneumonia is characterized by a slow onset with an extended incubation period of 2-3 weeks before appearance of flu-like symptoms including nonproductive cough, fever, chills and generalized aches and pains. *M. pneumoniae*, *Chlamydia pneumoniae*, *Chlamydia psittaci*, *Coxiella burnetii*, *Legionella* spp, *Histoplasma capsulatum*, *Coccidioides immitis*, *Pneumocystis carinii*, and respiratory viruses are among infectious agents associated with atypical pneumonia (Krause and Taylor-Robinson 1992). In contrast, typical pneumonia has an abrupt onset following an incubation period of only 1-3 days, a productive cough with rust colored sputum in the case of *Streptococcus pneumoniae* infections, high fever, chest consolidation, rales, pleuritic chest pain, and neck stiffness (Helms 1978). Typical pneumonia is associated with infectious agents including *S. pneumoniae*, Influenza viruses A and B, *Haemophilus influenzae*, and *Staphylococcus aureus*. Incidence rates of 36 to 40 cases of pneumonia per 1000 children under the age of 5 and 11 to 16 cases per 1000 children between 5 and 14 have been reported for the United States and Finland (Jokinen *et al.*, 1993; Murphy *et al.*, 1981). Poor countries in Africa and Asia have a reported 2-to-10 times greater incidence of infection (Pechere 1995), and pneumonia is one of the leading causes of hospitalization

and death in these countries (Nascimento-Carvalho 2001). *S. pneumoniae* is widely recognized as the most common cause of community acquired pneumonia, and along with, *H. influenzae* and respiratory syncytial virus, is responsible for most serious cases of pneumonia (Nascimento-Carvalho 2001). Epidemiological statistics concerning *M. pneumoniae* infection are generally only collected from individuals seeking medical attention and their families or contacts. Likely, less than 10% of infected individuals seek medical attention (Cassell and Cole 1981; Clyde 1983) and about 25% of *M. pneumoniae* infections are subclinical/preclinical or asymptomatic (Cassell *et al.*, 1985). Thus epidemiological reports probably underestimate the actual number of infections. However, various studies report that *M. pneumoniae* is responsible for up to 30% of pneumonias in the general population (Clyde 1983; Murray *et al.*, 1975; White *et al.*, 1981). Therefore, *M. pneumoniae* is a significant human pathogen.

Mycoplasmal pneumonia is a community-acquired disease requiring close contact for transmission. The community-acquired nature of the disease predisposes households, schools, college dorms, military barracks, and nursing homes as sites of epidemics. Up to 81% of children in a household can be infected in a family epidemic (Hanukoglu *et al.*, 1986). Children over the age of 5 and young adults are the demographic most commonly affected by *M. pneumoniae*. An estimated 9 to 42% of children over the age of five with community-acquired pneumonia are infected with *M. pneumoniae* (Block *et al.*, 1995; Harris *et al.*, 1998; Heiskanen-Kosma *et al.*, 1998; Wubbel *et al.*, 1999). However, recent studies show an increasing number of children under 5 diagnosed with *M. pneumoniae* infection (Principi and Esposito 2001). Epidemiological studies have shown that *M. pneumoniae* infections are endemic and not particularly seasonally variable

(Mansel *et al.*, 1989) with cyclic epidemics occurring every 4 to 7 years (Krause and Taylor-Robinson 1992).

Mycoplasma infections can involve the nasopharynx, throat, bronchus, and bronchioles, but rarely the alveoli (Krause and Taylor-Robinson 1992). Tracheobronchitis (dry cough and low grade fever) is the most common manifestation of *M. pneumoniae* infection (Clyde 1983). Atypical pneumonia develops in 3 to 10% of infected individuals (Cassell and Cole 1981; Clyde 1983), while on average, 5 to 10% of persons seeking medical attention required hospitalization (Helms *et al.*, 1979; Mansel *et al.*, 1989). Of those seeking medical attention, dry cough was the most common complaint (97%) followed by low-grade fever (85%) (Mansel *et al.*, 1989). Other symptoms can include, malaise, rhinorrhea, otitis media, pharyngitis, bronchitis, nausea vomiting, anorexia, diarrhea and scattered rales and consolidation (Mansel *et al.*, 1989). Reinfections are not uncommon (Jacobs *et al.*, 1988) and sequelae such as sinusitis, otitis media, erythema multiforme, exudativum, central nervous system, hemolytic anemia, myocarditis, pericarditis, and asthma have been documented (Clyde 1979).

M. pneumoniae infections are difficult to diagnose and are most commonly determined by assessing clinical findings and ruling out other causes. Pathology shows that the predominant lesion is a dramatic increase in macrophages and neutrophils in the lungs at some stage of disease (Cassell *et al.*, 1985). All reports agree that radiographic patterns associated with *M. pneumoniae* infection are quite variable. Unilateral or bilateral involvement of lower lobes is common with some upper lobe involvement. Consolidation is rare (Mansel *et al.*, 1989). Serological testing is often effective only for retrospective diagnosis since samples are required from both the acute and the

convalescent phase of illness in order to show the required fourfold increase in antibody titer (Principi and Esposito 2001). One means for early diagnosis (1 to 2 weeks following infection) is the production of cold agglutinins. Cold agglutinins are IgM autoantibodies that agglutinate human erythrocytes at 4°C and are found in 33 to 76% of patients with confirmed *M. pneumoniae* infection (Scully *et al.*, 1983). Unfortunately cold agglutinins are not produced by all individuals, are particularly infrequently seen in young children infected with *M. pneumoniae*, and can also be caused by a number of other agents of respiratory disease (Nelson 2002; Principi and Esposito 2001). *M. pneumoniae* can be isolated from culture, however this is extremely slow, generally requiring 8-to-25 days of incubation for detection (Dorman *et al.*, 1983). Productive samples have been obtained from nasopharyngeal, oropharyngeal or throat swab, tracheal aspirate and lung tissue biopsy (Clyde 1979). Enzyme immunoassay measuring specific IgM or IgG can also be used for diagnosis (Principi and Esposito 2001). PCR-based tests are being developed, although at this time they are generally regarded as less sensitive than serology (Principi and Esposito 2001) and are not accessible to most clinicians (Nelson 2002).

M. pneumoniae infections are generally self-limiting, with most symptoms resolving in less than two weeks, although, the cough can persist for months (Mansel *et al.*, 1989). Previously, many believed that antibiotics were not necessary due to the self-limiting nature of the illness. However, more recently it has been shown that antibiotic therapy is effective in shortening the duration of illness (Principi and Esposito 2001). Following antibiotic therapy thoracic radiographs showed clearing in the majority of individuals within four weeks, and nearly all were clear by eight weeks (Mansel *et al.*, 1989). Effective antibiotics include tetracyclines, chloramphenicol, streptomycin, and

erythromycins or other macrolides in young children. Azithromycin has been gaining in popularity due to several characteristics. It is as effective as erythromycin but has a much more palatable taste, requires a single daily dose, a shorter course of treatment (5 days) (Powers 1996), has enhanced activity against respiratory pathogens *S. pneumoniae* and *H. influenzae* (Klein 1997), and lower incidence of gastrointestinal side-effects than erythromycin or clarithromycin (Nelson 2002). These antibiotics are not mycoplasmacidal (Clyde 1979).

Prevention of mycoplasmal disease has been the goal of a number of research projects. Studies have shown that antibiotic prophylaxis simply delays onset of illness until after antibiotic therapy is discontinued (Clyde 1979). In one vaccine trial, while one group of volunteers developed a measurable antibody response to inoculation with the proposed vaccine, another group did not. The group that developed antibodies was protected when challenged. However, upon challenge, the group that did not respond to the vaccine had more severe illness than the uninoculated control group (Smith 1967). In yet another study, only those volunteers shown to have preexisting mycoplasma antibodies mounted a response to the vaccine (Brown *et al.*, 1972).

Morphology and Ultrastructure.

M. pneumoniae cells are not shaped like the typical rod, coccoid or even spiral bacteria. Wild-type *M. pneumoniae* cells are spindle shaped, long filaments (approximately 2 μm long by 100-300 nm wide) with an asymmetrically located distended area (cell body) approximately 2-3 times wider than the filament. The longer filamentous extension is known as the trailing filament, while the shorter filament, the

attachment organelle, tapers and then flares into a knob-like structure. Since *M. pneumoniae* cells lack a cell wall, cell morphology is somewhat plastic, and populations are pleiomorphic. The morphology described above is by far the most predominant in wild-type populations, but many *M. pneumoniae* cells have altered morphologies, often with branches.

The attachment organelle is composed of a complex assemblage of proteins that are specifically localized to this structure and coordinately stabilized. They include the major adhesin, protein P1 (Baseman *et al.*, 1982b; Feldner *et al.*, 1982; Hu *et al.*, 1982), and cytoadherence-accessory proteins HMW1, HMW2, HMW3, B, C, P200, P65, and P30 (Baseman and Tully 1997; Franzoso *et al.*, 1993; Jordan *et al.*, 2001; Proft and Herrmann 1994; Stevens and Krause 1991; Stevens and Krause 1992). The attachment organelle is believed to play a role in gliding motility, attachment, and cell division (Boatman 1979b; Kirchhoff 1992; Razin 1999). Through analysis of mutants with defects in various attachment organelle proteins we are beginning to understand how this structure is assembled. The current model proposes that proteins are incorporated into the attachment organelle via two pathways and that the proteins of each individual pathway stabilize one another upon incorporation. It is hypothesized that first HMW1 and HMW2, then HMW3 and P30 and finally P65 are incorporated by one pathway, while proteins B, C and P1 are incorporated by a different pathway (Krause and Balish 2001; Seto *et al.*, 2001). Work is underway to determine how these proteins physically interact to form a stable, functional attachment organelle.

Electron microscopic examination of thin sections of *M. pneumoniae* cells has revealed details about the ultrastructure of the cells, which are surrounded by a single

trilaminar membrane 75-100 Å thick (Domermuth *et al.*, 1964). There is generally a thin slime layer outside the membrane that thickens around the attachment organelle, perhaps providing additional support (Domermuth *et al.*, 1964; Wilson and Collier 1976). At the pole corresponding to the attachment organelle an electron-dense rod shaped structure was visualized. The structure is surrounded by an electron-lucent area (Biberfeld and Biberfeld 1970; Domermuth *et al.*, 1964) and is often referred to as the electron-dense core. The electron-dense core appears to have some degree of periodicity (Wilson and Collier 1976).

When *M. pneumoniae* cells are extracted with the nonionic detergent Triton X-100 a triton-insoluble fraction (triton shell) containing a minimum of 100 proteins can be isolated (Regula *et al.*, 2001). This fraction by definition comprises the mycoplasmal cytoskeleton. The cytoskeleton is thought to function in maintenance of the cell shape, proper localization of certain membrane proteins, cell division, and protection of the mycoplasma cell from osmotic lysis. Visualization of *M. pneumoniae* cells grown on grids and extracted with Triton X-100 reveals a striated rod that corresponds to the electron dense core seen in thin sections (Meng and Pfister 1980). Protruding from this rod is a network of fibrils (Meng and Pfister 1980). A number of the components of the triton insoluble fraction have been identified by Western immunoblotting or liquid chromatography-mass spectrophotometric analysis. Many components of the attachment organelle are also components of the cytoskeleton, including HMW1, HMW2, HMW3, B, C, P65, P200 and to a small extent P1 (Regula *et al.*, 2001).

P1 Adhesin.

Characterization of the *M. pneumoniae* adhesin began with studies suggesting its proteinaceous nature (Feldner *et al.*, 1979; Feldner *et al.*, 1981; Hu *et al.*, 1977). In a 1982 study Hu *et al.* isolated a monoclonal antibody to the P1 protein, demonstrating adherence-inhibiting properties of this antibody and describing antibodies reactive with the same protein in *M. pneumoniae*-infected hamsters, rabbits and humans (Hu *et al.*, 1982), indicating that P1 is likely an adhesin and is immunogenic. In a separate study, Feldner *et al.* (1982) generated a monoclonal antibody that blocked adherence to erythrocytes and plastic and inhibited motility. Indirect immunofluorescence using this antibody revealed trypsin-sensitive, polar consolidation of fluorescence. Cells probed with this monoclonal antibody and immunoferritin were labeled primarily at their attachment organelles. Finally, this antibody bound to a band with hemolytic properties in the 160-190 kDa region of a polyacrylamide gel (Feldner *et al.*, 1982). The authors did not attempt to define the epitope. However, since these properties are all characteristics of P1, it seems likely that this antibody reacted with protein P1. Another study compared four classes of hemadsorption negative mutants (Krause *et al.*, 1982) to the wild-type, hemadsorption positive strain. Perplexingly, three of these mutant classes expressed apparently wild-type levels of protein P1, yet exhibited reduced levels of attachment (Baseman *et al.*, 1982b; Hansen *et al.*, 1979a; Hansen *et al.*, 1979b; Krause *et al.*, 1982). Lactoperoxidase-catalyzed radioiodination revealed that with the exception of one mutant (class IV) that apparently lacked P1 altogether, P1 was equally surface-exposed on all mutants. Using monospecific antisera generated against P1, clustering of this protein at the attachment organelle of wild-type cells, with a small degree of labeling

on the rest of the cell was confirmed (Baseman *et al.*, 1982a). Conversely, no polar clustering of P1 was seen in the nonadhering mutants, providing an explanation for loss of adherence in these mutants despite wild-type levels of P1, and suggesting that clustering of P1 at the attachment organelle is a prerequisite for attachment (Baseman *et al.*, 1982). Sequencing of the class IV mutant identified an insertion of a single adenine into a stretch of 7 adenines at nucleotide positions 13-18 of the *p1* gene, resulting in a frameshift and premature termination (Su *et al.*, 1989).

Two independent efforts to sequence the gene encoding P1 generated somewhat contradictory results (Inamine *et al.*, 1988; Su *et al.*, 1987). While the 4881 nt sequence attributed to the *p1* gene was identical in the two studies, controversy arose concerning the flanking region. Su *et al.* reported that *p1* was monocistronic, while Inamine *et al.* identified flanking ORFs suggesting that *p1* might be cotranscribed. This debate was resolved upon sequencing of an 18 kb region including *p1* (Inamine *et al.*, 1988) which revealed two ORFs of 723 and 3654 nt, respectively, bordering the *p1* gene. These ORFs are hereafter referred to as ORF4 and ORF6, with the gene order ORF4-*p1*-ORF6. While no consensus ribosome binding site or Shine-Dalgarno sequence was identified preceding *p1* or ORF6, such sequences were identified upstream of ORF4 (Inamine *et al.*, 1988). A primer extension product correlated a transcription start site with the predicted promoter region upstream of ORF4. Moreover, no predicted transcriptional terminator sequence could be identified immediately downstream of ORF4 or *p1*, but a likely stem-loop structure ($\Delta G = -8.6$ kcal/mol) was identified downstream of ORF6 (Inamine *et al.*, 1988). Therefore, although an mRNA corresponding to this message was never identified, it seems probable that these genes encompass an operon. The loss of the ORF6 products in

conjunction with the frameshift mutation in the P1 gene is consistent with this conclusion.

P1 may delay or avoid activation of a host immune response by antigenic variation utilizing P1 sequences dispersed on the genome. The first evidence that regions of the *p1* gene exist as multiple copies on the genome came in 1988 (Su *et al.*, 1988). ³²P-labeled *p1* probes hybridized to multiple bands in Southern blots of digested chromosomal *M. pneumoniae* DNA. To better assess which regions of *p1* were present in multicopy, the *p1* gene was divided into 14 fragments by restriction digestion and subcloned. Each fragment was labeled with ³²P and used to probe genomic DNA under stringent conditions. Results indicated that the DNA corresponding to the middle and C-terminal regions was present in single copy on the chromosome, while the DNA encoding the remaining two-thirds of the protein was present to various degrees as multicopy (Su *et al.*, 1988). Another study showed that two regions of P1 are repeated within the genome. The sequence designated RepMP4 is within the 5' region of *p1*, and a similar sequence is found in 7 other instances on the chromosome, while RepMP2/3 is within the 3' region of the *p1* gene and is repeated nearly identically 9 additional times in the genome (Ruland *et al.*, 1990). Interestingly, a 13-amino-acid region determined to be required for adherence was present in only one copy, emphasizing the importance of this region (Su *et al.*, 1988). Comparison of independently isolated clinical samples has confirmed at least two variable regions within the *p1* coding sequence with high degree of similarity to RepMP4 and Rep Mp2/3, suggesting homologous recombination between these regions could serve as a means to vary P1 antigenically (Dorigo-Zetsma *et al.*, 2000; Dorigo-Zetsma *et al.*, 2001; Kenri *et al.*, 1999; Su *et al.*, 1990).

P1 is an immunodominant protein in *M. pneumoniae* infection. Much work has been done to characterize immunogenic regions of the protein as well as the receptor-binding sites. Jacobs *et al.* attempted to identify B cell epitopes using overlapping octapeptides encompassing approximately one-fifth of the amino acid sequence of P1 as antigens in ELISA probed with human antisera collected from individuals with confirmed mycoplasmal pneumonia (Jacobs *et al.*, 1990). The data revealed three highly antigenic domains: aa 803 to 816, aa 1119 to 1128 and aa 837-854. Significantly, two of these regions shared sequence similarity with the 140 kDa *M. genitalium* adhesin protein (Jacobs *et al.*, 1990). These results were expanded upon in a follow-up study by Gerstenecker and Jacobs in which monoclonal antibodies were generated by immunization of mice with an N-terminal synthetic peptide, whole *M. pneumoniae* or purified P1 protein (Gerstenecker and Jacobs 1990). Hybridomas were screened for adherence-inhibiting antibodies reactive with P1, and 5 monoclonal antibodies were selected for further study. Octapeptides encompassing the N-terminus of the protein (aa 172-343) and two previously identified antigenic domains: aa 841 to 941 (domain D1) and aa 1241 to 1441 (domain D2) were screened for binding by monoclonal antibodies. Results revealed that a single antibody was capable of binding epitopes within region D1 and D2 and another antibody bound regions within both the N-terminus and D1. Once the epitopes bound by each antibody were determined, competitive ELISAs were done using multiple antibodies in order to explore the native conformation of P1. These data suggest that P1 exists in the membrane as at least three loops that are in close association with one another (Gerstenecker and Jacobs 1990).

Cytadherence-Accessory Proteins.

Krause *et al.* reported isolation and preliminary characterization of 22 spontaneously arising, nonhemadsorbing *M. pneumoniae* mutants (Krause *et al.*, 1982). Variants were assigned to one of four different classes (I-IV) based on protein profiles (Table 1). All mutants were nonadherent to hamster tracheal rings, and when inoculated into hamsters, none of these strains resulted in pneumonia (Krause *et al.*, 1982). Moreover, reacquisition of proteins deficient in each mutant resulted in a reversion to a wild-type phenotype (Krause *et al.*, 1983). Analysis of each of these mutant classes and other mutants that have since been isolated (Layh-Schmitt *et al.*, 1995; Willby and Krause 2002) has broadened our understanding of requirements for attachment, identifying a number of nonadhesin proteins that are essential for attachment to host cells. These proteins are referred to as cytheadherence-accessory proteins and include HMW1, HMW2, HMW3, B, C, P65, and P200 (Krause *et al.*, 1982; Proft and Herrmann 1994). We have begun to characterize interactions among these proteins in an attempt to define the sequence of events that leads to formation of a functional attachment organelle.

Preliminary reports describing class I mutants, in particular, mutant I-2 (mutant class I, isolate number 2) describe reduced levels of HMW1 and absence of HMW2 and HMW3 (Krause *et al.*, 1982). Further characterization of this mutant demonstrated the insertion of a single adenine in a run of adenines within *hmw2* (Fisseha *et al.*, 1999). Hedreyda and Krause (1995) reported that transposon insertion into the *hmw2* gene of wild-type *M. pneumoniae* cells resulted in loss of proteins HMW1 and HMW3 in addition to HMW2. Pulse chase analysis of mutant I-2 and *hmw2* transposon insertion mutants revealed that HMW1 and HMW3 are transcribed at wild-type levels in these

mutants, but established the loss of both HMW1 and HMW3 proteins over time, suggesting proteolysis in the absence of HMW2 (Popham *et al.*, 1997). Additionally, pulse-chase analysis of HMW1 followed by Triton fractionation showed that in wild-type cells, HMW1 is synthesized in a Triton-soluble form, but over time becomes Triton-insoluble. However, in mutant I-2, HMW1 becomes insoluble with a much lower efficiency, with degradation apparently occurring in the soluble fraction (Balish *et al.*, 2001). Interestingly, transformation of mutant I-2 with a recombinant *hmw1* allele encoding a truncated HMW1 missing the C-terminal 112 amino acids results in moderate steady-state levels of this protein, emphasizing the C-terminal region in turnover (Hahn *et al.*, 1996). Several double-serine containing motifs were identified in the C-terminus of HMW1 (Popham *et al.*, 1997). These motifs are reminiscent the region following the proteolytic processing site in *M. pneumoniae* ORF6 and may be a target sequence for turnover of HMW1 (Popham *et al.*, 1997; Sperker *et al.*, 1991). Perhaps in the absence of HMW2, HMW1 does not form stabilizing interactions with the cytoskeleton, resulting in increased accessibility to proteolytic processing.

Sequencing efforts revealed that the genes encoding HMW1 and HMW3 along with the coding sequence for P30, ribosomal protein S4, and six additional less characterized open reading frames, are components of a gene cluster flanked by putative transcriptional termination sequences (Dirksen *et al.*, 1996; Himmelreich *et al.*, 1996; Krause and Lee 1991; Waldo *et al.*, 1999). S1 nuclease protection assays and primer extension were used to identify transcription start sites within this region. Four such sites each with upstream sequence homology to the consensus Pribnow-Schaller box (Pribnow 1975) were identified; two at the 5' end of the gene cluster, one near its midpoint and one

at the 3' end (Waldo *et al.*, 1999). Additionally, transcriptional linkage of genes within this cluster was confirmed via RT-PCR spanning intergenic sequences. Consequently, these genes appear to be transcribed from overlapping transcripts, perhaps reflecting a mechanism for generating a stoichiometric balance between important cytoadherence related proteins (Waldo *et al.*, 1999).

Sequence analysis of the gene encoding HMW1 revealed a 1018-amino-acid protein with a predicted molecular mass of 112,177 Da, much smaller than the 210,000 relative molecular weight observed by SDS-PAGE (Dirksen *et al.* 1996; Krause *et al.*, 1982). HMW1 has a deduced pI of 3.79, with an internal acidic domain and high concentration of Glu (13.3%), Val (12.4%), and Pro (9.6%) residues. It is hypothesized that the unusual charge distribution and amino acid composition of this protein slows its migration by SDS-PAGE, resulting in the inconsistency between predicted and observed sizes. HMW1 is largely hydrophilic with no typical membrane-spanning sequences. Furthermore, HMW1 can be divided into three domains based on its amino acid sequence. The N-terminal domain (Domain I) has a fairly typical amino acid composition and is predicted to form mostly β -sheets. Glu, Val and Pro residues arranged in repeating motifs referred to as acidic proline rich (APR) domains make up about 60% of the central region of the protein (Domain II) of HMW1. This region is predicted to be quite rigid due to the high Pro content with secondary structure consisting mostly of α -helices and a few turns. Domain III, the C-terminus of HMW1, has a more commonplace amino acid composition and is predicted to form a mixture of β -sheets, α -helices and turns. HMW1 is phosphorylated by an ATP-dependent Ser/Thr kinase

(Dirksen *et al.*, 1996). Analysis of the amino acid sequence for likely phospho-acceptor sites revealed an unexpectedly high number within Domain III (Dirksen *et al.*, 1996).

Immunoelectron microscopy studies have placed HMW1 at the attachment organelle and on trailing filaments of the wild-type mycoplasma cell (Stevens 1991). Treatment of *M. pneumoniae* with the detergent Triton X-100 allows isolation of Triton-soluble and Triton-insoluble fractions, the latter including the mycoplasmal cytoskeleton. HMW1 has been shown to be mostly triton-insoluble and is almost certainly a component of the *M. pneumoniae* cytoskeleton. Furthermore, when *M. pneumoniae* cells attached to glass coverslips are treated with Triton X-100, the triton-soluble material is lost and the triton-insoluble material remains attached to the coverslips (Gobel *et al.*, 1981). When this material was probed with antisera against HMW1 and an immunogold-conjugated secondary antibody, HMW1 was again visualized on the filamentous portions of the cell, confirming both its insolubility and its polar localization (Stevens and Krause 1991).

Assessing the subcellular location of HMW1 relative to the cell membrane has been more problematic. While HMW1 is phosphorylated and does not have any predicted membrane-spanning regions (Dirksen *et al.*, 1996), it appears to be a peripheral membrane protein associated with the outer leaflet of the membrane (Balish *et al.*, 2001). This conclusion was based on a number of experiments. HMW1 partitioned with isolated membrane (Proft and Herrmann 1994), and was released from membrane pellets solubilized by alkali treatment (Balish *et al.*, 2001). Whole cells were reproducibly labeled with HMW1 antibodies in immunoelectron microscopy studies (Stevens and Krause 1991) and immunofluorescence microscopy with antibodies generated to Domains I-III confirmed that these domains are on the cell exterior (Balish *et al.*, 2001).

Moreover, HMW1 was precipitated by whole-cell radioimmunoprecipitation (RIP). However, slightly more HMW1 was precipitated from lysates than from whole cells, suggesting that not all of HMW1 is antibody-accessible on the mycoplasma cell surface (Balish *et al.*, 2001; Dirksen *et al.*, 1996).

Other studies have focused on characterizing the function of HMW1 within the attachment organelle, including its associations with other proteins. Immunoelectron microscopy of mutant I-2 probed with antiserum against P1 revealed that P1 was no longer properly localized in this mutant, implicating HMW1-HMW3 in P1 localization (Baseman *et al.*, 1982b). Complementation of the M6 mutant with a recombinant *p30* by transposon delivery resulted in the first mutant lacking only HMW1 (Hahn *et al.*, 1998). Like the M6 mutant itself, these transformants were hemadsorption negative, had an irregular morphology and did not localize P1 (Hahn *et al.*, 1998), implicating HMW1 in these activities.

Sequence analysis of *hmw3* revealed a 672 amino acid protein with a molecular mass of 73,725 daltons. While database searches do not reveal significantly homologous sequences, deduced HMW1 and HMW3 do have common characteristics. The sequence of HMW3 is largely hydrophilic, with a deduced pI of 4.4. Like HMW1, it contains a relatively high concentration of Glu and Asp (13.3% by weight) and Pro (12% by weight). The N-terminus of HMW3 has an approximately equal acidic vs. basic amino acid content, the central region contains APR domains making it acidic, and the C-terminus is basic. Several repetitive motifs consisting of between 3 and 10 amino acids are present within the N-terminal and central regions of the protein (Ogle *et al.*, 1992). Secondary structural predictions based on the algorithms of Chou and Fasman (Chou and

Fasman 1978) and Garnier *et al.* (Garnier *et al.*, 1978) predict mostly β -sheets and loops or turns with few α -helices within HMW3. The high Pro content is likely to encourage an extended conformation (Ogle *et al.*, 1992). No typical membrane spanning sequences were identified (Ogle *et al.*, 1992). As with HMW1 and likely for the same reasons as HMW1, the relative mobility of HMW3 by SDS-PAGE (140,000) is much larger than the deduced molecular mass.

HMW3 is a component of the *M. pneumoniae* cytoskeleton, partitioning with the Triton X-100 insoluble fraction (Stevens and Krause 1992). Immunogold labeling of whole cells demonstrated discrete localization of HMW3 at the attachment organelle, specifically the distal, bulbous region. Whole-cell labeling was, however, accomplished only after extended incubation with high-titered, affinity-purified anti-HMW3 antibodies, suggesting surface exposure is limited at best. Immunogold labeling of thin sections and triton shells showed the same HMW3 distribution. However, RIP failed to precipitate HMW3, suggesting that surface accessibility by immuno-electron microscopy may be an artifact of sample preparation (Stevens and Krause 1992). While, potassium iodide extraction of triton shells resulted in some removal of HMW3, it appeared that the extracted protein remained associated in clusters, implying that HMW3 is a component of a multimeric complex (Stevens and Krause 1992).

As previously mentioned, HMW3 is present at reduced levels in the class I mutants (Krause *et al.*, 1982), and like HMW1, HMW3 is proteolytically degraded in the absence of HMW2 (Fisseha *et al.*, 1999; Hedreyda and Krause 1995; Popham *et al.*, 1997). However, turnover of HMW3 is considerably slower than that of HMW1 (Popham *et al.*, 1997). Also like HMW1, the C-terminus of HMW3 contains sequences

similar to the ORF6 proteolytic processing site, suggesting that these proteins may be lost by a similar mechanism in mutant I-2 (Popham *et al.*, 1997; Sperker *et al.*, 1991).

Cytoskeletal proteins P65 and P200 were identified using an *E. coli* expression library generated from *M. pneumoniae* genomic DNA (Proft and Herrmann 1994). P200 is similar to HMW1 and HMW3 in a many respects. Based on its amino acid sequence, P200 has a molecular weight of 116,914 Da, however its relative mobility by SDS-PAGE is approximately 200,000. Its protein sequence is not significantly homologous to other proteins thus far identified including HMW1, HMW3 and P65. P200 has a low pI (3.9) and a high Pro (6.5%) and Glu (14.8%) content. Like HMW1 and HMW3, the central region of the protein has an especially high concentration Pro and acidic amino acids (APR domain). This region also contains repeated sequences. Predictions based on the amino acid sequence suggest a hydrophilic protein with no typical membrane-spanning sequences. P200 has no predicted coiled-coils but is dominated by α -helices and turns (Proft *et al.*, 1996). Presence of P200 in the cytoskeleton as well as its similarities with demonstrated cytodherence-accessory proteins HMW1 and HMW3 suggest that P200 may also be involved in cytodherence.

The gene encoding P65, along with genes encoding HMW2 and two other ORFs were localized to an operon located 160 kb from the HMW operon (Krause 1997). Comparisons of P65 from two *M. pneumoniae* strains revealed a slight size polymorphism as a result of presence or absence of a 54-bp repeat within the *p65* coding region (Proft *et al.*, 1995). Protein database searches revealed no significant homologs to this protein. However, P65 also has a number of properties in common with cytoskeletal proteins HMW1 and HMW3. It is deduced to be a 409-amino-acid protein with a

molecular mass of 47,304 Da, much less than the 65,000 relative molecular weight predicted by SDS-PAGE. Like HMW1 and HMW3, the aberrant electrophoretic mobility is probably a function of the amino acid composition including a high (9.1%) Pro content, as well as an above average concentration of Asp and Glu residues (15.6% together) and the resulting acidic pI (4.09). P65 can be divided into three domains based on secondary structure predictions. The N-terminus (domain I) is predicted to be mostly turns and coils. This domain has a disproportionately high Pro and Asp content (APR domain) and contains several repeated sequences. The central domain (domain II) is estimated to be primarily α -helical with a high probability of forming coiled-coils, and the C-terminus of the protein (domain III) is predicted to be composed of α -helices, β -sheets, and turns (Proft *et al.*, 1995). Like HMW1 and HMW3, P65 is predicted to be predominately highly hydrophilic with no membrane spanning-sequences (Proft *et al.*, 1995).

As previously mentioned, P65 is a cytoskeletal protein. Biochemical analysis suggests that it is more loosely associated with the cytoskeleton than are HMW1 and HMW3 (Proft *et al.*, 1995). P65 was detected by immunofluorescent labeling of whole-cells, albeit not as intensely as P1, suggesting that P65 is surface exposed to some extent (Proft, *et al.*, 1995). Limited trypsin sensitivity also suggests surface exposure of this protein.

P65 is found at reduced steady state levels along with HMW1 and HMW3 in mutant I-2, apparently also as the result of accelerated proteolytic turnover (Jordan *et al.*, 2001; Krause *et al.*, 1997). Additionally, Western blotting showed reduced levels of P65 in mutants II-3, II-7 (mutant class II, isolates 3 and 7) and M6 (Jordan *et al.*, 2001).

These mutants have in common absent or reduced P30, predicting an association between P65 and P30 (Jordan *et al.*, 2001).

P65 was localized to the attachment organelle of wild-type *M. pneumoniae* via immunofluorescence (Jordan *et al.*, 2001; Seto *et al.*, 2001). Polar labeling of P65 in mutant II-3, II-7, III-4 and IV-22 was also observed, however P65 appeared to be distributed throughout mutant I-2 and M6 (Jordan *et al.*, 2001). Therefore, while stability of P65 seemed to depend on P30, localization of P65 was dependent on HMW1, HMW2, and/or HMW3.

HMW2 is not a member of the family of related proteins that includes HMW1, HMW3, P200 and P65. HMW2 has a deduced molecular mass 215,620 Da and a similar relative mobility of 190,000. HMW2 has a basic pI (9.8) and is largely composed of four amino acids: E (11.6%), K (12.3%), L (13.5%), and Q (13%) arranged in numerous heptad repeats (Krause *et al.*, 1997). Structural algorithms predict coiled-coils along the length of HMW2 with intermittent disruptions. Additionally, five leucine zippers are predicted in the center of the protein. Protein database searches do not reveal homologs to HMW2, although, the coiled-coil regions of the protein are reminiscent of similar structures in other proteins, myosin type II heavy chain from chicken, for example. The presence of coiled-coil and leucine zipper motifs implies that HMW2 may exist as a multimer or perhaps interact with other *M. pneumoniae* proteins (Krause *et al.*, 1997).

Loss of HMW2 either through transposon insertion (*crl* mutant; Hedreyda and Krause 1995) or frameshift mutation (mutant I-2; Fisseha *et al.*, 1999; Krause *et al.*, 1997) results in subsequent accelerated turnover of HMW1, HMW3, and P65 (Jordan *et al.*, 2001; Krause *et al.*, 1982; Popham *et al.*, 1997). Mutant I-2 cells transformed with

recombinant *hmw2* expressed somewhat variable levels of HMW2. Mutants with wild-type levels of HMW2 regained wild-type levels of HMW1, HMW3, and P65 and were fully hemadsorption-positive. Cells producing lower levels of HMW2 regained wild-type levels of HMW3, but HMW1 and P65 levels were proportional to the amount of HMW2 produced, and hemadsorption was intermediate, reinforcing the relationship between HMW1, HMW3, P65 and HMW2 (Fisseha *et al.*, 1999). Finally, a 28 kDa protein (P28) is likely the result of internal translation from *hmw2* (Fisseha *et al.*, 1999). The role if any that this protein plays in cytheadherence is not known.

P1 and two additional open reading frames (ORF4 and ORF6) make up the P1 operon, with a gene order of ORF4-P1-ORF6 (Inamine *et al.*, 1988). ORFs 4 and 6 are predicted to encode 28- and 130-kDa proteins respectively. Very little work has been done on ORF4, and no cognate protein has yet been identified. The ORF6 gene product is predicted to be a membrane protein. It has typical signal and stop transfer sequences located at its N-terminus and a single hydrophobic region of adequate length to span the membrane (Inamine *et al.*, 1988). Although protein database searches failed to yield homologs to ORF6 in other organisms, ORF6 has striking similarity to the C-terminus of *M. pneumoniae* protein P1. While no 130 kDa protein was reactive with antisera generated against an ORF6 fusion proteins, two smaller (40 and 90 kDa) proteins did react (Sperker *et al.*, 1991). These antisera failed to react with cytheadherence mutants of class III or class IV, suggesting that the 90- and 40-kDa proteins correspond to proteins B and C, respectively, previously reported to be absent in these mutants (Hansen *et al.*, 1979a; Krause *et al.*, 1982). N-terminal sequencing of the 90 kDa protein confirmed that it is the product of central and C-terminal ORF6 sequences, with the 40 kDa protein the

product of the 5' end of ORF6. Although only protein C has a signal sequence, both B and C are proposed membrane proteins and accessible to trypsin and peroxidase-mediated iodination (Layh-Schmitt and Herrmann 1992). Franzoso *et al.* (1993) localized B to the attachment organelle, and Layh-Schmitt and Herrmann (1992; 1994) demonstrated crosslinking of both B and C to P1 using 3,3'-dithiobis(sulfosuccinimidylpropionate) .

Initial characterization of hemadsorption negative mutants of class II failed to identify any protein deficiencies in these mutants (Krause *et al.*, 1982). Subsequently, antisera specific for a 32 kDa *M. pneumoniae* protein were unreactive in an ELISA assay using several different Class II isolates as antigen (Baseman *et al.*, 1987). Additionally, while this antisera precipitated a 32 kDa protein from both wild-type and class II hemadsorption positive revertants, it failed to precipitate any protein from class II isolates (Baseman *et al.*, 1987). These data suggest that loss of this 32 kDa protein (called P30) may contribute to the hemadsorption negative phenotype of class II mutants.

Characterization of P30 revealed that it is somewhat sensitive to a number of proteases, suggesting surface accessibility. Additionally, *M. pneumoniae* infected hamsters produce antibodies specific for it (Baseman *et al.*, 1987). Electron microscopy and colloidal gold labeling demonstrated localization of P30 at the attachment organelle (Baseman *et al.*, 1987). Preincubation of *M. pneumoniae* with monoclonal antibodies against P30 inhibited attachment suggesting a role for P30 in adherence (Morrison-Plummer *et al.*, 1986). However, to date, the possibility that loss of adherence was nonspecifically occluded by antibody binding to another attachment organelle protein was not explored.

The gene encoding P30 was identified and has subsequently localized to the HMW gene locus (Dallo *et al.*, 1990; Wenzel *et al.*, 1992). The gene is predicted to encode a 29,743 kDa protein with a potential signal sequence at its N-terminus (Dallo *et al.*, 1990). The C-terminus of the protein is characterized by three different types of repeated amino acid motifs. These motifs have in common a high concentration of proline (Dallo *et al.*, 1989a; Dallo *et al.*, 1989b). This region of the protein is predicted to be hydrophilic and appears to be flanked by two membrane spanning regions (Dallo *et al.*, 1996). Antibodies generated to the C-terminal region of P30 precipitated a 30 kDa protein in whole cell RIPs, suggesting surface accessibility of this region. Conversely, antibodies directed against the N-terminus of P30 were unreactive in whole cell RIP experiments (Dallo *et al.*, 1996). P30 is homologous over approximately 40% of its sequence to the C-terminal sequence of P1. Both these proteins share homology with eukaryotic matrix proteins such as fibrinogen, myosin, actin, collagen, keratin, and vitronectin, and immunologic cross reactivity has been demonstrated to fibrinogen, myosin and keratin, perhaps one explanation for autoimmune pathologies associated with *M. pneumoniae* infection (Dallo *et al.*, 1989a; Dallo *et al.*, 1996).

Further analysis of class II mutants revealed two subclasses. One subclass, represented by mutant II-3 failed to produce any P30. A frameshift mutation was discovered at nucleotide 453 resulting in an altered protein with a distinct C-terminus that was only a single amino acid shorter than the wild-type protein (Romero-Arroyo *et al.*, 1999). However, this protein was not detected with antisera specific for the altered sequence and appears to be unstable (Jordan, submitted). The other class II subclass, represented by mutant II-7, produces a 25 kDa protein reactive with anti-P30 antisera.

Sequence analysis of II-7 revealed an in-frame deletion of 144 nucleotides in the 3' coding region, drastically reducing the number of C-terminal proline-rich repeats. Characterization via SEM revealed that mutant II-3 has an altered morphology with a disproportionately large population of branched cells. Mutant II-7 had a morphology nearer to that of wild-type *M. pneumoniae*. As previously mentioned, loss of cytoadherence-accessory proteins HMW1, HMW2, and HMW3 were shown to affect the localization of P1 at the attachment organelle (Baseman *et al.*, 1982b; Hahn *et al.* 1998); mutants II-3 and II-7, however, localized P1 properly (Romero-Arroyo *et al.*, 1999). Therefore, unlike in other mutants, inability of class II cells to attach is not a function of inability of P1 to localize properly. Thus, P30 is involved in attachment and morphological development with its C-terminal domain required for the former process.

CHAPTER II

MATERIALS AND METHODS

Bacterial strains and culture conditions.

E. coli. *Escherichia coli* cells were cultured in LB broth or on LB agar plates at 37°C in the presence of 100 µg/ml ampicillin for maintenance of plasmids (Sambrook *et al.*, 1989). For the DHFR-ΔHMW1 construct, following transformation with plasmid pKV204, eighteen colonies were randomly selected and analyzed by Western blot for production of an approximately 41-kDa protein reactive with DHFR-specific antisera (1:200). Plasmid DNA was isolated from a positive clone, sequenced to verify its accuracy, and transformed into protease-deficient strains: SG22165 (*lacI^q clpP::catΔlon*), SG22166 (*lacI^q ftsH1*), SG22174 (*lacI^q clpP::cat*), and SG22186 (*lacI^q Δlon rcsA51::kan*), and the parental strain SG22163 (*lacI^q*) (generously provided by S. Gottesman, NIH, Bethesda, MD). Plasmid, pQE41 was transformed into these strains as a control.

M. pneumoniae. Wild-type *M. pneumoniae* strain M129-B18 (Lipman *et al.*, 1969) and mutants I-2 (Krause *et al.*, 1982) and M6 (Layh-Schmitt, *et al.* 1995; Table 1) were cultured in Hayflick medium or on PPLO agar plates at 37°C as previously described (Hahn *et al.*, 1996). Gentamicin (18 µg/ml) was included for culture of transposon-containing transformants. Individual colonies were isolated from PPLO agar plates incubated 7-9 d at 37°C, after application of a sheep blood overlay and additional

incubation for 2 d (Hahn *et al.*, 1996). Hemolytic plaques were picked with a sterile Pasteur pipette and expanded in fresh Hayflick medium. To ensure that resulting phenotypes from mycoplasma transformations were not a consequence of the transposon insertion site, 3-5 independent transformants were analyzed for each construct; representative results are shown here. The *hmw3::Tn4001*mod transformant was filter cloned as described (Tully 1983), to obtain a clonal population.

Plasmid Construction.

DHFR-ΔHMW1 fusions. Construction of a mouse dihydrofolate reductase (DHFR) fusion to the C-terminus of HMW1 (DHFR-ΔHMW1) was accomplished by PCR amplification of the C-terminus (amino acids 906-1008) of HMW1 using pKV37 (contains *hmw1*) as template DNA and introducing an in-frame stop codon 10 amino acids upstream of the actual HMW1 stop codon (Table 2; Table3). The expression vector, pQE41 (Qiagen, Chatsworth, CA) contains the coding sequence for DHFR followed by a polylinker including *Bgl*II and *Hind*III restriction sites. The PCR product was digested with *Bam*HI and *Hind*III and ligated to *Bgl*II/*Hind*III digested pQE41 (Fig. 1) resulting in a translational fusion between DHFR and the C-terminus of HMW1 (hereafter referred to as DHFR-ΔHMW1) and transformed into electrocompetent SURE strain *E. coli* cells (Stratagene, La Jolla, CA).

HMW1 deletion derivatives. Plasmids were isolated using QIAprep Spin Miniprep Kit (Qiagen, Santa Clarita, CA), Qiagen Plasmid Maxi Kit or alkaline lysis (Sambrook *et al.*, 1989). Four regions of interest were identified within the C-terminus of HMW1 for deletion based on the presence of a paired Ser motif (Fig. 2A, underlined;

TABLE 2. Construction of HMW1 truncation/deletion derivatives

Plasmid	Protein expressed	Upstream primer	Downstream primer^a	Nucleotides amplified^b	Amino acids encoded
pKV201	Δ1-2	ttaaaccttgatttagat	accgtttccattagttcatc	2864-3033	955-1011
pKV202	Δ1-4	--	--	--	1-905
pKV203	Δ2-4	ttaagcacaatcaacacggt	caagagatct aa ataatggc	1783-2790	1-927
pKV205	Δ4	ggatggcgaagctagacag	at ggatcct atggctctaac	2666-2942	1-978
pKV213	reHMW1	ggatggcgaagctagacag	ggc gg atccttgaataactacc	2666-3116	1-1018
pKV219	Δ1	tg ggatcct ggacttctcc	ggc gg atccttgaataactacc	2778-3116	1-905, 928-1018
pKV204	DHFR- ΔHMW1	ggatggcgaagctagacag	tcccca agct tttacattagttc	2666-3039	906-1008

^a Altered nucleotides are shown in bold.

^b Numbers represent nucleotide position within the coding sequence of *hmw1*.

Table 3. Conditions for PCR Amplification of Plasmid Inserts.

Plasmid	Polymerase	PCR Steps						
		1	2	3	4	5	6	7
pKV201	<i>Taq</i> ^a	95°C 5 min	95°C 2 min	55°C 1 min	72°C 2 min	30 x to step 2	72°C 2 min	4°C
pKV204	<i>Taq</i> ^a	95°C 5 min	95°C 2 min	45°C 1 min	72°C 2 min	30 x to step 2	72°C 2 min	4°C
pKV203	<i>Taq</i> ^a	95°C 2 min	95°C 2 min	45°C 1 min	72°C 2 min	30 x to step 2	72°C 2 min	4°C
pKV205	<i>Taq</i> ^a	95°C 5 min	95°C 2 min	45°C 30 min	72°C 2 min	30 x to step 2	72°C 2 min	4°C
pKV213	Platinum <i>Pfx</i> ^b	94°C 2 min	94°C 20 sec	53°C 40 sec	68°C 30 min	35 x to step 2	4°C	—
pKV219	Platinum <i>Taq</i> High Fidelity ^c	94°C 2 min	94°C 30 sec	52°C 30 sec	68°C 21 sec	35 x to step 2	68°C 21 sec	4°C

^aPromega

^bLife Technologies

FIG. 1. Plasmid map illustrating pKV204. Nucleotides 2666-3039 of *hmw1* were amplified by PCR, digested with *Bam*HI and *Hind*III , and ligated into *Bgl*II-and *Hind*III-digested pQE41 (Qiagen, Chatsworth, CA) to generate pKV204. The resulting recombinant allele encodes the C-terminus of HMW1 fused in frame to the C-terminus of mouse DHFR. *dhfr*, sequence encoding mouse DHFR; *hmw1'*, PCR generated 3' fragment of *hmw1*; *bla*, β -lactamase gene.

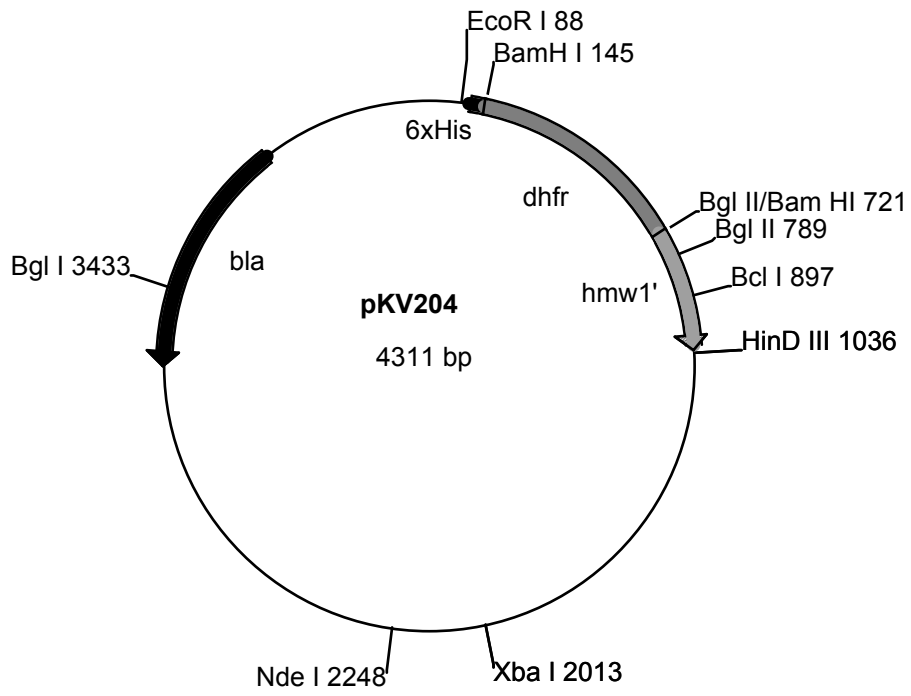
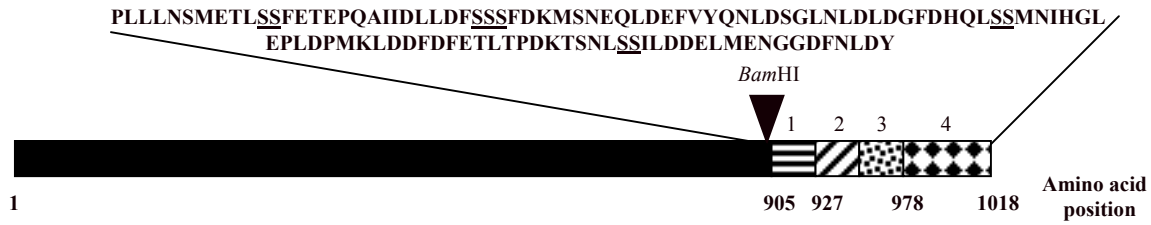


FIG. 2. Schematic diagram of HMW1 and recombinant HMW1 constructs. (A) HMW1 with the sequence of the C-terminal 112 amino acids shown above (double serines underlined) and the four regions of interest represented by striped, hatched, stippled and checkered boxes. Amino acid positions corresponding to each region are indicated below the diagram, and the *Bam*HI site is shown for reference. (B) HMW1 truncation/deletion derivatives depicting the region of HMW1 encoded by each construct. The plasmid containing each construct as well as the designation used for each recombinant protein is indicated to the right of the corresponding cartoon. Not to scale. (C) and (D) Schematic of relevant regions of plasmids pKV74 and pKV37, respectively. Bent arrow indicates the IS256 inward reading promoter. Not to scale. Restriction sites: E, *Eco*RI; B, *Bam*HI; K, *Kpn*I . Gm^r: Gentamicin resistance gene.

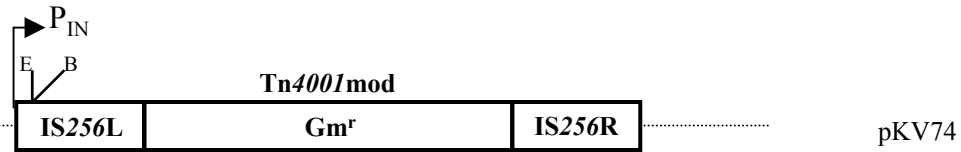
A.



B.



C.



D.

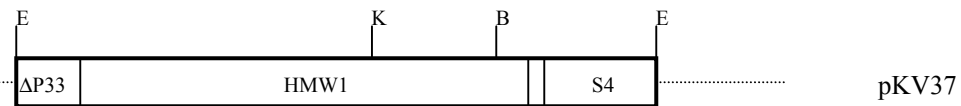


Fig. 2B). Plasmid pKV74 (Fig. 2C; Hahn *et al.*, 1998) contains a derivative of the Tn4001 engineered from plasmid pISM2062 (Knudtson and Minion 1993) in which the *Sma*I restriction site was replaced with an *Eco*RI site (Hahn *et al.*, 1998). pKV37 (Fig. 2D) contains the region of the *M. pneumoniae* chromosome encompassing the *hmw1* gene. pKV37 was digested with *Eco*RI and *Bam*HI to release a 3496-bp fragment encoding all but the last 112 amino acids of HMW1. This fragment was cloned into Tn4001 following digestion of pKV74 with *Eco*RI/*Bam*HI, to create pKV202 (Fig. 2), which served as the cloning vector for most of the deletion derivatives engineered for this study. Various segments of the 3' of *hmw1* were amplified by PCR using pKV37 as template DNA (Table 2; Table 3), digested with *Bam*HI, and ligated into pKV202 to generate pKV205, pKV213 and pKV219 (Fig. 2B). All downstream PCR primers introduced a *Bam*HI restriction site and an in-frame stop codon, except where the actual *hmw1* stop codon was present in the amplicon (Table 2). The upstream primer used to generate pKV219 introduced a *Bam*HI site (Table 2).

pKV203 was constructed using an alternate strategy whereby pKV37 was digested with *Eco*RI and *Kpn*I, and the 2598-bp fragment containing the 5' region of *hmw1* was isolated. Nucleotides 1783-2790 of *hmw1* were amplified via PCR, introducing an in-frame stop codon (Table 2; Table 3). This PCR product is flanked by *Kpn*I and *Bgl*II sites on its 5' and 3' ends, respectively, and was digested with both enzymes and ligated along with the *Eco*RI/*Kpn*I fragment isolated from pKV37 into *Eco*RI/*Bam*HI-digested pKV74. Electrocompetent *E. coli* Sure strain cells (Stratagene, La Jolla, CA) were transformed with plasmid DNA by standard methods (Sambrook *et*

al., 1989). Mycoplasma cells were transformed with plasmid DNA containing recombinant transposons as described previously (Hedreyda *et al.*, 1993).

Polymerase Chain Reaction.

The changing availability of polymerases necessitated the use of a variety of enzymes and programs for polymerase chain reaction (PCR) of plasmid inserts, as indicated in Table 3. The following program was used for mapping the transposon insertion in *hmw3::Tn4001mod* using chromosomal DNA from this strain as template: heat at 95°C for 5 min, denature at 95°C for 2 min, anneal at 50°C for 1 min, extend at 72°C for 1 min, repeat the last three steps 40 times, and extend at 72°C for 10 min. Sequencing of PCR products was carried out by the University of Georgia Molecular Genetics Instrumentation Facility as described elsewhere (Dirksen *et al.*, 1996). Sequences were analyzed using GCG software (Wisconsin Package version 10.1, Genetics Computer Group, Madison, WI).

Isolation of an *hmw3* Insertion Mutant.

In order to generate translational fusion between DHFR and region 4 of HMW1 (Fig. 2) an *EcoRI* linker (5'-ccggaattccgg-3') was ligated into the *SmaI* site of pQE41(Qiagen, Santa Clara, CA). The resulting plasmid was digested with *EcoRI* and 663 bp *EcoRI* fragment containing a ribosome binding site, 6 x His tag, and *dhfr* was isolated. This fragment was ligated into *EcoRI* digested pKV74 (Fig. 2) to generate pKV158. Plasmid pKV192 was generated by PCR amplification of regions 3 and 4 of *hmw1* (Table 2; Table3; Fig. 2) using pKV37 (Fig. 2) as template. The resulting PCR

fragment was gel purified (BIO101 GeneClean Spin Kit, Vista, CA) and ligated into the TA cloning vector pCR2.1 (Invitrogen, Carlsbad, CA) to generate pKV192. This plasmid was digested with *Bam*HI and *Sph*I. A 255 bp fragment was isolated and digested with *Bst*YI and *Sph*I. The resulting 142 bp fragment was isolated and ligated into *Bgl*III/*Sph*I digested pKV158 to generate pKV201. Thus, pKV201 contains a translational fusion between *dhfr* and region 4 of *hmw1*. This plasmid was transformed into wild-type *M. pneumoniae* and transformants were isolated as described above. A number of transformants were inoculated into liquid culture. After incubation at 37°C for 3 days I identified one transformant that poorly attached to the plastic tissue culture flask. Western blots revealed that this transformant lacked HMW1 (Fig. 3).

Isolation of *hmw3*::Tn4001mod Excision Revertants.

Strain *hmw3*::Tn4001mod was passaged 5 times in 5 mL Hayflick broth in the absence of gentamicin in 25-cm² tissue culture flasks. For each passage, cultures were grown to mid-log phase as indicated by the phenol red pH indicator, the spent medium was decanted, and the monolayer was washed three times with 10 mL cold PBS and gently scraped into 10 mL PBS. Twenty-five to 50 μ L of the cell suspension was then used to inoculate 5 mL of fresh Hayflick broth without gentamicin. Following the fifth passage, cells were washed and scraped as described above, and dilutions were plated on PPLO agar and incubated at 37°C for 7-9 days. Colonies were tested for hemadsorption, and ten hemadsorption-positive colonies were picked as described previously (Hedreyda and Krause 1995) and inoculated into 1 mL Hayflick broth. The resulting cultures were re-plated and tested for a hemadsorption-positive phenotype. Gentamicin sensitivity of

each isolate was tested by growth in Hayflick broth with or without gentamicin in 24-well tissue culture dishes. Production of HMW3 was monitored by SDS-PAGE as described below.

SDS-PAGE and Western Immunoblot Analysis.

M. pneumoniae cultures were harvested as described previously (Hahn *et al.*, 1996), and total protein was quantitated by the bicinchoninic acid assay (Pierce, Rockford, IL). Evaluation of the steady state levels of *M. pneumoniae* proteins and turnover of DHFR- Δ HMW1 in *E. coli* protease-deficient strains was based upon SDS-PAGE and Western immunoblotting as described previously (Hahn *et al.*, 1996), using anti-HMW3, 1:5,000 (Stevens and Krause 1992); anti-HMW1, 1:10,000 (Stevens and Krause 1991); anti-HMW2, 1:7,500 (Krause *et al.*, 1997); anti-P30, 1:3,000 (Jordan *et al.*, 2001); anti-B, 1:5000 (Sperker *et al.*, 1991); anti-P1, 1:1,000 (MAB134P, Maine Biotechnology Services, Inc.); anti-P65, 1:1,000 (Proft and Herrmann 1994); anti-P43 1:100 (provided by J.L. Jordan, University of Georgia); and anti-DHFR 1:200.

DHFR- Δ HMW1 Turnover Assays in *E. coli*.

Previous studies suggested that the C-terminus of HMW1 contains a proteolytic target sequence (Hahn *et al.*, 1996; Popham *et al.*, 1997). To determine the destabilizing capacity of the C-terminus of HMW1, we developed a construct encoding a DHFR- Δ HMW1 fusion protein and transformed it into a collection of *E. coli* strains carrying a variety of protease mutations for Lon, FtsH, and ClpP. Stability of the fusion protein was monitored in each strain as follows (modified from Leffers and Gottesman 1998). One

hundred μL was removed from a 2-mL overnight culture and pelleted. Pellets were used to inoculate 20-mL LB with glucose added to a final concentration of 2% for repression of the *lac* promoter. Cultures were grown to an ABS_{600} of 0.4-0.6 at 37°C. At this point the temperature was increased to 42°C in experiments with the temperature-sensitive strain SG22166 (*ftsH*). In all strains expression was induced for 2 min by the addition of 0.02% isopropyl- β -D-thiogalactopyranoside, then blocked with 700 $\mu\text{g/mL}$ spectinomycin. Five hundred μL samples were removed every 15 minutes, precipitated with 55 μL TCA on ice for 5 min, centrifuged for 5 min at 4 °C, suspended in 1 M Tris base and analyzed by SDS-PAGE and Western immunoblotting.

Triton X-100 Extraction.

Association with the cytoskeleton was assessed by fractionation with the nonionic detergent Triton X-100. Cell preparations were extracted with Triton X-100 (2% vol/vol) as described in detail previously (Balish *et al.*, 2001). Ten percent (vol/vol) trichloroacetic acid was added to the resulting detergent-soluble fractions, mixed and incubated on ice for 30 min to collect the detergent-soluble protein. Samples were centrifuged at 13,000 x g for 5 min and the supernatants discarded. Pellets were washed with 500 μL cold acetone and centrifuged as before. The supernatants were discarded, and pellets were air-dried, suspended in 1 M Tris base, combined with SDS-PAGE sample buffer, and analyzed by SDS-PAGE and Western immunoblotting.

Pulse-Chase Analysis of Recombinant HMW1 Derivatives.

Pulse-chase analysis was employed to assess the stability of newly synthesized HMW1 derivatives, as described previously (Popham *et al.*, 1997) with modifications. Briefly, 25-ml cultures were grown to mid-log phase and harvested, and the resulting pellets were suspended in 5 ml Dulbecco's Modified Eagle's Medium (DMEM) supplemented with 10% dialyzed fetal bovine serum (FBS) and all essential amino acids except methionine. Samples were incubated for 30 min at 37°C with [³⁵S] methionine at 67 µCi/ml (>1,000 Ci/mmol; 1 Ci = 37 GBq; Amersham, Piscataway, NJ), washed with 5 ml DMEM/FBS containing 1 mM methionine at 4°C, suspended in 3-ml fresh Hayflick medium by passage through a 25 gauge needle, and aliquoted into 1-ml portions. Aliquots were incubated at 37°C for the indicated time periods, at which point cell suspensions were centrifuged and washed three times with cold PBS (pH 7.2), then suspended in 200 µl TDSET (1% Triton X-100, 0.2% sodium deoxycholate, 0.1% SDS, 10 mM tetrasodium EDTA, 10 mM Tris-HCl, pH 7.8)/1 mM phenylmethylsulfonyl fluoride using a 25 gauge needle. After a 10-min incubation at 37°C, suspensions were centrifuged at 50,000 x g for 30 min at 4°C, and the supernatants were collected and analyzed by SDS-PAGE and autoradiography. It should be noted that the 0-h time point is loosely defined, given the time required to process the samples after the pulse.

Hemadsorption Analysis.

M. pneumoniae cultures were assessed qualitatively for hemadsorption as detailed elsewhere (Hahn *et al.*, 1996). Quantitative hemadsorption assays were performed as described by Fisseha *et al.* (1999) with modifications. *M. pneumoniae* cultures were

inoculated from frozen stocks into 15 mL Hayflick broth containing 200 μCi [^3H]thymidine (6.7 Ci/mmol; Dupont NEN, Boston, MA) and incubated at 37°C to mid-log phase. Cells were harvested, washed twice in cold PBS (pH 7.2), and suspended in 3 mL Hayflick broth by repeated passage through a 25-gauge needle. Suspensions were centrifuged for 5 min at 123 x g in a clinical centrifuge (International Equipment Company, Needham Heights, MA) to remove any remaining aggregates. Six 100- μL aliquots were removed; three were incubated at 4°C and three were incubated at 37°C, each for 30 min. A 1:1 suspension of fresh chicken erythrocytes in Alsever's solution was washed twice with phosphate buffered saline (PBS, pH 7.2) and then the erythrocytes were suspended in PBS (pH 7.2) to 4% (vol/vol). Fifty microliters of the 4% red blood cell suspension was added to each 100- μL aliquot of *M. pneumoniae* cells and incubated at 4°C or 37°C for an additional 30 min. The *M. pneumoniae*/erythrocyte mixtures were then overlaid onto 150 μL of 40% sucrose and centrifuged at 1690 x g for 90 sec. The resulting pellets were suspended in 100 μL PBS, 10 μL 10% SDS was added, and the incubation was continued overnight at room temperature. The following day, 5 μL H_2O_2 was added, and samples were incubated an additional 2 h at 37°C, after which, scintillation fluid was added and radioactivity was measured.

Microscopy.

Mycoplasma cell pellets from 25-mL cultures were suspended in fresh Hayflick medium, passed repeatedly through a 25-gauge needle to disperse the cells, and filtered (1.2 μm pore diameter) to remove aggregates. The suspensions were used to inoculate 24-well dishes containing either Formvar-coated, carbon-coated nickel grids (for

antibody labeling and transmission electron microscopy [TEM]) or glass coverslips (for scanning electron microscopy [SEM]). Grids and coverslips were precoated with poly-L-lysine (Stevens and Krause 1992), to promote attachment of the mutants to these surfaces, and UV sterilized. After incubation of the cultured for 1 to 4 hours at 37°C, grids and coverslips were removed and processed for fixation and antibody labeling (Stevens and Krause 1991; Stevens and Krause 1992). Briefly, grids and coverslips were rinsed with washing buffer [25 mM HEPES (N-[2-Hydroxyethyl]piperazine-N'-[2-ethanesulfonic acid])-0.8% NaCl (pH 7.4)], and transferred to fixative (1% paraformaldehyde, 1% glutaraldehyde, 0.1% picric acid, 0.1 M cacodylic acid [pH 7.4]) for 1 h at 4°C. Next, for SEM, coverslips were rinsed twice with washing buffer and once with 0.1 M sodium cacodylate buffer (pH 7.4). Coverslips were then treated sequentially (10 min each) with 30, 50, 70, 85, and 95% ethanol; treated twice with 100% ethanol; and critical point dried. Chromium was evaporated over the samples, which were then examined with a LEO 982 field emission SEM. For TEM, grids were rinsed with washing buffer and blocked in 4% calf serum in 0.2 M Tris-HCl (pH 8.2)-0.8% NaCl for at least 30 minutes at room temperature in a moisture chamber. The primary antibody was mouse monoclonal anti-P1 immunoglobulin (MAB134P, Maine Biotechnology Services, Inc.), which was used at a dilution of 1:75 to 1:500 overnight at 4°C. The secondary antibody was 10-nm-diameter colloidal gold-conjugated goat anti-mouse immunoglobulin (Amersham, Arlington Height, IL), which was used at a dilution of 1:10. Grids were rinsed well with washing buffer, counterstained in 2% aqueous urinal acetate, and examined with a JEOL 100CX II TEM.

Cells were prepared for fluorescence microscopy as previously described (Jordan *et al.*, 2001) and examined using a Nikon TE300 epifluorescence microscope with a tetramethyl rhodamine isothiocyanate filter cube (528 to 552 nm) and equipped with phase-contrast optics. Samples were probed with P65-specific antibodies diluted 1:100 and indocarbocyanine (Cy3)-conjugated donkey anti-rabbit immunoglobulin G antibody (Jackson ImmunoResearch Laboratories, West Grove, PA) diluted 1:75, and images were digitized using a Micromax CCD camera (Princeton Scientific Instruments, Monmouth Junction, N.J.) with an exposure time of 0.1 s for phase contrast images and 0.5 s for fluorescent images.

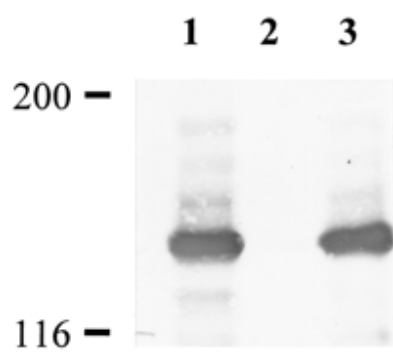
For ultrastructural examination, 50-mL mid-log phase cultures were harvested by gently scraping adherent cells into the spent medium and centrifuging at 20,000 x g for 20 min at 4°C. After three washes in cold PBS, the cells were divided into two 1.5-mL Eppendorf tubes. Subsequent washes were done in Sorensen's phosphate buffer (pH 7.2) (Bozzola and Russell 1992). Samples were fixed 1 h at 4°C in 2% glutaraldehyde/2% paraformaldehyde, washed overnight at 4°C and washed two more times for 30 min each the following day. Samples were then post-fixed in 1% OsO₄ 1 h at room temperature, washed twice, 3 min each, and dehydrated by transfer through a series of ethanol concentrations (30, 50, 70, 85, 95, 100, and 100%), 10 min each, followed by two 15-min incubations in propylene oxide. Samples were incubated overnight in 1:1 propylene oxide:Epon 812 at room temperature followed by 2 h in 100% Epon 812, and embedding in Epon 812 for 24 h at 60°C. Thin sections were cut with a diamond knife and collected on formvar-coated nickel grids. Grids were stained in 2% aqueous uranyl acetate-4.4% lead citrate before examination.

CHAPTER III
FUNCTIONAL ANALYSIS OF HMW3
RESULTS AND DISCUSSION

Identification of an *hmw3* Insertion Mutant.

As part of a separate study wild-type *M. pneumoniae* was transformed with pKV201, a derivative of the modified Tn4001 containing pISM2062 (Knutson and Minion 1993) into which a translational gene fusion encoding mouse dihydrofolate reductase (DHFR) and a very small fragment of *hmw1* had been cloned. Gentamicin-resistant transformants were isolated from agar plates and inoculated into Hayflick broth. With one transformant cells were observed floating in the growth medium as well as attached to the flask, suggesting that cytoadherence was impaired. Significantly, this phenotype was unique to this particular transformant; all other transformants examined attached normally to plastic, suggesting that the loss of attachment was insertion-site specific. Western blots of this transformant probed individually with antisera against various cytoadherence-associated proteins indicated that HMW3 was completely absent (Fig. 3), raising the possibility of a fortuitous transposon insertion within or near the *hmw3* gene. The original focus of this transformation, the DHFR fusion protein, was not detected in Western blots (data not shown) and is thought to be extremely unstable or not expressed.

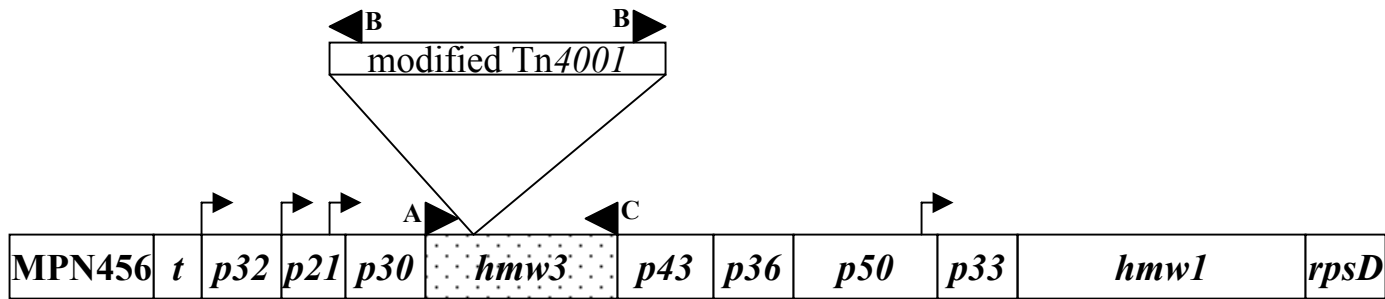
FIG. 3. Western immunoblot analysis of *M. pneumoniae* with anti-HMW3 serum. Equal amounts of total protein were electrophoresed on an SDS-4.5% polyacrylamide gel, transferred to nitrocellulose, and probed with antisera (1:10,000). Lanes: 1, wild-type *M. pneumoniae*; 2, *hmw3::Tn4001*mod transformant; 3, transformant control (modified *Tn4001* transposon inserted elsewhere). Protein size standards are indicated in kilodaltons.



Following filter cloning of this transformant to ensure a clonal population, I verified the site of transposon insertion by PCR amplification and nucleotide sequencing. *Mycoplasma* cells were harvested, and DNA was isolated as described elsewhere (Wenzel and Herrmann 1988). The transposon insertion was localized to the 5' end of *hmw3* by PCR of genomic DNA from the transformant with three primers that I designed for this purpose (Fig. 4). Primer A was complementary to a sequence immediately upstream of *hmw3*, primer C was complementary to the 3' end of *hmw3*, and primer B was complementary to the inverted repeat of the IS element of Tn4001 (Byrne *et al.*, 1989). The estimated size of PCR products generated using primer combinations A/B and B/C and analyzed by agarose gel electrophoresis approximated position of the insertion within *hmw3*. Sequencing of a PCR product generated using primer pair A/B localized the insertion precisely between nucleotide 267 and 268 in the *hmw3* coding region. Analysis of the composite sequence *hmw3*::Tn4001mod revealed an in-frame stop codon 13 bp into the IS element of the transposon. I did not detect a truncated HMW3 protein on Western blots probed with polyclonal antibodies prepared against full-length HMW3 (data not shown).

Several scenarios could account for the failure to isolate an *hmw3* mutant in prior studies (Hedreyda and Krause 1995; Krause *et al.*, 1982). The most likely explanation, however, is that mutations affecting cytoadherence were identified previously by screening for complete loss of attachment (Baseman *et al.*, 1982b), in some cases including enrichment steps for non-adherent cells (Hedreyda and Krause 1995). Loss of HMW3 resulted in only a partial reduction in cytoadherence, hence *hmw3* mutants might have been overlooked in those studies. Significantly, a 1999 study in which *M. pneumoniae*

FIG. 4. Schematic of the *hmw* operon (Dirksen, *et al.*1996;Tully1983) illustrating the point of insertion of the transposon into *hmw3* (shaded). Arrowheads indicate the positions of primers used for PCR analysis. Arrows indicate the positions of the promoters within the operon. Insertion of the transposon immediately downstream of nucleotide 267 was determined by sequencing the PCR product generated using primer pair A/B. The diagram is not drawn to scale.



hmw operon

and *Mycoplasma genitalium* were both subjected to global transposon mutagenesis yielded a transposon insertion in the *M. genitalium hmw3* homologue (Hutchison *et al.*, 1999), hinting that this protein is dispensable *in vitro* at least in *M. genitalium*, and by correlation in *M. pneumoniae*.

Only the Steady State Level of P65 is Reduced in the Absence of HMW3.

I examined the consequences of loss of HMW3 on the steady-state levels of other cytoadherence-related proteins. Western blots were prepared and probed with antisera directed against cytoadherence-associated proteins HMW1, HMW2, B, P65, and P30 (Fig. 5) as well as P1 and P28 (data not shown). Examination of these blots revealed wild-type levels of all proteins tested except P65, which was decreased in the *hmw3::Tn4001mod* transformant to nearly the same level as that seen in the *hmw2* mutant I-2 (Fig. 5). Levels of all proteins examined including P65 were indistinguishable in wild-type *M. pneumoniae* and a transformant thereof having *Tn4001mod* inserted elsewhere (Fig. 5).

The gene for HMW3 is part of a large transcriptional unit (Waldo *et al.*, 1999) (Fig. 4) and is followed immediately by and possibly transcriptionally linked to the gene for P43 (Dirksen *et al.*, 1996). To determine whether transposon insertion in *hmw3* might have polar consequences, we compared P43 levels in wild-type *M. pneumoniae* and the *hmw3::Tn4001mod* transformant by Western immunoblotting. No decline in P43 levels was evident (Fig. 6), indicating that the gene for P43 is expressed in this mutant, probably from an outward-reading promoter in the IS element of *Tn4001* (Byrne *et al.*, 1989).

FIG. 5. Western immunoblot analysis of *M. pneumoniae* to assess steady-state levels of certain cytoadherence-associated proteins. Equal amounts of protein were electrophoresed on either a 4.5% (A, B, and D) or a 10% (C and E) polyacrylamide gel, transferred to nitrocellulose, and probed with the following antisera: A, anti-HMW1; B, anti-HMW2; C, anti-P30; D, anti-B; E, anti-P65. Lanes: 1, wild-type, *M. pneumoniae*; 2, *hmw3::Tn4001*mod transformant; 3, transformant control; 4, (panel E only), mutant I-2. Protein size markers are given in kilodaltons to the left of each blot, and arrowheads designate proteins of interest.

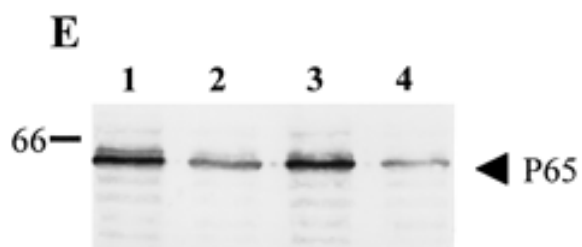
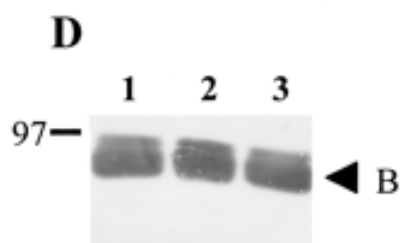
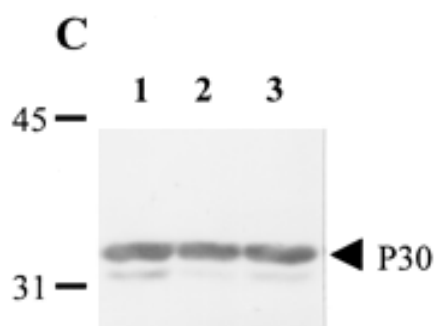
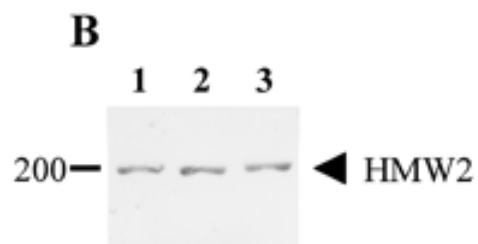
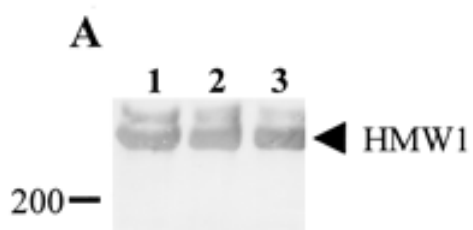
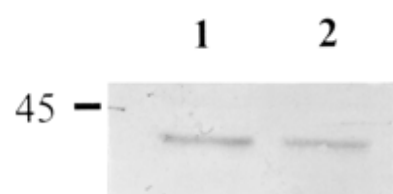


FIG. 6. Western immunoblot analysis of *M. pneumoniae* to compare levels of protein P43. Equal amounts of protein were electrophoresed on a 12% polyacrylamide gel, transferred to nitrocellulose, and probed with antisera (1:100). Lanes: 1, wild-type *M. pneumoniae*; 2, *hmw3::Tn4001*mod transformant. The protein size standard is indicated in kilodaltons.



Many *M. pneumoniae* cytoadherence-associated proteins identified to date exhibit a stabilizing interdependency, most likely reflecting a complex web of interactions (Krause and Balish 2001). For example, loss of HMW2 results in accelerated turnover of several proteins including P65, which is encoded by the gene immediately upstream of *hmw2* (Krause *et al.*, 1997), and HMW1 and HMW3 (Popham *et al.*, 1997), proteins encoded by the *hmw* operon, quite some distance from *hmw2*. Similarly, the loss of HMW1 is associated with reduced levels of HMW3, HMW2 (Willby *et al.*, in preparation) and P65 (Jordan *et al.*, 2001). However, loss of HMW3 in the *hmw3::Tn4001*mod transformant affected only the level of P65. Significantly, reduction in the level of HMW3 was the single common denominator for decreased levels of P65 in *hmw1*, *hmw2*, and *hmw3* mutants, suggesting a role for HMW3 in P65 stabilization, and expanding the functional relationship between the protein products of the two operons. However, HMW3 is not sufficient to stabilize P65, as defects involving protein P30, encoded by the gene preceding *hmw3*, do not affect levels of HMW3 but result in diminished P65 levels (Jordan *et al.*, 2001; Krause and Balish 2001). Therefore, both HMW3 and P30, encoded by adjacent genes in the *hmw* operon, are likely required for stabilization of P65. Furthermore, this correlation between the levels of HMW3 and P65 may indicate a physical interaction between these two proteins that stabilizes P65 within the attachment organelle.

Morphology and Ultrastructure are Aberrant in HMW3-Deficient Cells.

Wild-type *M. pneumoniae* cultures are typically pleomorphic, with the predominant morphology an asymmetric spindle with a polar attachment organelle (Fig.

7). The spindle shape results from the presence of a distended area (cell body) adjacent to the attachment organelle, with a width approximately 2-3 times that of the flanking filaments. Cells of the *hmw3::Tn4001mod* transformant were also pleomorphic (Fig. 7) but distinct from wild-type populations. In particular, the prototypical, filamentous wild-type morphology was much less common in the *hmw3* mutant population. The most striking morphological feature of this mutant was the unusually large number of cells having multiple branches or greater than one distended area. The transformant control containing the modified *Tn4001* in another site on the chromosome was morphologically indistinguishable from wild-type *M. pneumoniae* (Fig. 7).

The characteristic ultrastructural feature of wild-type *M. pneumoniae* cells is the electron-dense core that defines the attachment organelle (Fig. 8A, B). This core structure terminates in a bulbous knob and can be easily identified in thin sections of wild-type cells (Biberfeld and Biberfeld 1970). Studies using immunoelectron microscopy localized HMW3 to this knob and along the shaft of the electron dense core (Stevens and Krause 1992). Somewhat surprisingly, despite the loss of HMW3 in the *hmw3::Tn4001mod* mutant, many cells contained wild-type-like cores, with a single electron-dense rod (Fig. 8C). However, in at least 20% of the cells the core was not seen as a single electron-dense rod as it was in 100% of the wild-type cells, but rather was V-shaped with the vertex distal, suggesting spreading at the base of the core and a potential role for HMW3 in holding the core together (Fig. 8D, arrowhead).

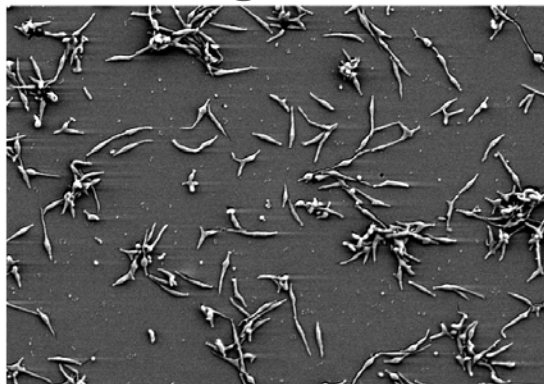
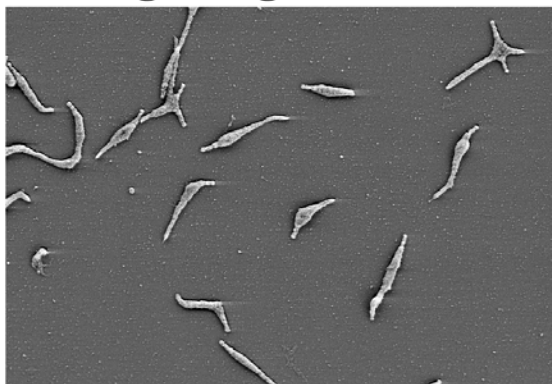
Thus, the *hmw3* mutant is striking morphologically and ultrastructurally. While the classic, wild-type spindle morphology was not completely absent in *hmw3::Tn4001mod* cultures (Fig. 7), most cells had multiple branches and numerous distended areas.

FIG. 7. Morphological analysis of wild-type (A), transformant control with Tn4001mod inserted elsewhere (B), and *hmw3::Tn4001mod* (C) *M. pneumoniae* by SEM. A high-magnification image is shown on the left, and a lower-magnification survey shot is shown on the right so that individual cells, as well as populations of cells, can be examined.

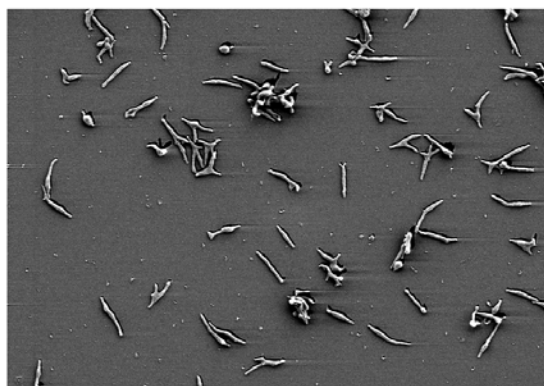
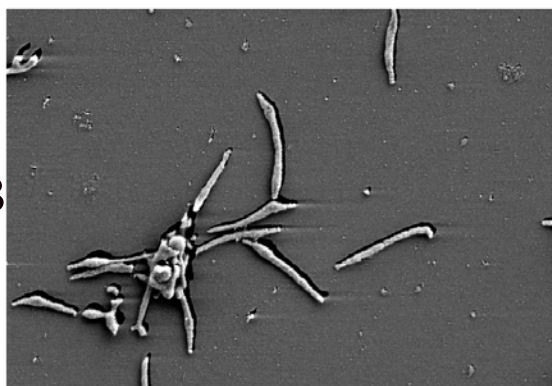
high magnification

low magnification

A



B



C

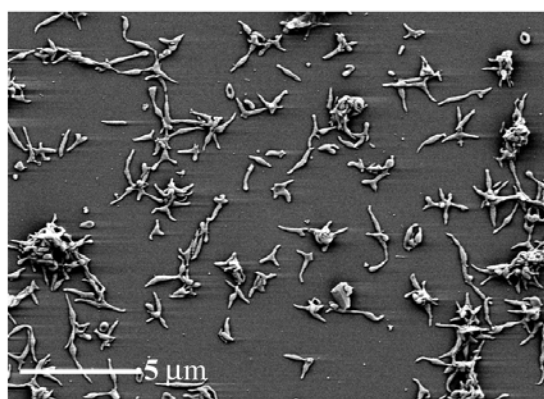
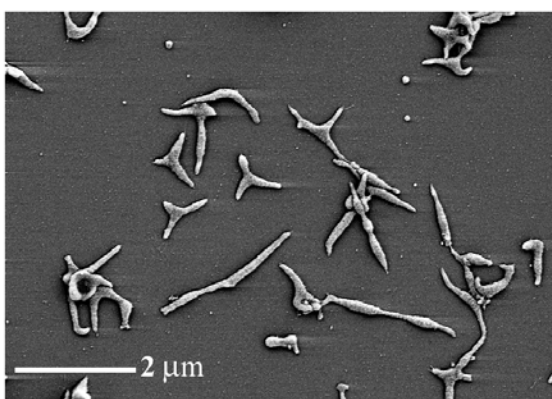
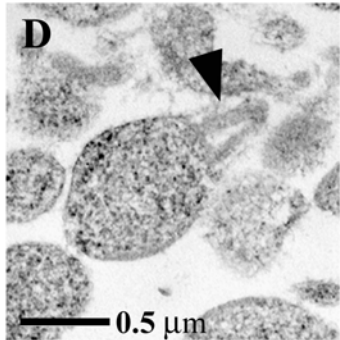
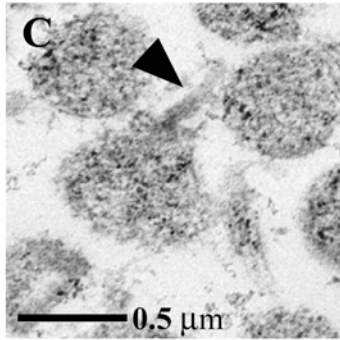
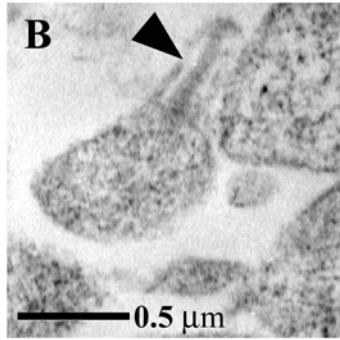
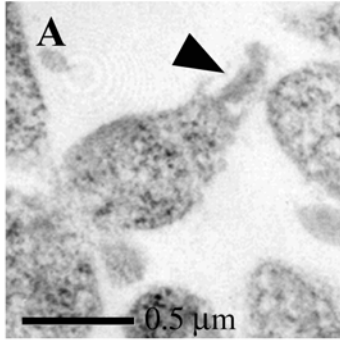


FIG. 8. Transmission electron microscopic analysis of thin sections of *M. pneumoniae* cells showing the electron-dense core (arrowheads). (A) wild-type *M. pneumoniae*, (B) transformant control, (C) *hmw3::Tn4001mod* transformant with wild-type core, (D) *hmw3::Tn4001* transformant with altered core.



Branched cells are a common feature of cell division abnormalities in *E. coli* and other bacteria (Akerlund *et al.*, 1993) and might indicate a similar consequence of loss of HMW3. Significantly, defects in P30, the gene for which precedes the gene for HMW3, likewise result in a branched morphology (Romero-Arroyo *et al.*, 1999), as does loss of other cytodherence proteins (Hahn *et al.*, 1998; Romero-Arroyo *et al.*, 1999; Seto *et al.*, 2001). The electron-dense cores observed in thin sections of *hmw3::Tn4001*mod cells in many cases appeared similar to those of wild-type cells (Fig. 8). Due to the nature of sectioning such small organisms, it is difficult to determine in cells with multiple branches whether more than one branch contains a core, so I could not assess whether the increased number of branches in the HMW3 mutant correlates with an increased number of cores. However, V-shaped cores were also identified in the mutant and these might actually represent a cross-section of a cone. V-shaped cores accounted for approximately 20% of the cores seen in the *hmw3::Tn4001*mod transformant. It is likely that this number is an underestimation of the actual number of abnormal cores present in the mutant since the sectioning process is arbitrary and the ability to distinguish V-shaped cores depends on the plane through which the cell is sectioned. Regardless, cores with this appearance have not been reported in wild-type cells or other mutants, suggesting that loss of HMW3 promotes a defect either in core structure or in the regulation of core construction. Previous studies indicated that polymers of HMW3 might surround the core and the terminal button in a linear pattern (Stevens and Krause 1992), possibly serving to stabilize this structure. In the absence of HMW3 the core may be less stable, leading to the V- or possibly cone-shape. Alternatively, this shape may reflect a change in the frequency at which new cores form prior to cell division, as formation of a second

attachment organelle is thought to be an early step in this process (Boatman 1979b; Stevens and Krause 1992).

Loss of HMW3 Results in an Intermediate Cytadherence Phenotype.

Adsorption of erythrocytes by *M. pneumoniae* (hemadsorption) correlates strongly with adherence to the respiratory epithelium (Sobeslavsky *et al.*, 1968) and was assessed qualitatively and quantitatively in the *hmw3* mutant (Fig. 9). Qualitative examination revealed that the majority of *hmw3::Tn4001mod* transformant colonies had erythrocytes attached only around their periphery (Fig. 9C), whereas wild-type (Fig. 9A) and transformant control colonies (*Tn4001mod* inserted elsewhere; data not shown) were uniformly coated with erythrocytes, and colonies of the nonadherent mutant II-3 had no attached erythrocytes (Fig. 9B). Results from the quantitative assay indicated an intermediate level of hemadsorption by the *hmw3::Tn4001mod* transformant ($22 \pm 5.3\%$ of wild-type), compared with $0 \pm 3.3\%$ of wild-type for the negative control (mutant II-3) and $108 \pm 6.1\%$ of wild-type for the transformant control. The intermediate hemadsorption phenotype of *hmw3::Tn4001mod* is consistent with the qualitative hemadsorption findings as well as the original observation that these cells adhered only poorly to the plastic tissue culture flask.

P1 and P65 have Altered Localization Patterns in the Absence of HMW3.

The adhesin protein P1 localizes primarily to the attachment organelle in wild-type *M. pneumoniae* (Fig. 10A) (Baseman *et al.*, 1982b; Feldner *et al.*, 1982; Hu *et al.*, 1982). Immunogold labeling was used to examine P1 localization in the

FIG. 9. Qualitative hemadsorption assay of wild-type (A), cytadherence mutant II-3 (B), and *hmw3::Tn4001*mod transformant (C).

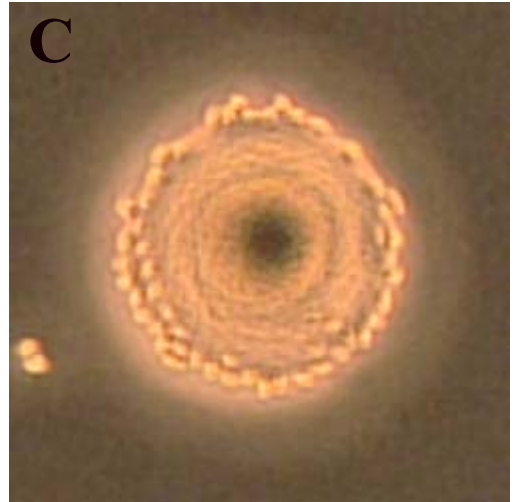
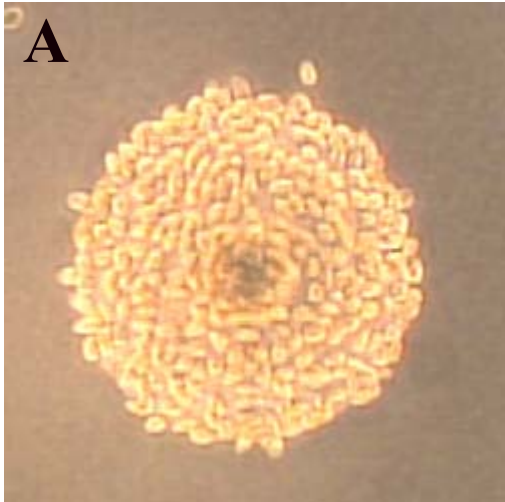
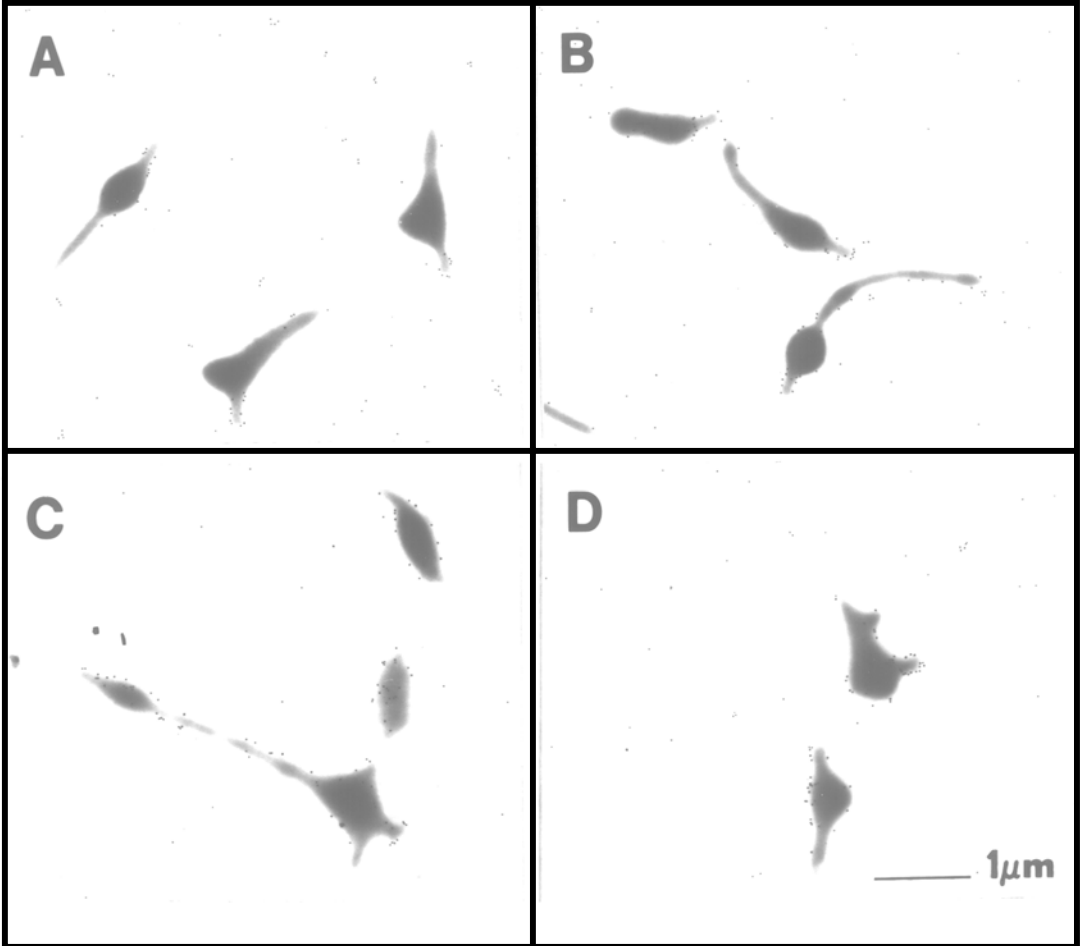


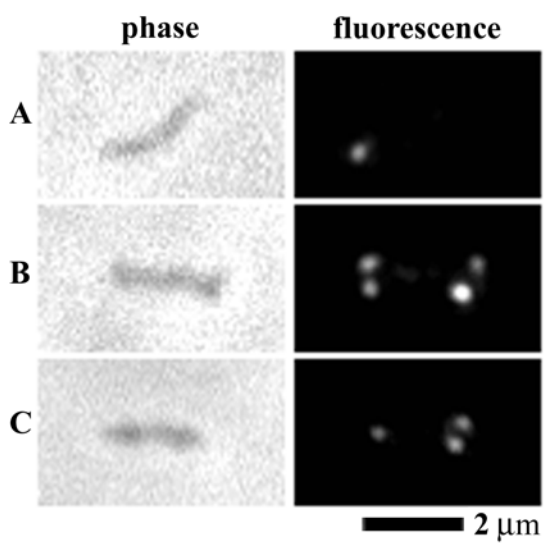
FIG. 10. Distribution of protein P1 on wild-type and transformant *M. pneumoniae* cells. (A) wild-type *M. pneumoniae*, (B) transformant control, (C and D) *hmw3::Tn4001*mod transformant.



*hmw3::Tn4001*mod transformant. Due to the abnormal morphology of the mutant it was often difficult to identify attachment organelles with complete certainty, yet some cells exhibited a local concentration of P1 on one or two branches in addition to the P1 scattered on the rest of the cell (Fig. 10D). However, this pattern was the exception and was only seen in approximately 10% of *hmw3::Tn4001*mod cells compared with approximately 60% of wild-type cells. In a majority of *hmw3::Tn4001*mod cells, the labeling was dispersed along the cell surface (Fig. 10C). No obvious correlation was apparent between presence or absence of P1 clustering and cell morphology. Some cells morphologically similar to prototypical wild-type cells exhibited no attachment organelle-localized P1, while other cells that were morphologically irregular exhibited P1 clustering. The transformant control was indistinguishable from wild-type cells (Fig. 10B).

Recent studies reported localization of P65 to the attachment organelle of wild-type *M. pneumoniae* using immunofluorescent labeling (Jordan *et al.*, 2001; Seto *et al.*, 2001). P65 is predicted to be incorporated late in the assembly of this structure (Krause and Balish 2001). Additionally, the data revealing reduced levels of P65 concurrent with loss of HMW3 suggest an interaction between these two proteins. Therefore, I examined whether loss of HMW3 had consequences on the localization of P65 (Fig. 11). Cells were labeled with anti-P65 antibody and a fluorescent secondary antibody and examined by fluorescence/phase contrast microscopy. *hmw3::Tn4001*mod transformant cells generally had a minimum of one fluorescent focus (usually polar) with patchy fluorescence on the rest of the cell (Fig. 11B) similar to the patchy labeling pattern of

FIG. 11. Localization of P65 protein in wild-type *M. pneumoniae* (A), mutant I-2 (B), and an *hmw3::Tn4001*mod transformant (C). On the left are individual cells viewed by phase-contrast microscopy, and on the right are the corresponding fluorescent images. The contrast was adjusted to compensate for protein levels among the strains (see Table 1).



mutant class I cells (Jordan *et al.*, 2001). This is in contrast to the exclusively polar labeling observed with wild-type cells and the transformant control (Fig. 11A, C).

The major adhesin P1 is concentrated at the attachment organelle but present to a lesser extent along the rest of the wild-type *M. pneumoniae* cell (Baseman *et al.*, 1982b; Feldner *et al.*, 1982; Hu *et al.*, 1982). The clustering of P1 presumably enhances attachment of the bacterium to host cells. The loss of cytoadherence-accessory protein HMW1 or HMW2 affects the ability of P1 to localize properly (Baseman *et al.*, 1982b; Hahn *et al.*, 1998). Likewise, while some cells of the *hmw3::Tn4001*mod transformant showed clustered P1 on branches, most did not, a finding that is consistent with poor adherence to plastic and an intermediate hemadsorption phenotype. It is difficult to know whether these rare clusters of P1 are significant since it is possible that in cells with randomly distributed P1, local concentrations of the adhesin could occur by chance along the length of the cell. HMW3 is thought to associate with the cytoplasmic surface of the cell membrane of the attachment organelle with no exposure on the mycoplasma cell exterior (Stevens and Krause 1992). Therefore, while HMW3 does not appear to play a direct role in attachment, loss of HMW3 results in defective P1 localization and consequently the dramatic decline in attachment efficiency as revealed by qualitative and quantitative hemadsorption assays.

It is reasonable to assume that the interactions among cytoadherence-associated proteins not only serve to stabilize one another, but also assist in achieving and maintaining the appropriate distribution of these proteins within the cell. Recent studies using fluorescence microscopy have shown that P65 is localized to a single pole in wild-type *M. pneumoniae* cells (Jordan *et al.*, 2001; Seto *et al.*, 2001), the same pole at which

P1 is found (Seto *et al.*, 2001). These studies also showed wild-type localization of P65 in mutants in cytoadherence proteins A, B, C, P1 and P30, but patchy distribution of P65 in mutants with absent or reduced levels of HMW1, HMW2 and HMW3 (mutants I-2 and M6; Jordan *et al.*, 2001). In the current study, in the absence of HMW3, P65 was not confined to a single focus. Patches of P65 were dispersed throughout the cell, though often with a dense cluster still identifiable at a pole. Therefore, wild-type levels of HMW1 and HMW2 alone are not sufficient for proper localization of P65; HMW3 is also required. In contrast, preliminary studies reveal HMW1 consolidated in a discrete focus in the *hmw3::Tn4001mod* transformant (data not shown) as is seen with wild-type cells (Seto, *et al.* 2001; Stevens and Krause 1991).

Isolation and Characterization of *hmw3::Tn4001mod* Excision Revertants.

The *hmw3::Tn4001mod* transformant was passaged five times in the absence of gentamicin; resulting colonies that were gentamicin-sensitive regained the ability to adsorb erythrocytes, implying excision of the transposon. Gentamicin-sensitive, hemadsorption-positive colonies were selected and cultured in Hayflick broth. All putative excision revertants analyzed by Western immunoblotting regained wild-type levels of full-length HMW3 (data not shown). One revertant was characterized further. DNA sequencing of the *hmw3* gene confirmed precise excision of the transposon, consistent with reacquisition of HMW3. Likewise, this revertant exhibited a characteristic wild-type phenotype with respect to protein profile, hemadsorption, cell morphology, and P1 and P65 localization (data not shown), establishing a clear

correlation between insertional inactivation of *hmw3* and the altered phenotype described here.

Summary.

Studies based on the *hmw3::Tn4001mod* mutant have advanced our understanding of *M. pneumoniae* on two related fronts. First, we examined more directly the function of HMW3, and secondly, we were able to lend weight to the model of attachment organelle assembly proposed by Krause and Balish (2001). Based on this model, proteins are incorporated into the attachment organelle via one of two pathways. Proteins HMW2, HMW1, HMW3, P30 and P65 follow one pathway and stabilize one another as they associate with the nascent attachment organelle. In this study we showed that HMW1 was stable in the absence of HMW3, suggesting that it precedes HMW1 in incorporation into the nascent attachment organelle. P65 is neither stable in the absence of HMW3, nor is it properly localized (Fig. 5; Fig. 11), supporting the theory that P65 is incorporated into the attachment organelle after both HMW1 and HMW3. P1, on the other hand, was only occasionally found in polar clusters in *hmw3::Tn4001mod* cells (Fig. 10). Krause and Balish propose that P1 is incorporated into the attachment organelle via a separate pathway from HMW1 and HMW3 (Krause and Balish 2001). The two pathways intersect in the attachment organelle where proteins from each pathway likely interact resulting in a functional structure. Its association with the attachment organelle, cytoskeleton and cell membrane positions HMW3 to secure interactions with proteins found in each of these sites, for instance maintaining localization of P1 to the attachment organelle and holding together the electron-dense

core. Consistent with this hypothesis is the apparent ability of HMW3 to exist in multimeric form or as part of a complex of proteins (Stevens and Krause 1992), as HMW3 released from cells extracted sequentially with Triton X-100 and potassium iodide takes the form of clusters and chains (Stevens and Krause 1992). Furthermore, while HMW3 is a peripheral membrane protein, it pellets with alkali-treated cell membranes (Balish and Krause, unpublished data), suggesting that it is highly insoluble, perhaps attributable to its presence within a complex of proteins.

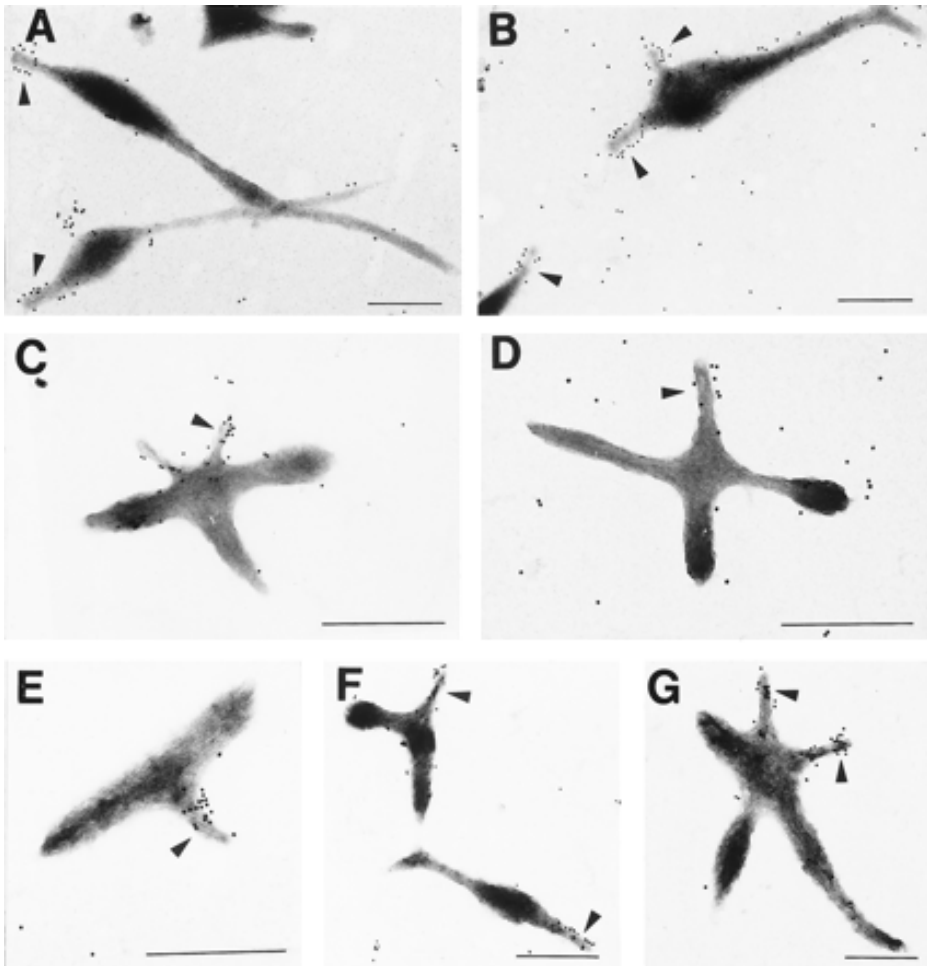
I hypothesize that HMW3 is not essential for formation of the attachment organelle, but as one of the early proteins incorporated into this structure it may be required for proper timing of its duplication or for stabilization or maintenance of its structure. Additionally, the attachment organelle is believed to function in adherence, motility and cell division. The absence of HMW3 resulted in an intermediate hemadsorption phenotype. Colonial morphology of *M. pneumoniae* strains grown on soft agar with a liquid overlay has been correlated with presence or absence of motility in *M. pneumoniae* strains (Jordan and Krause submitted). I observed the *hmw3::Tn4001*mod transformant under these conditions and, based on preliminary observations believe that this mutant has very limited motility in the absence of HMW3. Furthermore, the ultrastructural and morphological abnormalities associated with loss of HMW3 suggest a defect in cell division, a conclusion supported by the fact that HMW3 is located in the region of the cell where early steps in cell division are thought to occur. Thus, loss of HMW3 has effects on all of the functions thought to be associated with the attachment organelle, underscoring its fundamental importance.

CHAPTER IV
STRUCTURE-FUNCTION ANALYSIS OF HMW1
RESULTS AND DISCUSSION

Altered Morphology and P1 Localization in the Absence of HMW1.

The absence of wild-type levels of proteins HMW1-HMW3 in mutant I-2 confers an altered morphology, and P1 is not localized at the attachment organelle (Baseman *et al.*, 1982b). However, it was impossible to determine which of the absent proteins was responsible for these defects. The more recently isolated M6 mutant lacks HMW1 and produces a truncated P30 (Table 1) making it a viable tool for assessing the phenotypes associated with loss of HMW1 (Layh-Schmitt *et al.*, 1995). However, in order to use this mutant to study HMW1 function, the effects, if any, of truncation of P30 must be determined. Two P30 mutants have been isolated. Mutant II-3 is completely deficient in P30, but mutant II-7 expresses a C-terminally truncated P30 protein identical to that in mutant M6 (Dallo *et al.*, 1996; Krause *et al.*, 1982). Previous morphological analysis of these mutants showed that while mutant II-3 has an abnormal, branched morphology mutant II-7 exhibits a near wild-type morphology (Romero-Arroyo *et al.*, 1999). We used monoclonal P1 antibodies and immunogold labeling to address P1 localization in each of these isolates. Mutant II-7 localized P1 properly (Fig. 12E to G). Moreover, in spite of its altered morphology, mutant II-3 appeared to cluster P1 specifically on one or rarely two branches (Fig. 12C and D). Thus, these studies suggest that the truncated P30

FIG. 12. Immunogold labeling of wild-type *M. pneumoniae* (A and B) and mutants II-3 (C and D) and II-7 (E to G) with monoclonal anti-P1 antibodies (1:75 dilution). Arrows indicate likely attachment organelles. Scale bar, 0.5 μm .



produced in mutant M6 should have little or no effect on morphology or P1 localization and that mutant M6 can be used to assess the role of HMW1 in these phenotypes.

SEM examination of mutant M6 revealed a distinctly non-wild-type morphology (Fig. 13B). While wild-type cells were long and filamentous (Fig. 13A), M6 cells were short, broad and often branched with multiple distended areas (Fig 13B). Furthermore, wild-type cells had a characteristic tapering at the attachment organelle, but all poles were rounded in M6 cells making visual identification of an attachment organelle impossible. Transformation of M6 cells with recombinant full-length *hmw1*, but not *p30* (Hahn *et al.*, 1998) restored a near wild-type morphology (Fig. 13C, D) lending weight to the conclusion that HMW1 is required for wild-type cell shape.

The function of HMW1 in localization of P1 to the attachment organelle was addressed by analysis of P1 distribution in M6 cells by immunogold labeling. P1 was scattered across the entire surface of M6 cells (Fig 14C). The same labeling pattern was generally seen on M6 cells transformed with recombinant *p30* (Fig 13F) (Hahn *et al.*, 1998), while M6 cells transformed with recombinant *hmw1* (Fig 12E; Hahn *et al.*, 1998) had more wild-type like P1 distribution. Quantitative assessment of P1 distribution was accomplished by counting gold particles on 70-90 cells, categorizing them as either polar or not polar and averaging counts for each category. M6 mutant cells had approximately 3-fold greater numbers of gold particles in the nonpolar category compared with the polar category (3.7 versus 13.9 particles per cell, respectively). However, wild-type *M. pneumoniae* and mutant M6 transformed with *hmw1* had more polar than nonpolar gold particles (8.3 and 7.5 versus 5.6 and 6.0 particles per cell, respectively). These data were analyzed statistically by one-way analysis of variance and the Student-Newman-Keuls

FIG. 13. SEM analysis of wild-type, mutant, and transformant *M. pneumoniae*. (A) wild-type *M. pneumoniae*, (B) mutant M6, (C) mutant M6 + P30, and (D) M6 + HMW1. The elongated morphology with tapered tip structures was only observed with the wild-type and M6 + HMW1 cells.

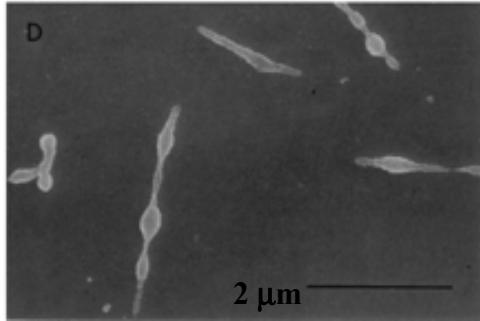
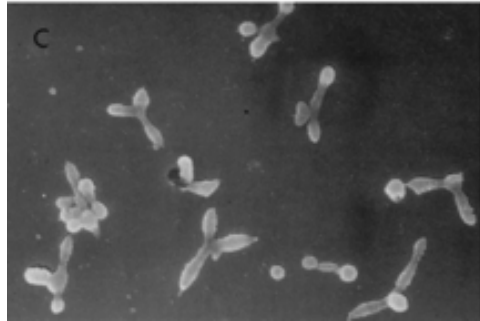
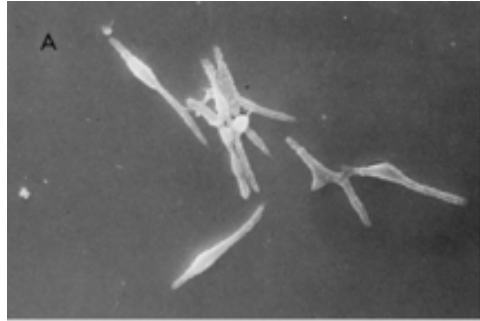
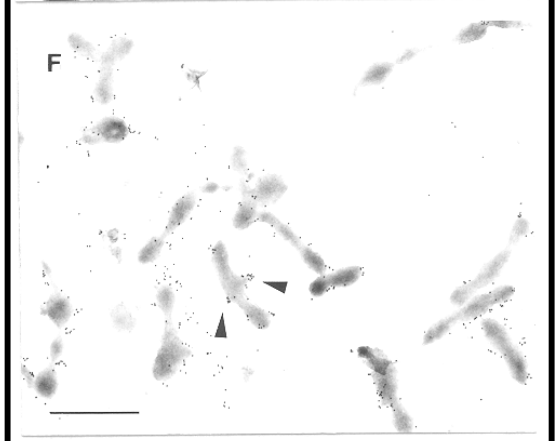
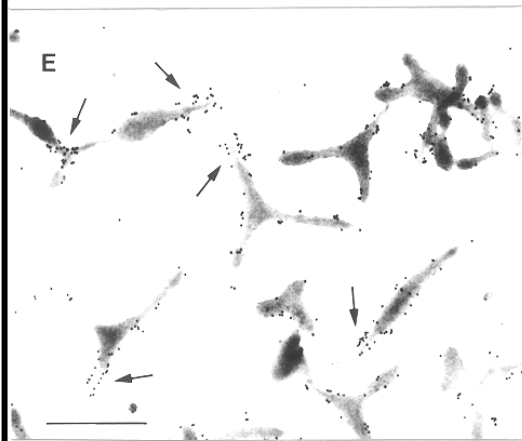
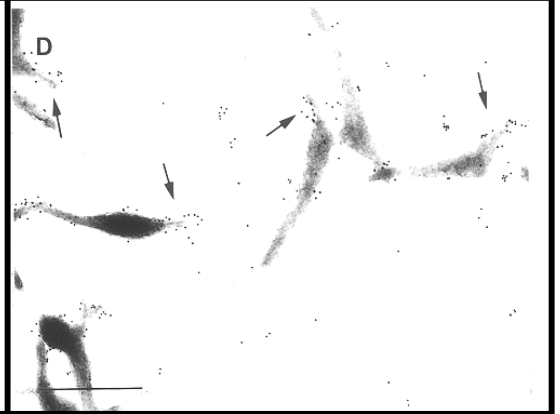
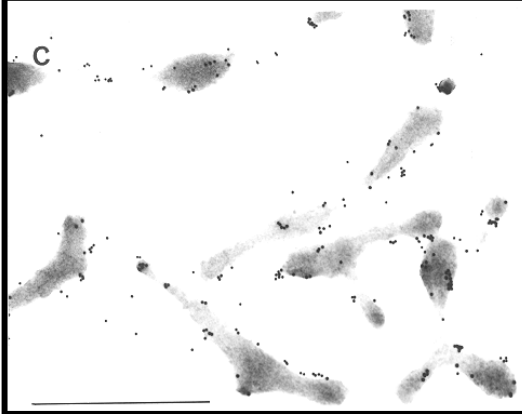
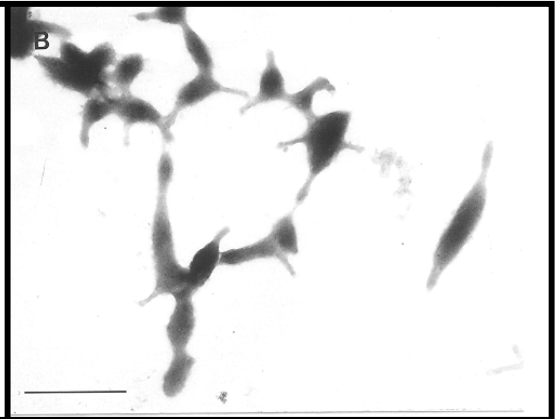
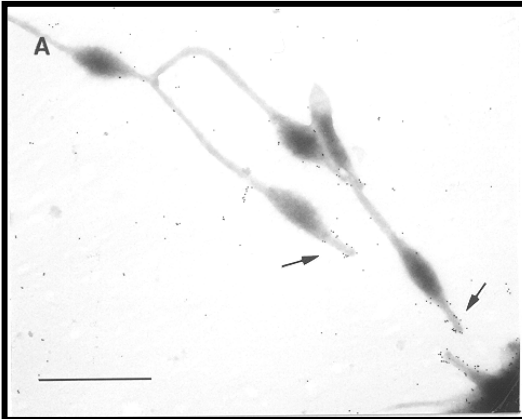


FIG. 14. Immunogold labeling wild-type, mutant, and transformant *M. pneumoniae* strains with anti-P1 antiserum. (A) wild-type *M. pneumoniae*, (B) P1⁻ mutant control, (C) mutant M6, (D) mutant II-7, (E) mutant M6 + HMW1, and (F) mutant M6 + P30. Arrows indicate tip structures where high density of labeling was observed. Arrowheads indicate zones of dense antibody labeling on some M6 + P30 cells. Bar, 1 μ m.



multiple comparisons test. A significant difference ($P < 0.001$) was noted in polar labeling between M6 and wild-type *M. pneumoniae* and between M6 and M6 transformed with *hmw1*.

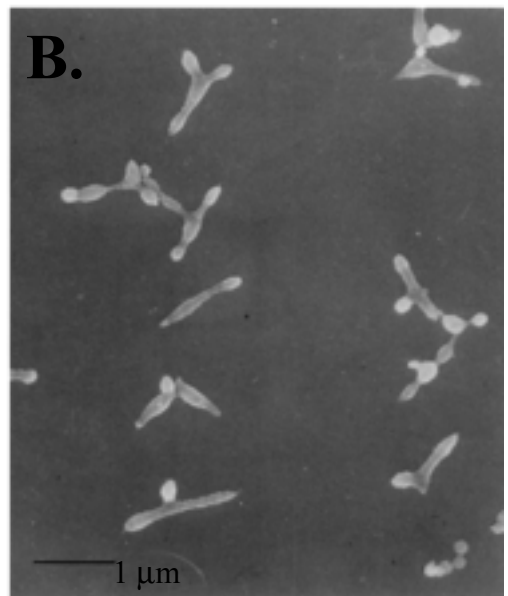
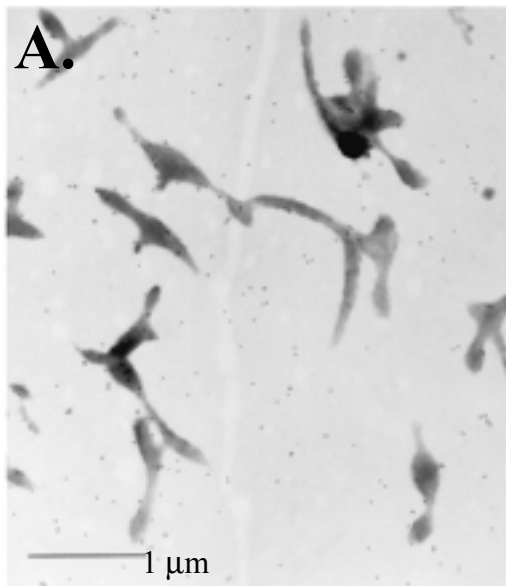
HMW1 is a component of the *Mycoplasma* cytoskeleton and localizes largely on the filamentous extensions but not on the cell body of *M. pneumoniae* (Stevens and Krause 1991). Based upon differences in P1 localization in the M6 mutant and M6 transformed with HMW1, HMW1 could be part of a molecular conduit for directing P1 to the terminal organelle, such that in its absence P1 is inserted into the membrane, but not concentrated at the attachment organelle.

C-terminally Truncated HMW1 Fails to Restore Morphology or P1

Localization.

The C-terminal 112 amino acids of HMW1 were shown to function in turnover of the protein in mutant I-2 (Hahn *et al.*, 1996; Popham *et al.*, 1997). Does this same region contribute to HMW1 function in morphology and P1 trafficking? I tested M6 cells transformed with a 3'-truncated recombinant *hmw1* (*hmw1'*; Hahn *et al.*; 1998), for these phenotypes. These transformants were indistinguishable from M6 in terms of morphology (Fig. 15B) and P1 localization (Fig. 15A; 4.2 polar vs. 10.4 nonpolar gold particles per cell) revealing a function for the C-terminus of HMW1 in morphology and P1 localization.

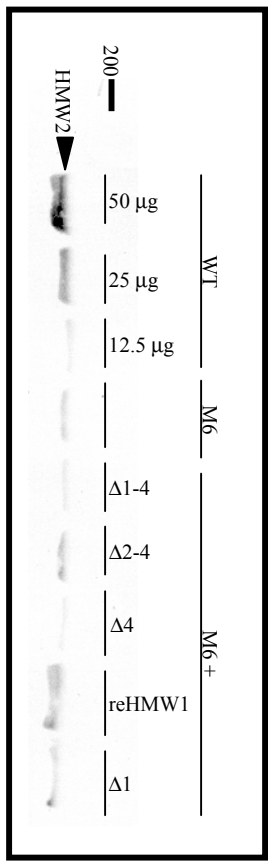
FIG. 15. Characterization M6 + HMW1' by anti-P1 immunogold labeling (A) and SEM (B). Immunogold labeling of M6 + HMW1' transformants with anti-P1 antibodies revealed scattered labeling of the entire cell (A). SEM analysis demonstrated an M6-like morphology for M6 + HMW1' (B).



Loss of HMW1 Leads to Decreased Stability of HMW2.

The original description of mutant M6 reported only the loss of HMW1 due to a frameshift in the *hmw1* gene, and a truncated protein P30 as a result of a deletion near the 3' end of the corresponding gene (Layh-Schmitt *et al.*, 1995). In subsequent studies characterizing M6 transformants producing recombinant full-length and truncated HMW1 (Hahn *et al.*, 1998), we likewise failed to recognize an additional defect in this mutant. However, recent examination of mutant M6 revealed an approximately 4-fold decrease in the steady-state level of HMW2 (Fig. 16). Furthermore, complementation of M6 with full-length recombinant HMW1 notably increased HMW2 levels, but a truncated HMW1 derivative lacking the C-terminal 112 amino acids (HMW1 Δ 1-4) did not (Fig. 16). Pulse-chase analysis confirmed that HMW2 loss occurred post-translationally (data not shown). It should be noted that the HMW1 derivative HMW1 Δ 1-4 is identical to HMW1'. These proteins are given separate designations to reflect different transcriptional origin. The cloned *M. pneumoniae* DNA from which HMW1' is expressed contains part of the coding sequence for P50 and the entire P33 coding sequence and includes the promoter region thought to direct *hmw1* transcription (Fig. 4). The DNA from which HMW1 Δ 1-4 is expressed contains only part of the P33 coding sequence. Transcription of *hmw1* is directed by the P_{IN} promoter in Tn4001mod (Fig 2). To define more precisely the specific region(s) within the C-terminus of HMW1 required to restore HMW2 stability, deletion derivatives of HMW1 (Fig. 2) were tested for their ability to restore HMW2 levels in mutant M6. The gene encoding each was cloned into pKV74 and transformed into mutant M6, and transformants were assessed for restoration

FIG. 16. Western immunoblot analysis of *M. pneumoniae* to assess steady-state levels of HMW2. Protein was electrophoresed on a 4.5% polyacrylamide gel, transferred to nitrocellulose, and probed with the anti-HMW2 antisera at a concentration of 1:7,500. The lanes labeled WT contained 50, 25 and 12.5 μg of wild-type *M. pneumoniae* protein as indicated. Lane labeled M6 contained 50 μg M6 protein. Lanes labeled M6 + contained 50 μg of M6 expressing the indicated HMW1 derivative (Fig 2B; Table 2). Protein size markers are given in kilodaltons to the left of the blot. Arrowhead designates HMW2.



of HMW2 levels. None of the HMW1 deletion-derivatives fully restored HMW2 stability, which required full-length HMW1 (Fig. 16).

Associations among components of the attachment organelle have consequences at multiple levels. Thus, newly synthesized HMW1 appears to shift from the Triton X-100-soluble fraction to a transiently insoluble fraction, to a stable, insoluble state on the *Mycoplasma* cell surface (Balish *et al.*, 2001). In the absence of HMW2 this process is much less efficient, therefore some detergent-insoluble HMW1 returns to the detergent-soluble fraction, from whence it is degraded (Balish *et al.*, 2001). It seems likely that a similar scenario exists for other components of the attachment organelle, with complexed proteins more stable than their uncomplexed counterparts. This process may reflect an important check-point in the assembly process, serving to maintain proper stoichiometry among attachment organelle proteins. The requirement for HMW2 to stabilize HMW1 and the importance of proper stoichiometry in the interplay between HMW1 and HMW2 were demonstrated previously. The current study establishes the reciprocal nature of this relationship, with HMW2 likewise dependent on HMW1 for stability. Only full-length recombinant HMW1 resulted in a notable increase in HMW2 stability.

Stability of Recombinant HMW1 Derivatives is Affected by Elements of its C-terminal Domain.

The C-terminal 112 amino acids of HMW1 were previously correlated with instability of HMW1 in mutant I-2. In order to identify more specifically regions of HMW1 required for turnover of the protein, four C-terminal truncations were generated based on the four instances of double serines in this region of the protein (Fig. 2).

Double serines were identified preceding the known processing site of the ORF6 gene product, and it was thought that they might be part of a consensus processing sequence in *M. pneumoniae* (Layh-Schmitt and Herrmann 1992; Popham *et al.*, 1997). Additionally, I constructed an *hmw1* allele encoding a protein with amino acids 905 through 927 deleted. Each construct was transformed into wild-type, mutant I-2 and mutant M6 *M. pneumoniae*, and the stability of each the recombinant HMW1 derivative was analyzed. In the wild-type background, levels of HMW1 Δ 1-4 and HMW1 Δ 1 were comparable to that of the resident full-length protein, HMW1 Δ 2-4 was substantially less abundant, and HMW1 Δ 4 was present at intermediate levels (Fig. 17A). Steady-state levels of each recombinant protein reflected post-translational turnover (Fig. 17B). Additionally, the level of total HMW1 in wild-type *M. pneumoniae* + reHMW1 did not appear to double, as might be expected with two wild-type *hmw1* alleles, perhaps a reflection of the importance of HMW1/HMW2 stoichiometry.

A similar pattern was observed in the mutant M6 background. The full-length recombinant HMW1 (reHMW1) and HMW1 Δ 1 were observed at steady-state levels similar to those of HMW1 in wild-type *M. pneumoniae* (Fig. 18A). In contrast, HMW1 Δ 2-4 was barely detectable, while HMW1 Δ 1-4 and HMW1 Δ 4 were observed at intermediate steady-state levels. Pulse-chase analysis likewise confirmed that loss of these HMW1 derivatives occurred post-translationally (Fig. 18B). While difficult to discern for HMW1 Δ 2-4 given its instability and the time frame required for sample processing in pulse-chase experiments, a rapid disappearance with time was nevertheless apparent.

FIG. 17. Analysis of HMW1 derivatives in the wild-type *M. pneumoniae* background. (A) Western immunoblot analysis. Equal amounts of protein were electrophoresed on a 4.5% polyacrylamide gel, transferred to nitrocellulose, and probed with the anti-HMW1 antisera at a concentration of 1:10,000. Lanes: WT, protein from untransformed wild-type cells; WT +, protein from WT cells expressing the indicated HMW1 derivative (Fig 2B; Table 2). (B) Pulse-chase analysis of recombinant HMW1 synthesis and turnover. Cells were treated as described above, and equal volumes of cell lysates were analyzed by SDS-PAGE (3% stacking, 4.5 % resolving gel). Gels were dried and exposed to film for 3-7 days. Lanes: WT, protein from untransformed WT cells; WT +, the HMW1 derivative indicated in the WT background (Fig 2B; Table 1). (A and B) The single band visible in lanes labeled reHMW1 encompasses both the recombinant protein and the protein expressed from the resident allele (since these two proteins are identical). Protein size markers are given in kilodaltons on the right. Arrowhead designates HMW1, and stars designate each HMW1 derivative.

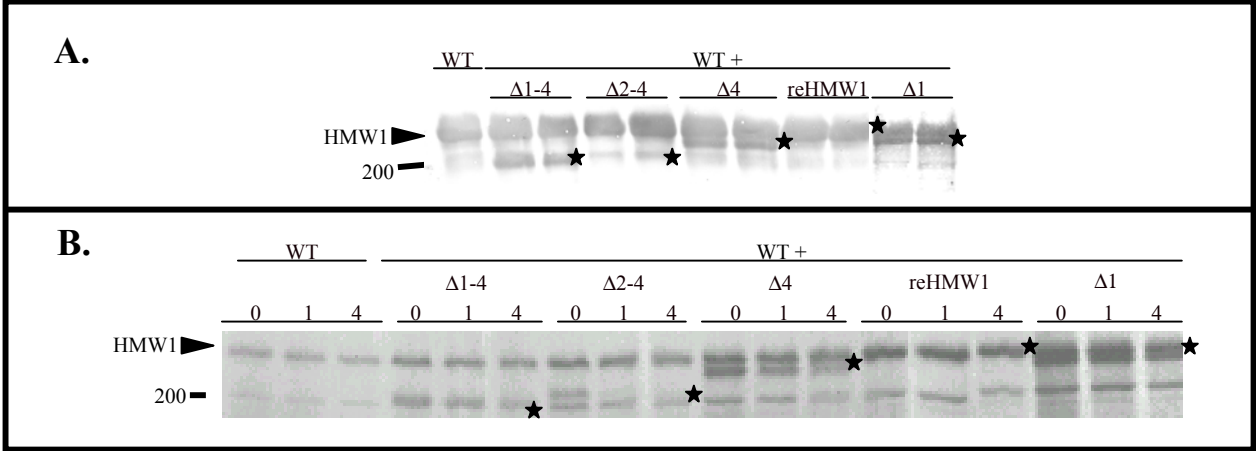
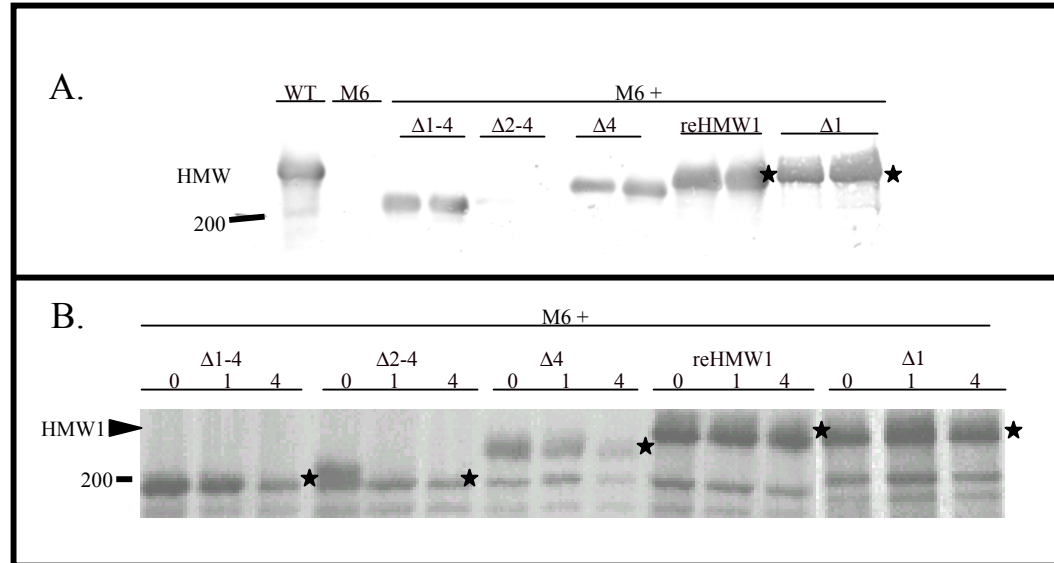


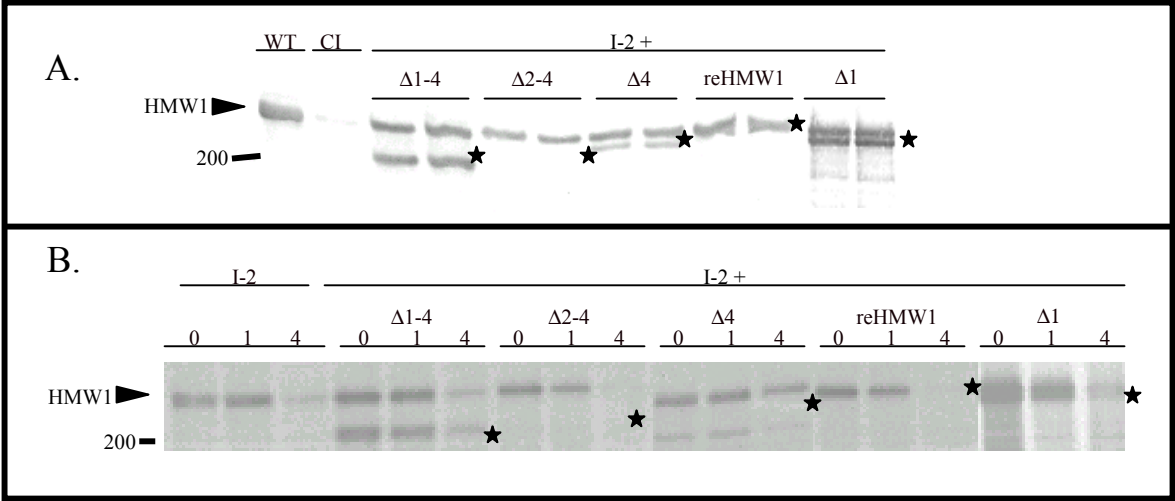
FIG. 18. Analysis of HMW1 derivatives in the *M. pneumoniae* mutant M6 background. (A) Western immunoblot analysis. Equal amounts of protein were electrophoresed on a 4.5% polyacrylamide gel, transferred to nitrocellulose, and probed with the anti-HMW1 antisera at a concentration of 1:10,000. Lanes: WT and M6, protein from untransformed wild-type and mutant M6 cells respectively; M6 +, protein from M6 cells expressing the indicated HMW1 derivative (Fig 2B; Table 2). (B) Pulse-chase analysis of recombinant HMW1 synthesis and turnover. Cells were treated as described, and equal volumes of cell lysates were analyzed by SDS-PAGE (3% stacking, 4.5 % resolving gel). Gels were dried and exposed to film for 3-7 days. Lanes contain the HMW1 derivative indicated in the M6 background (Fig 2B; Table 1). (A and B) Protein size markers are as indicated on the right in kilodaltons. Arrowhead designates HMW1, and stars designate each HMW1 derivative.



I observed resident HMW1 at very low, somewhat variable steady-state levels in the *hmw2⁻* mutant I-2, as reported previously (Fig. 19A) (Krause *et al.*, 1982). Significantly, transformation of mutant I-2 with each recombinant *hmw1* derivative resulted in a higher steady-state level and slower turnover of the resident HMW1 compared to untransformed mutant I-2 (Fig 19A and 19B, arrowhead) and may reflect the titration of an element involved in accelerated HMW1 turnover. HMW1 Δ 1-4 and HMW1 Δ 1 were observed at steady-state levels higher than that of the resident HMW1 in untransformed mutant I-2 and comparable to that of the stabilized resident full-length HMW1 in the transformants. HMW1 Δ 2-4 and HMW1 Δ 4 were again significantly less abundant, with HMW1 Δ 2-4 undetectable on most blots (Fig 19A). Pulse-chase data confirmed that the loss of each HMW1 derivative occurred post-translationally (Fig. 19B). Thus, HMW1 Δ 2-4 was considerably less abundant in all backgrounds due to its rapid turnover relative to the other HMW1 derivatives tested, while HMW1 Δ 1-4 and HMW1 Δ 1 were observed at the highest levels in all backgrounds. Region 1 (residues 906-927) in particular appeared to contribute to instability, while regions 2-4, and especially region 4, appeared to reverse this instability in the presence of HMW2.

Previous studies indicated that the C-terminal 112-amino acid domain of HMW1 may be targeted for accelerated turnover of HMW1 in the absence of HMW2 (Hahn *et al.*, 1996; Popham *et al.*, 1997). Complete removal of the C-terminal 112 amino acids (HMW1 Δ 1-4) rendered the protein only slightly unstable in all backgrounds including the HMW2⁻ mutant. However, deletion of only the last three regions (HMW1 Δ 2-4) resulted in a dramatic increase in instability, based both on steady-state levels and on pulse-chase analysis. This instability was particularly pronounced in HMW2 deficient

FIG. 19. Analysis of HMW1 derivatives in the *M. pneumoniae* mutant I-2 background. (A) Western immunoblot analysis. Equal amounts of protein were electrophoresed on a 4.5% polyacrylamide gel, transferred to nitrocellulose, and probed with the anti-HMW1 antisera at a concentration of 1:10,000. Lanes: WT and I-2, protein from untransformed wild-type and mutant I-2 cells respectively; I-2 +, protein from mutant I-2 cells expressing the indicated HMW1 derivative (Fig 2B; Table 2). (B) Pulse-chase analysis of recombinant HMW1 synthesis and turnover. Cells were treated as described, and equal volumes of cell lysates were analyzed by SDS-PAGE (3% stacking, 4.5 % resolving gel). Gels were dried and exposed to film for 3-7 days. Lanes: I-2, protein from untransformed I-2 cells; I-2 +, the HMW1 derivative indicated in the mutant I-2 background (Fig 2B; Table 1). (A and B) The single band visible in lanes labeled reHMW1 encompasses both the recombinant protein and the protein expressed from the resident allele (since these two proteins are identical). Protein size markers are given on the right in kilodaltons. Arrowhead designates HMW1, and stars designate each HMW1 derivative.



mutants I-2 and M6. Or considered another way, the addition of amino acids 906-927 appeared to destabilize HMW1 Δ 1-4. Conversely, deletion of only region 1 (amino acids 906-927) from otherwise full-length HMW1 resulted in near-normal stability in wild-type and mutant M6 backgrounds, and a stability comparable to HMW1 Δ 1-4 in mutant I-2. HMW1 Δ 4 was more stable than HMW1 Δ 2-4 but less stable than full-length HMW1 in both the wild-type and the mutant M6 backgrounds. Furthermore, reHMW1, differing from HMW1 Δ 4 by only the presence of region 4 (amino acid residues 979-1018), was stable at wild-type levels in M6. Thus, regions 2-4, and region 4 in particular, appeared to stabilize HMW1 under circumstances where HMW2 was present. The destabilizing effect of region 1 might be explained by accessibility to protease, presence of a specific amino acid motif, or the ability to disrupt folding of upstream regions of HMW1. The addition of regions 2-4 to HMW1 Δ 2-4 might reduce accessibility of protease to region 1 or overcome its possible destabilizing effects. Nevertheless, the difference in stability of HMW1 Δ 2-4 in the presence or absence of wild-type levels of HMW2 raises the possibility that this domain interacts with HMW2 or an HMW2-dependent protein that is absent or present at reduced levels in mutant I-2 and M6. Thus, in the absence of a binding partner this region is exposed in HMW2 mutants, permitting targeting for proteolysis.

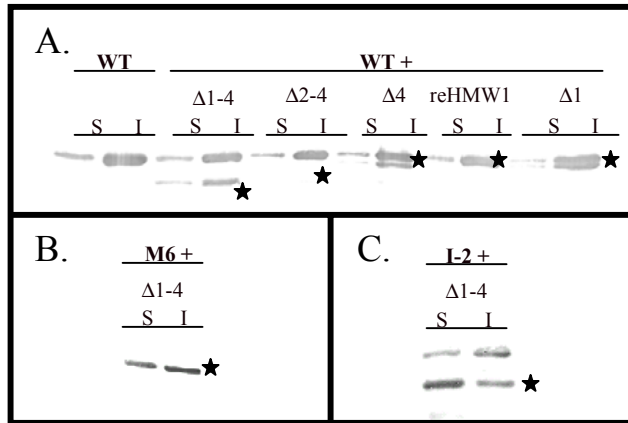
One unanticipated observation from these studies was the increase in the steady-state level of full-length HMW1 in mutant I-2 transformed with an HMW1 deletion derivative (Fig. 19A). In retrospect, this is consistent with limiting factors involved in proteolytic removal of HMW1 or deletion derivatives thereof not properly bound to a partner protein. Thus, recombinant HMW1 deletion derivatives may compete with

resident HMW1 for access to the protease(s) or a component of the proteolytic pathway responsible for turnover in mutant I-2. Furthermore, the increased stability of HMW1 Δ 1-4 over resident full-length HMW1 in mutant I-2 was originally attributed to the absence of possible protease recognition site(s) in the deletion derivative. The current findings indicate that titration of an essential element for accelerated turnover may also contribute to this observation.

The C-terminal Domain of HMW1 Influences its Association with the Cytoskeleton.

The Triton X-100-insoluble fraction of *M. pneumoniae* contains its cytoskeleton. HMW1 partitions predominantly (70-80%) in the insoluble fraction (Fig. 20). I examined Triton-fractionated wild-type and mutant *M. pneumoniae* producing recombinant HMW1 deletion derivatives to determine if the C-terminal domain of HMW1 might contribute to its association with the cytoskeleton. Each HMW1 derivative in wild-type *M. pneumoniae* partitioned primarily in the detergent-insoluble fraction, similar to full-length HMW1 (Fig. 20). However, the partitioning of HMW1 Δ 1-4 was atypical in mutant M6, where soluble and insoluble HMW1 Δ 1-4 were approximately equal, and in mutant I-2 where a greater proportion of HMW1 Δ 1-4 partitioned in the soluble fraction than in the insoluble fraction. Analysis of HMW1 Δ 2-4 fractionation was difficult due to its extreme instability. Other recombinant proteins fractionated similarly to full-length HMW1 in the mutant backgrounds (data not shown). These data suggest that regions 2-4 of the C-terminal domain of HMW1 contribute to the association of HMW1 with the cytoskeleton and may thereby account for the ability of these regions to overcome

FIG 20. Western immunoblot analysis of Triton X-100 solubility of HMW1 derivatives in WT (A), mutant M6 (B), and mutant I-2 (C) *M. pneumoniae* backgrounds. Equal amounts of protein were treated with Triton as described previously to obtain triton-soluble (S) and triton insoluble (I) fractions. Fractions were electrophoresed on a 4.5% polyacrylamide gel, transferred to nitrocellulose, and probed with the anti-HMW1 antisera at a concentration of 1:10,000. Lanes: WT, protein from untransformed wild-type cells; WT +, M6 +, or I-2 +, protein from wild-type, M6 or mutant I-2 cells respectively, expressing the indicated HMW1 derivative (Fig 2B; Table 2). The single band visible in the lane labeled reHMW1 encompasses both the recombinant protein and the protein expressed from the resident allele (since these two proteins are identical). Stars designate each HMW1 derivative.

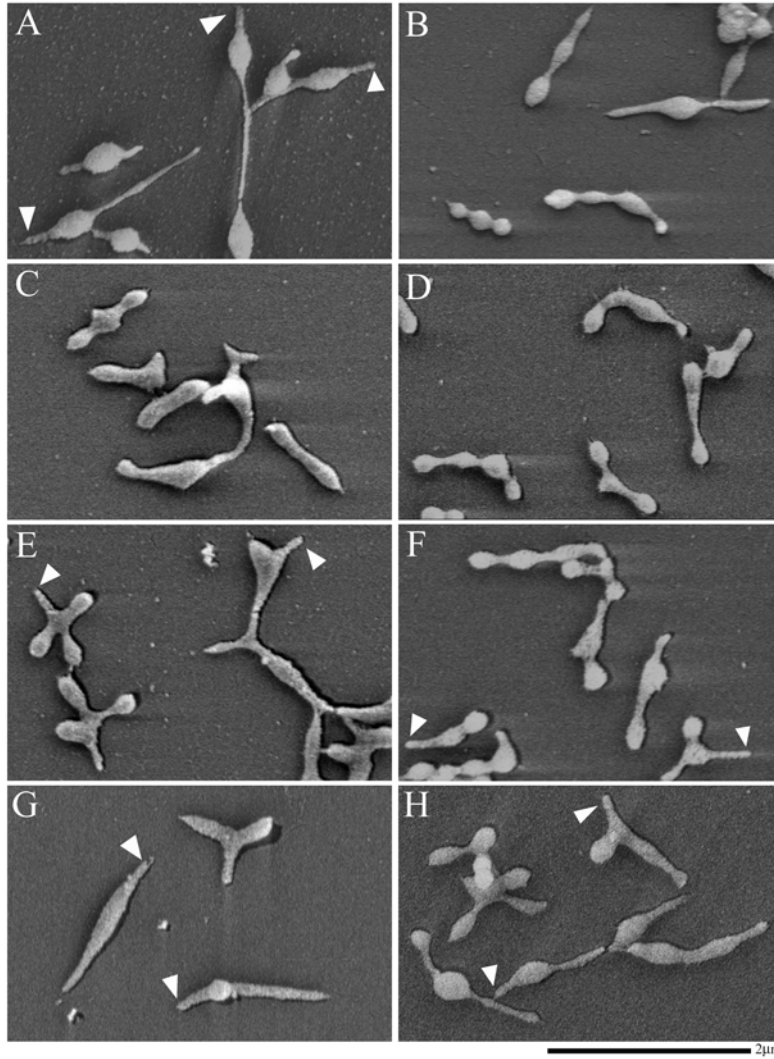


partially the instability of HMW1 Δ 2-4. Previous studies correlated the stability of HMW1 with its ability to associate efficiently with the Triton X-100-insoluble, cytoskeletal fraction (Balish *et al.*, 2001). Since stability is associated with detergent insolubility, and the C-terminus of HMW1 provides the protein with a measure of stability, I investigated the Triton X-100-insolubility of each HMW1 deletion derivative. Each partitioned identically to full-length HMW1 in wild-type *M. pneumoniae*, suggesting that the C-terminus is not essential for cytoskeletal association in this background. However, a different pattern emerged in the mutant I-2 and M6 backgrounds, where HMW1 Δ 1-4 was found in a substantially higher proportion in the detergent-soluble fraction than is normally seen with wild-type *M. pneumoniae* (Fig. 20). Interestingly, full-length HMW1 expressed from the resident allele in a mutant I-2 strain also expressing HMW1 Δ 1-4 fractionated normally (Fig. 20). Thus HMW2 or an HMW2-dependent protein likely influences the stable incorporation of a portion of HMW1 into the cytoskeletal fraction (Balish *et al.*, 2001), and this process appears to require the C-terminal domain of HMW1. Interestingly, HMW1 Δ 1-4 is relatively stable in mutant I-2 despite inefficient incorporation into the detergent-insoluble fraction, again underscoring the importance of the C-terminal domain in the targeting of unbound HMW1 for turnover.

The C-terminus of HMW1 is Required for Wild-type Morphology.

Hahn *et al.* (1998) reported that full-length recombinant HMW1 restores a near-wild-type morphology to mutant M6, while HMW1', lacking the C-terminal 112 amino acids did not (Fig. 21). I evaluated the morphology of mutant M6 cells producing the

FIG. 21. Scanning electron micrographs of wild-type *M. pneumoniae* and mutant M6 expressing recombinant *hmw1* alleles. (A) wild-type *M. pneumoniae*, (B) mutant M6, (C) M6 + HMW1 Δ 1-4, (D) M6 + HMW1 Δ 2-4, (E), M6 + HMW1 Δ 4, (F) M6 + HMW1 Δ 1, (G and H) M6 + reHMW1. Arrowheads indicate wild-type like, tapered attachment organelles.



HMW1 truncation/deletion derivatives by SEM. As was the case with M6 cells producing HMW1', HMW1 Δ 1-4 did not restore wild-type morphology to the M6 mutant. M6 cells producing HMW1 Δ 2-4 were multi-lobed, with multiple distended areas and rounded poles, similar to untransformed M6 cells. Although most cells still resembled untransformed mutant M6, cells with tapered attachment organelles could be seen in populations of M6 + HMW1 Δ 4 and M6 + HMW1 Δ 1. However, the cells most like wild-type were M6 + the full length recombinant HMW1.

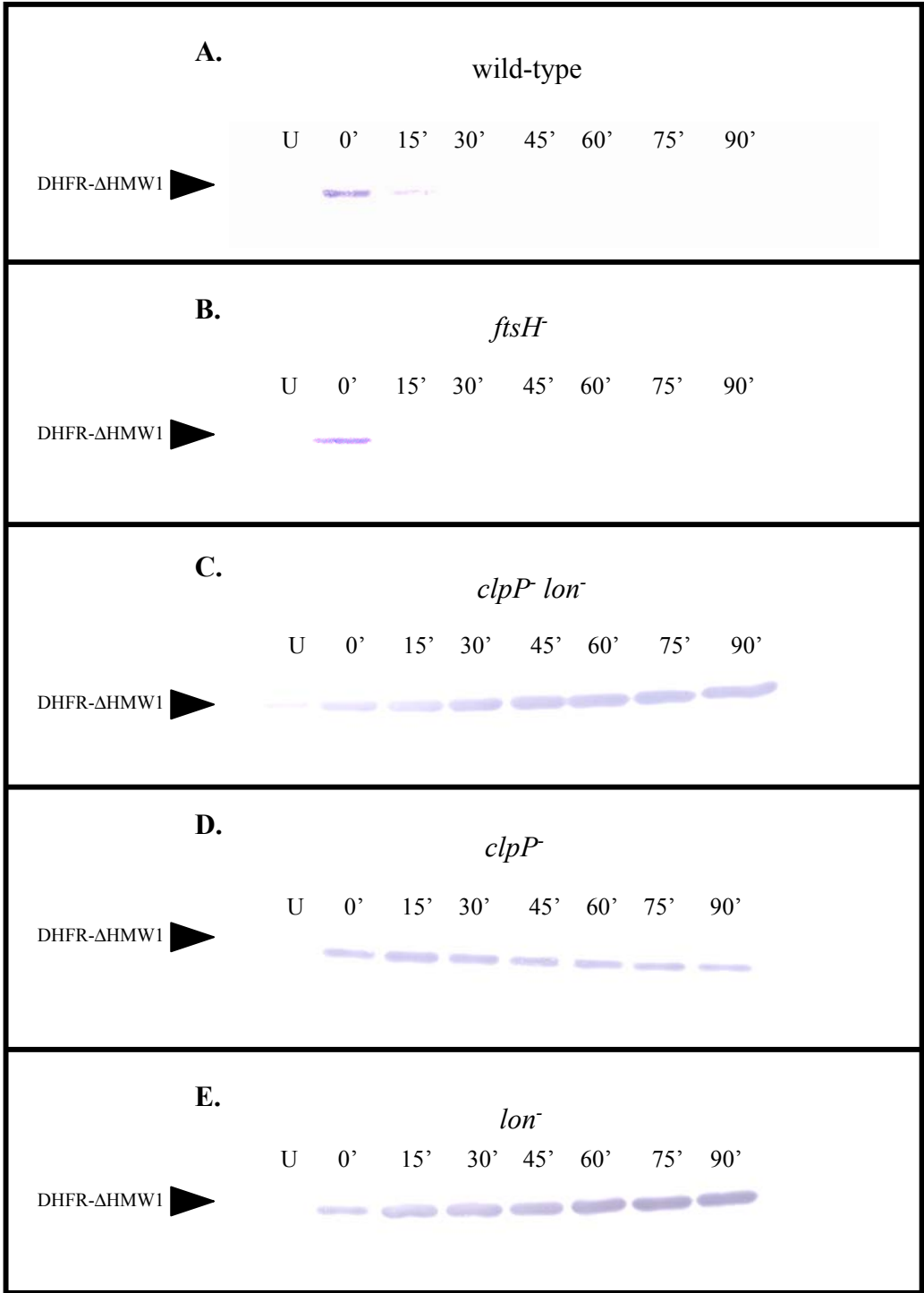
Thus, C-terminal region of HMW1 seems to be required for HMW1 to confer a tapered attachment organelle, with expression of full-length *hmw1* resulting in cells with the greatest degree of morphological similarity to wild-type cells. As mentioned previously, it is possible that the multiple branches and distended areas characteristic of mutant M6 are the result of defective cell division. It is noteworthy that only M6 cells producing reHMW1 had wild-type levels of HMW2, thus, restoration of morphology is likely a consequence of the presence of both of these attachment organelle-associated proteins at normal levels. Perhaps presence of HMW1 and HMW2 results in a mostly functional attachment organelle (tapered poles), leading to successful and efficient cell division (filamentous cells without multiple branches or distended areas).

Functional ClpP and Lon Proteases are Required for Turnover of DHFR- Δ HMW1 in *E. coli*.

Much of the regulatory proteolytic turnover in bacterial cells is accomplished by energy dependent proteases such as ClpP, Lon or FtsH. Although, no ClpP homolog has been identified in *M. pneumoniae*, sequences corresponding to both Lon and FtsH have

been identified, and one of these proteases may be responsible for turnover of HMW1. We assembled a collection of *E. coli* strains with mutations in each of these proteases. Full-length HMW1 cannot be easily expressed in *E. coli* since it contains 2 UGA codons, which in *E. coli* signal a translational stop. I designed a reporter system whereby the C-terminal region of HMW1 was fused to mouse DHFR (DHFR-ΔHMW1) with transcription under the control of *lac* operator sequences (Fig. 1). Plasmid DNA containing this reporter fusion was transformed into the parental *E. coli* strain (all proteases functional) and each mutant strain. Cultures were grown to mid-log phase under conditions that repressed expression of DHFR-ΔHMW1 and then induced for two minutes by the addition of IPTG. Spectinomycin (700 μg/ml) was added to inhibit further protein synthesis, and samples were removed at various time points and analyzed by Western blot with DHFR-specific antisera to monitor stability of DHFR-ΔHMW1 in each strain (Fig. 22). As a control, I confirmed the stability of unfused DHFR in each background (data not shown). While DHFR-ΔHMW1 was unstable in the parental strain in which all proteases were functional (Fig. 22A) it was completely stable in Lon deficient strains (Fig. 22C and E) and mostly stable in ClpP-deficient strains (Fig. 22C and D). Conversely, DHFR-ΔHMW1 was turned over in the FtsH-deficient strain (Fig. 22B), suggesting that *E. coli* FtsH and by extension possibly *M. pneumoniae* FtsH does not act on HMW1. Surprisingly, it appears that in *E. coli*, Clp and Lon are both required for turnover of DHFR-ΔHMW1. Degradation of photo-damaged D1 protein of photosystem II reaction center in chloroplasts requires an initial cleavage event by the protease DegP1 in order for FtsH to complete turnover of the protein (Adam and Ostersetzer 2001). Therefore, it is possible, however unlikely, that both proteases are

FIG. 22. Stability of DHFR- Δ HMW1 in *E. coli* strains transformed with pKV204. Cells were grown in LB medium supplemented with 2% glucose to an ABS_{600} of 0.4-0.6, induced for two minutes with IPTG (0.02%) to express DHFR- Δ HMW1, and treated with spectinomycin (700 μ g/ml) to inhibit protein synthesis. Samples were removed before induction (U), immediately following addition of spectinomycin (0') and every 15 minutes thereafter and precipitated with TCA. Pellets were suspended in 1M Tris base and analyzed by SDS-PAGE (3% stacking, 10% resolving). (A) SG22163 (*lacI^q*), (B) SG22166 (*lacI^q ftsH1*), (C) SG22165 (*lacI^q clpP::cat Δ lon*), (D) SG22174 (*lacI^q clpP::cat*), and (E) SG22186 (*lacI^q Δ lon rcsA51::kan*).



needed for turnover of DHFR-ΔHMW1 in *E. coli*. Clp and Lon proteases have been reported to utilize a similar mechanism to recognize substrates (Smith *et al.*, 1999). No ClpP homolog has been identified in *M. pneumoniae* (Himmelreich *et al.*, 1996). Therefore, in this organism the substrate specificity of Lon may be somewhat more broader. It could also be possible that chaperones contribute to recognition of a larger array of substrates by Lon in *M. pneumoniae*. Perhaps HMW1 is a substrate for Lon in *M. pneumoniae*, however it is not particularly good substrate for either Lon or Clp in *E. coli*, requiring both proteases for appreciable turnover in this organism. Regardless, since *M. pneumoniae* does not appear to encode Clp, if any correlation can be drawn between turnover of DHFR-ΔHMW1 in *E. coli* and turnover of HMW1 in *M. pneumoniae*, Lon may be the protease responsible for turnover of HMW1 in *M. pneumoniae*.

In summary, in the current study I assessed the role HMW1 in morphology, P1 localization and HMW2 stability and examined the role of specific regions within the C-terminal domain of HMW1 in its stability and function. Residues 906-927 appeared to be particularly important in the accelerated turnover of HMW1 in the absence of HMW2, while residues 928-1018 may be involved in the binding to HMW2 to an HMW2-dependent protein for proper function and to protect HMW1 from rapid turnover. Finally, HMW1 is required for the maintenance of HMW2 at wild-type levels, demonstrating a reciprocal relationship between these cytoadherence-associated proteins.

CHAPTER V

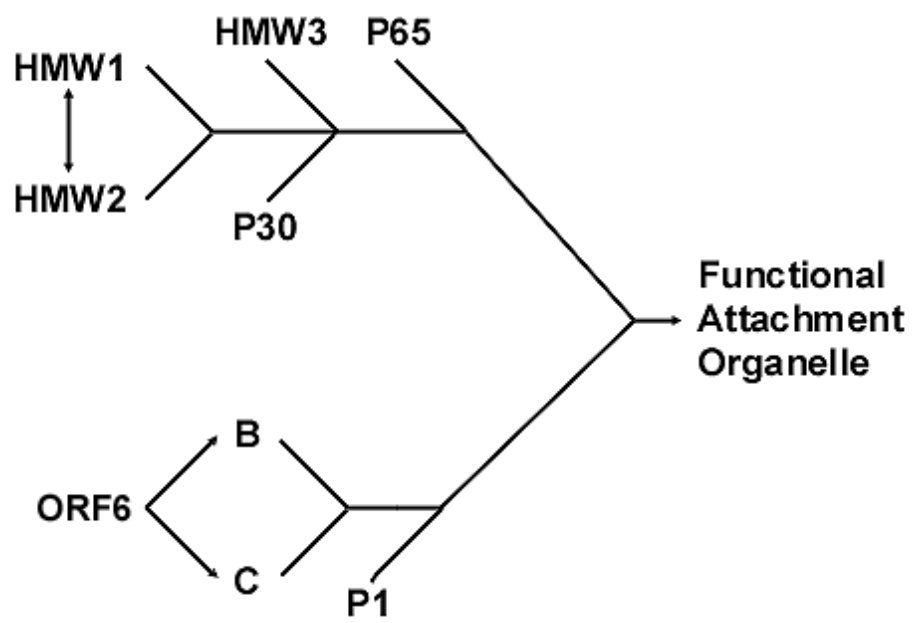
CONCLUSIONS

Bacterial genes encoding functionally related proteins must be regulated such that those proteins are produced in appropriate amounts at the appropriate times. Such genes are commonly organized into a single regulatory unit, an operon, or into several operons coordinately controlled as a regulon. Contemporaneous expression of such genes contributes to the presence of their products in stoichiometric amounts at the correct time. Genes encoding components of the *M. pneumoniae* attachment organelle are not found in a single operon, but are located in at least three different operons widely dispersed on the chromosome. How the components of the attachment organelle come together in proper stoichiometric amounts to form a highly organized structure presents an intriguing question. Only a single sigma factor is predicted in the *M. pneumoniae* genome sequence precluding regulation by multiple sigma factors. There is some evidence for translational coupling of attachment organelle proteins encoded by the *p1* operon (proteins P1, B, and C; Inamine *et al.*, 1988; Su *et al.*, 1989). Regulation some of the components of the *hmv* operon are via this strategy is also a possibility particularly due to the short intergenic regions separating most if its constituents (Himmelreich *et al.*, 1996). Additional evidence indicates that both HMW1 and HMW2 are phosphorylated, another widely used regulatory strategy (Dirksen *et al.*, 1994; Krebs *et al.*, 1995). Other mechanisms of control including mRNA stability, antisense RNA, transcriptional activators or

repressors, and proteolytic turnover have not been thoroughly examined. Recent studies of *M. pneumoniae* mutants have allowed us to make progress in this area while learning more about the function of specific proteins and the assembly of the nascent attachment organelle prior to cell division.

The relationships among HMW2 and other cytoadherence proteins including HMW1 and HMW3, whereby loss of HMW2 leads to accelerated turnover of these proteins, has been previously described. I have shown a reciprocal relationship between HMW1 and HMW2 in that amino acids 906-927 destabilize HMW1, particularly when HMW2 is reduced or absent, and stability is restored with the addition of residues 928-1018, especially in the presence of HMW2. In addition, I showed a requirement for the C-terminal 112 amino acids of HMW1 for stabilization of HMW2. It appears that HMW1 and HMW2 interact, directly or indirectly, through the C-terminus of HMW1. The stabilizing effect of HMW1 is likely extended to HMW3 and P65 through its relationship with HMW2. Finally, in other studies I demonstrated that P65 stability is dependent in part on HMW3. Therefore, the relative amounts of these cytoadherence proteins are intricately interdependent. Furthermore, it has been hypothesized that components of the attachment organelle are incorporated into this structure via one of two pathways (Fig 23; Balish and Krause, 2002; Seto *et al.*, 2001). Components of each pathway are stabilized as they are sequentially incorporated into this structure (Balish *et al.*, 2001). HMW1 and HMW2 are predicted to be among the first components of the nascent attachment organelle. By revealing a mutually stabilizing relationship between these two proteins I have lent weight to the hypothesis that HMW1 and HMW2 are incorporated into the attachment organelle coordinately. Furthermore, the instability of

FIG. 23. Proposed model of assembly of identified protein components of the attachment organelle. Proteins are incorporated via one of two branches that come together to form a functional structure. Incorporation of each protein results in its stabilization. Downstream components cannot be incorporated prior to upstream components.



Molecular Biology and Pathogenicity of Mycoplasmas, 2002

P65 in this mutant likely reflects its inability to localize properly and suggests incorporation into the attachment organelle subsequent to HMW3. Likewise, the stability of other cytodherence proteins tested suggests that they are incorporated into the attachment organelle prior to or coincident with HMW3 or via the second pathway. Thus, studies using the *hmw3::Tn4001*mod transformant provide additional support the proposed model.

While turnover of unincorporated components of proteinaceous complexes is not as pervasive as other methods for achieving stoichiometric balance among proteins, it is nevertheless a widespread and important mechanism. For example, in *E. coli* and other Gram negative organisms, SecY, SecE, and SecG associate to form a channel through the inner membrane for protein secretion. A number of studies have shown that uncomplexed SecY is rapidly degraded by the protease FtsH (Baba *et al.*, 1994; Flower *et al.*, 1995; Kihara *et al.*, 1995; Matsuyama *et al.*, 1990; Taura *et al.*, 1993). Additionally, the F₀ portion of the *E. coli* ATPase serves as a proton channel across the bacterial membrane. It is composed of three subunits a, b, and c, all integral membrane proteins. Uncomplexed subunit a produced as a result of overexpression of the *atpB* gene does not accumulate in the membrane. Instead, like SecY, uncomplexed F₀ subunit a is turned over in an FtsH dependent manner (Akiyama *et al.*, 1996; Hermolin and Fillingame 1995). *Pseudomonas aeruginosa* proteins XcpZ and XcpY are components of a complex required for secretion of some proteins across the outer membrane. Like HMW1 and HMW2 of *M. pneumoniae*, XcpZ and XcpY have been shown to be mutually stabilizing. Neither protein is found at wild-type levels in the absence of its partner (Michel *et al.*, 1998). A similar phenomenon has been observed with homologous proteins in other

organisms (Possot *et al.*, 2000; Py *et al.*, 2001; Sandkvist *et al.*, 1995; Sandkvist *et al.*, 1999). However, preliminary studies have failed to reveal the protease responsible for turnover (Michel *et al.*, 1998).

Why did *M. pneumoniae* develop this interdependency among cytoadherence proteins? The presence of disproportionate amounts of F₀ subunit a was shown to be deleterious in *E. coli* (Eya *et al.*, 1989; von Meyenburg *et al.*, 1985). Perhaps the same is true for *M. pneumoniae* cytoadherence accessory proteins. There are a number of possible ways that this type of interdependency among proteins could facilitate formation of a functional attachment organelle in *M. pneumoniae*, a requirement for survival *in vivo*. For example, I showed that HMW1, including the entire C-terminus, contributes to the tapered appearance of the attachment organelle on the cell exterior, while HMW3 maintains the architecture of this structure from within. The interdependence of these proteins may assist in their concentration at the attachment organelle since mislocalized proteins are not likely to be complexed and so are more vulnerable to proteolytic degradation. Additionally, we assume that as with most organized complexes, there is a precise order of assembly of proteins into the attachment organelle (Balish *et al.*, 2001; Krause and Balish 2001; Seto *et al.*, 2001). As each protein in its turn is properly folded and assembled into this structure, it is stabilized. Proteins cannot associate with the complex prematurely because in the absence of proteins incorporated ahead of them into the attachment organelle, they are degraded. Moreover, interactions among partners keep proteins in the appropriate stoichiometric balance. It is likely that this stoichiometry is also crucial for function of the attachment organelle. For example, physical splitting of one electron-dense core into two is one possible means for duplication of this structure

prior to cell division. We suggest that HMW3 stabilizes the electron-dense core. Thus, an unusually high concentration of HMW3 might make it impossible for the core to divide, whereas too little HMW3 could result in a core that deteriorates leading to a nonfunctional attachment organelle. Therefore, *M. pneumoniae* may have elegantly achieved the localization, proper assembly, and stoichiometric balance of a number of proteins in the absence of any extraneous dedicated regulatory proteins.

REFERENCES

- Adam, Z., and O. Ostersetzer.** 2001. Degredation of unassembled and damaged thylakoid proteins. *Biochemical Society Transactions* **29**:427-430.
- Akerlund, T., K. Nordstrom, and R. Bernander.** 1993. Branched *Escherichia coli* cells. *Mol Microbiol* **10**:849-58.
- Akiyama, Y., A. Kihara, and K. Ito.** 1996. Subunit a of proton ATPase F₀ sector is a substrate of the FtsH protease in *Escherichia coli*. *FEBS Lett* **399**:26-8.
- Allen, P. Z., and B. Prescott.** 1978. Immunochemical studies on a *Mycoplasma pneumoniae* polysaccharide fraction: cross-reactions with type 23 and 32 antipneumococcal rabbit sera. *Infect and Immun* **20**:421-429.
- Almagor, M., S. Yatziv, and I. Kahane.** 1983. Inhibition of host cell catalase by *Mycoplasma pneumoniae*: a possible mechanism for cell injury. *Infect and Immun* **41**:251-256.
- Almagor, M., I. Kahane, and S. Yatziv.** 1984. Role of superoxide anion in host cell injury induced by *Mycoplasma pneumoniae* infection. A study in normal and trisomy 21 cells. *J Clin Invest* **73**:842-847.
- Almagor, M., I. Kahane, J. M. Wiesel, and S. Yatziv.** 1985. Human ciliated epithelial cells from nasal polyps as an experimental model for *Mycoplasma pneumoniae* infection. *Infect and Immun* **48**:552-555.
- Andreev, J., Z. Borovsky, I. Rosenshine, and S. Rottem.** 1995. Invasion of HeLa cells by *Mycoplasma penetrans* and the induction of tyrosine phosphorylation of a 145-kDa host cell protein. *FEMS Microbiol Lett* **132**:189-94.
- Baba, T., T. Taura, T. Shimoike, Y. Akiyama, T. Yoshihisa, and K. Ito.** 1994. A cytoplasmic domain is important for the formation of a SecY-SecE translocator complex. *Proc Natl Acad Sci U S A* **91**:4539-43.
- Balish, M.F., and D.C. Krause.** 2002. Cytadheence and the cytoskeleton, p.491-518. *In* S. Razin and R. Herrmann (ed.), *Molecular biology and pathogenicity of Mycoplasmas*. Kluwer Academic/Plenum Publishers, New York.

- Balish, M. F., T. W. Hahn, P. L. Popham, and D. C. Krause.** 2001. Stability of *Mycoplasma pneumoniae* cytoadherence-accessory protein HMW1 correlates with its association with the triton shell. *J Bacteriol* **183**:3680-8.
- Baseman, J. B., M. Banai, and I. Kahane.** 1982a. Sialic acid residues mediate *Mycoplasma pneumoniae* attachment to human and sheep erythrocytes. *Infect Immun* **38**:389-91.
- Baseman, J. B., R. M. Cole, D. C. Krause, and D. K. Leith.** 1982b. Molecular basis for cytoadsorption of *Mycoplasma pneumoniae*. *J Bacteriol* **151**:1514-22.
- Baseman, J. B., J. Morrison-Plummer, D. Drouillard, B. Puleo-Scheppke, V. V. Tryon, and S. C. Holt.** 1987. Identification of a 32-kilodalton protein of *Mycoplasma pneumoniae* associated with hemadsorption. *Isr J Med Sci* **23**:474-9.
- Baseman, J. B., S. F. Dallo, J. G. Tully, and D. L. Rose.** 1988. Isolation and characterization of *Mycoplasma genitalium* strains from the human respiratory tract. *J Clin Microbiol* **26**:2266-9.
- Baseman, J. B., M. Lange, N.L. Criscimanga, J.A. Giron, and C.A. Thomas.** 1995. Interplay between Mycoplasmas and host target cells. *Microb Patho* **19**:105-116.
- Baseman, J. B., and J. G. Tully.** 1997. Mycoplasmas: sophisticated, reemerging, and burdened by their notoriety. *Emerg Infect Dis* **3**:21-32.
- Biberfeld, G.** 1968. Distribution of antibodies with 19 S and 7 S immunoglobulins following infection with *Mycoplasma pneumoniae*. *J Immun* **100**:338-347.
- Biberfeld, G., and P. Biberfeld.** 1970. Ultrastructural Features of *Mycoplasma pneumoniae*. *J Bacteriol* **102**:855-861.
- Biberfeld, G., and G. Sterner.** 1971. Demonstrations of antibodies against *Mycoplasma pneumoniae* in bronchial secretion by immunofluorescence. *Ann NY Acad Sci* **177**:32-36.
- Biberfeld, G., P. Arneborn, M. Forsgren, L. V. von Stedingk, and S. Blomqvist.** 1983. Non-specific polyclonal antibody response induced by *Mycoplasma pneumoniae*. *Yale J Biol Med* **56**:639-642.
- Block, S., J. Hedrick, M. R. Hammerschlag, G. H. Cassell, and J. C. Craft.** 1995. *Mycoplasma pneumoniae* and *Chlamydia pneumoniae* in pediatric community-acquired pneumonia: comparative efficacy and safety of clarithromycin vs. erythromycin ethylsuccinate. *Pediatr Infect Dis J* **14**:471-7.
- Boatman, E. S.** 1979a. Morphology and ultrastructure of the Mycoplasmatales, p. 63-102. *In* S. Razin (ed.), *The mycoplasmas: cell biology*, vol. 1. Academic Press.

- Boatman, E. S.** 1979b. Morphology and ultrastructure of the mycoplasmatales. *In* S. Razin (ed.), *The mycoplasmas*, vol. 1. Academic Press, Washington, D.C.
- Bozzola, J. J., and L. D. Russell.** 1992. *Electron microscopy: principles and techniques for biologists*. Jones and Bartlett Publishers, Boston.
- Bredt, W.** 1968. Motility and multiplication of *Mycoplasma pneumoniae*. A phase contrast study. *Pathol Microbiol* **32**:321-6.
- Bredt, W., and D. Bitter-Suermann.** 1975. Interactions between *Mycoplasma pneumoniae* and guinea pig complement. *Infection and Immunity* **3**:497-504.
- Bredt, W.** 1979. Motility, p. 141-155. *In* S. Razin (ed.), *The mycoplasmas*, vol. 1. Academic Press, Washington, D.C.
- Brown, R. C., J. O. Hendley, and J. M. Gwaltney, Jr.** 1972. *Mycoplasma pneumoniae* vaccine: antigenicity of buffered antigens in volunteers. *Infect Immun* **5**:657-61.
- Byrne, M. E., D. A. Rouch, and R. A. Skurray.** 1989. Nucleotide sequence analysis of IS256 from the *Staphylococcus aureus* gentamicin-tobramycin-kanamycin-resistance transposon Tn4001. *Gene* **81**:361-7.
- Carson, J. L., A. M. Collier, and W. A. Clyde, Jr.** 1979. Ciliary membrane alterations occurring in experimental *Mycoplasma pneumoniae* infection. *Science* **206**:349-51.
- Carson, J. L., A. M. Collier, and S. C. Hu.** 1980. Ultrastructural observations on cellular and subcellular aspects of experimental *Mycoplasma pneumoniae* disease. *Infect Immun* **29**:1117-24.
- Cassell, G. H., and B. C. Cole.** 1981. Mycoplasmas as agents of human disease. *N Engl J Med* **304**:80-9.
- Cassell, G. H., W. A. Clyde, Jr., and J. K. Davis.** 1985. Mycoplasmal respiratory infections, p. 69-106. *In* S. Razin (ed.), *The Mycoplasmas: mycoplasma pathogenicity*, vol. IV. Academic Press, Inc, New York.
- Chambaud, I., H. Wroblewski, and A. Blanchard.** 1999. Interactions between *Mycoplasma* lipoproteins and the host immune system. *Trends Microbiol* **7**:493-9.
- Chambaud, I., R. Heilig, S. Ferris, V. Barbe, D. Samson, F. Galisson, I. Moszer, K. Dybvig, H. Wroblewski, A. Viari, E. P. Rocha, and A. Blanchard.** 2001. The complete genome sequence of the murine respiratory pathogen *Mycoplasma pulmonis*. *Nucleic Acids Res* **29**:2145-53.

- Chanock, R. M., and D. Riftkind.** 1961. Respiratory disease in volunteers infected with Eaton agent: a preliminary report. *Proc Natl Acad Sci U S A* **47**:887-890.
- Chanock, R. M., L. Hayflick, and M. F. Barile.** 1962. Growth on artificial medium of an agent associated with atypical pneumonia and its identification as a PPLO. *Proc Natl Acad Sci U S A* **48**:41-49.
- Chanock, R. M., L. Dienes, M. D. Eaton, D. G. Edward, E. A. Freunt, L. Hayflick, J. F. Hers, K. E. Jensen, C. Liu, B. P. Marmion, H. E. Morton, M. A. Mufson, P. F. Smith, N. L. Somerson, and D. Taylor-Robinson.** 1963. *Mycoplasma pneumoniae*: proposed nomenclature for atypical pneumonia organism (Eaton agent). *Science* **140**:662.
- Cherry, J. D., and D. Taylor-Robinson.** 1970. Growth and pathogenesis of *Mycoplasma mycoides* var. *capri* in chicken embryo tracheal organ cultures. *Infect Immun* **228**:1099-1100.
- Chou, P. Y., and G. D. Fasman.** 1978. Prediction of the secondary structure of proteins from their amino acid sequence. *Adv Enzymol Relat Areas Mol Biol* **47**:45-148.
- Clyde, W. A., Jr.** 1961. *Proc Soc Exp Biol Med* **107**:716-719.
- Clyde, W. A., Jr.** 1979. *Mycoplasma pneumoniae* infections of man, p. 275-306. *In* R. F. Whitcomb (ed.), *The Mycoplasmas: human and animal mycoplasmas*, vol. II. Academic Press, Inc, New York.
- Clyde, W. A., Jr.** 1983. *Mycoplasma pneumoniae* respiratory disease symposium: summation and significance. *Yale J Biol Med* **56**:523-7.
- Cocks, B. G., L. E. Pyle, and L. R. Finch.** 1989. A physical map of the genome of *Ureaplasma urealyticum* 960T with ribosomal RNA loci. *Nucleic Acids Res* **17**:6713-9.
- Cohen, G., and N. L. Somerson.** 1967. *Mycoplasma pneumoniae*: hydrogen peroxide secretion and its possible role in virulence. *Ann N Y Acad Sci* **143**:85-7.
- Collier, A. M., W. A. Clyde, Jr., and F. W. Denny.** 1969. Biologic effects of *Mycoplasma pneumoniae* and other mycoplasmas from man on hamster tracheal organ culture. *Proc Soc Exp Biol Med* **132**:1153-8.
- Collier, A. M., and W. A. Clyde.** 1971. Relationships Between *Mycoplasma pneumoniae* and Human Respiratory Epithelium. *Infection and Immunity* **3**:694-701.
- Collier, A. M.** 1972. Presented at the Ciba Foundation Symposium.

- Collier, A. M., and J. B. Baseman.** 1973. Organ culture techniques with mycoplasmas. *Annals of the New York Academy of Science* **225**:277-289.
- Dallo, S. F., A. Chavoya, C. J. Su, and J. B. Baseman.** 1989a. DNA and protein sequence homologies between the adhesins of *Mycoplasma genitalium* and *Mycoplasma pneumoniae*. *Infect Immun* **57**:1059-65.
- Dallo, S. F., J. R. Horton, C. J. Su, and J. B. Baseman.** 1989b. Homologous regions shared by adhesin genes of *Mycoplasma pneumoniae* and *Mycoplasma genitalium*. *Microb Pathog* **6**:69-73.
- Dallo, S. F., A. Chavoya, and J. B. Baseman.** 1990. Characterization of the gene for a 30-kilodalton adhesion-related protein of *Mycoplasma pneumoniae*. *Infect Immun* **58**:4163-5.
- Dallo, S. F., A. L. Lazzell, A. Chavoya, S. P. Reddy, and J. B. Baseman.** 1996. Biofunctional domains of the *Mycoplasma pneumoniae* P30 adhesin. *Infect Immun* **64**:2595-601.
- Dandekar, T., M. Huynen, J. T. Regula, B. Ueberle, C. U. Zimmermann, M. A. Andrade, T. Doerks, L. Sanchez-Pulido, B. Snel, M. Suyama, Y. P. Yuan, R. Herrmann, and P. Bork.** 2000. Re-annotating the *Mycoplasma pneumoniae* genome sequence: adding value, function and reading frames. *Nucleic Acids Res* **28**:3278-88.
- Dhandayuthapani, S., W. G. Rasmussen, and J. B. Baseman.** 2002. Stability of cytoadherence-related proteins P140/P110 in *Mycoplasma genitalium* requires MG218 and unidentified factors. *Arch Med Res* **33**:1-5.
- Dirksen, L.B., K.A, Krebs, and D.C. Krause.** 1994. Phosphorylation of cytoadherence-accessory proteins in *Mycoplasma pneumoniae*. *J Bacteriol* **176**:7499-505.
- Dirksen, L. B., T. Proft, H. Hilbert, H. Plagens, R. Herrmann, and D. C. Krause.** 1996. Sequence analysis and characterization of the *hmw* gene cluster of *Mycoplasma pneumoniae*. *Gene* **171**:19-25.
- Domermuth, C. H., M. H. Nielsen, E. A. Freundt, and A. Birch-Andersen.** 1964. Ultrastructure of *Mycoplasma* species. *J Bacteriol* **88**:727-744.
- Dorigo-Zetsma, J. W., J. Dankert, and S. A. Zaat.** 2000. Genotyping of *Mycoplasma pneumoniae* clinical isolates reveals eight P1 subtypes within two genomic groups. *J Clin Microbiol* **38**:965-70.

- Dorigo-Zetsma, J. W., B. Wilbrink, J. Dankert, and S. A. Zaat.** 2001. *Mycoplasma pneumoniae* P1 type 1- and type 2-specific sequences within the P1 cytoadhesin gene of individual strains. *Infect Immun* **69**:5612-8.
- Dorman, S. A., D. J. Wilson, and T. F. Smith.** 1983. Comparison of growth of *Mycoplasma pneumoniae* on modified New York City and Hayflick media. *Am J Clin Pathol* **79**:235-7.
- Duffy, M. F., I. D. Walker, and G. F. Browning.** 1997. The immunoreactive 116 kDa surface protein of *Mycoplasma pneumoniae* is encoded in an operon. *Microbiology* **143 (Pt 10)**:3391-402.
- Dybvig, K., and G. H. Cassell.** 1987. Transposition of gram-positive transposon Tn916 in *Acholeplasma laidlawii* and *Mycoplasma pulmonis*. *Science* **235**:1392-4.
- Eaton, M. D., G. Meiklejohn, and W. van Herick.** 1944. Studies on the etiology of primary atypical pneumonia. A filterable agent transmissible to cotton rats, hamsters, and chicken embryos. *Journal of Experimental Medicine* **79**:649-668.
- Eya, S., M. Maeda, K. Tomochika, Y. Kanemasa, and M. Futai.** 1989. Overproduction of truncated subunit a of H⁺-ATPase causes growth inhibition of *Escherichia coli*. *J Bacteriol* **171**:6853-8.
- Feldner, J., W. Brecht, and S. Razin.** 1979. Adherence of *Mycoplasma pneumoniae* to glass surfaces. *Infect Immun* **26**:70-5.
- Feldner, J., W. Brecht, and S. Razin.** 1981. Role of energy metabolism in *Mycoplasma pneumoniae* attachment to glass surfaces. *Infect Immun* **31**:107-13.
- Feldner, J., U. Gobel, and W. Brecht.** 1982. *Mycoplasma pneumoniae* adhesin localized to tip structure by monoclonal antibody. *Nature* **298**:765-7.
- Fernald, G. W.** 1979. Pathogenesis of *Mycoplasma pneumoniae* disease. *Zentralbl Bakteriol [Orig A]* **245**:139-43.
- Fisseha, M., H. W. Gohlmann, R. Herrmann, and D. C. Krause.** 1999. Identification and complementation of frameshift mutations associated with loss of cytoadherence in *Mycoplasma pneumoniae*. *J Bacteriol* **181**:4404-10.
- Flower, A. M., R. S. Osborne, and T. J. Silhavy.** 1995. The allele-specific synthetic lethality of *prlA-prlG* double mutants predicts interactive domains of SecY and SecE. *Embo J* **14**:884-93.
- Fox, G. E., E. Stackebrandt, R. B. Hespell, J. Gibson, J. Maniloff, T. A. Dyer, R. S. Wolfe, W. E. Balch, R. S. Tanner, L. J. Magrum, L. B. Zablen, R. Blakemore, R. Gupta, L. Bonen, B. J. Lewis, D. A. Stahl, K. R. Luehrsen, K.**

- N. Chen, and C. R. Woese.** 1980. The phylogeny of prokaryotes. *Science* **209**:457-63.
- Franzoso, G., P. C. Hu, G. A. Meloni, and M. F. Barile.** 1993. The immunodominant 90-kilodalton protein is localized on the terminal tip structure of *Mycoplasma pneumoniae*. *Infect Immun* **61**:1523-30.
- Fraser, C. M., J. D. Gocayne, O. White, M. D. Adams, R. A. Clayton, R. D. Fleischmann, C. J. Bult, A. R. Kerlavage, G. Sutton, J. M. Kelley, and et al.** 1995. The minimal gene complement of *Mycoplasma genitalium*. *Science* **270**:397-403.
- Freundt, E. A., and S. Razin.** 1984. Mycoplasma, p. 742-770. *In* J. G. Holt (ed.), *Bergey's Manual of Systemic Bacteriology*, vol. 1. Williams and Wilkins, Baltimore.
- Gabridge, M. G.** 1975. Oxygen consumption by trachea organ cultures infected with *Mycoplasma pneumoniae*. *Infect Immun* **12**:544-9.
- Gabridge, M. G.** 1976. Microrespirometer chamber for determinations of viability in cell and organ cultures. *J Clin Microbiol* **3**:560-65.
- Gabridge, M. G., C. C. Agee, and A. M. Cameron.** 1977a. Differential distribution of ciliated epithelial cells in the trachea of hamsters: implications for studies of pathogenesis. *J Infect Dis* **135**:9-19.
- Gabridge, M. G., Y. D. Barden-Stahl, R. B. Polisky, and J. A. Engelhardt.** 1977b. Differences in the attachment of *Mycoplasma pneumoniae* cells and membranes to tracheal epithelium. *Infect Immun* **16**:766-72.
- Gabridge, M. G., and Y. Dee Barden Stahl.** 1978. Role of cell-associated pathogen metabolism in infection of tracheal explants by *Mycoplasma pneumoniae*. *Med Microbiol Immunol (Berl)* **165**:153-61.
- Gabridge, M. G., and Y. D. Stahl.** 1978. Role of adenine in pathogenesis of *Mycoplasma pneumoniae* infections of tracheal epithelium. *Med Microbiol Immunol (Berl)* **165**:43-55.
- Garnier, J., D. J. Osguthorpe, and B. Robson.** 1978. Analysis of the accuracy and implications of simple methods for predicting the secondary structure of globular proteins. *J Mol Biol* **120**:97-120.
- Gerstenecker, B., and E. Jacobs.** 1990. Topological mapping of the P1-adhesin of *Mycoplasma pneumoniae* with adherence-inhibiting monoclonal antibodies. *J Gen Microbiol* **136**:471-476.

- Gobel, U., V. Speth, and W. Bredt.** 1981. Filamentous structures in adherent *Mycoplasma pneumoniae* cells treated with nonionic detergents. *J Cell Biol* **91**:537-43.
- Hahn, T. W., K. A. Krebs, and D. C. Krause.** 1996. Expression in *Mycoplasma pneumoniae* of the recombinant gene encoding the cytoadherence-associated protein HMW1 and identification of HMW4 as a product. *Mol Microbiol* **19**:1085-93.
- Hahn, T. W., M. J. Willby, and D. C. Krause.** 1998. HMW1 is required for cytoadhesin P1 trafficking to the attachment organelle in *Mycoplasma pneumoniae*. *J Bacteriol* **180**:1270-6.
- Hahn, T. W., E. A. Mothershed, R. H. I. Waldo, and D. C. Krause.** 1999. Construction and analysis of a modified Tn4001 conferring chloramphenicol resistance in *Mycoplasma pneumoniae*. *Plasmid* **41**:120-124.
- Hansen, E. J., R. M. Wilson, and J. B. Baseman.** 1979a. Two-dimensional gel electrophoretic comparison of proteins from virulent and avirulent strains of *Mycoplasma pneumoniae*. *Infect Immun* **24**:468-75.
- Hansen, E. J., R. M. Wilson, and J. B. Baseman.** 1979b. Isolation of mutants of *Mycoplasma pneumoniae* defective in hemadsorption. *Infect Immun* **23**:903-6.
- Hanukoglu, A., S. Hebroni, and D. Fried.** 1986. Pulmonary involvement in *Mycoplasma pneumoniae* infection in families. *Infection* **14**:1-6.
- Harris, J. A., A. Kolokathis, M. Campbell, G. H. Cassell, and M. R. Hammerschlag.** 1998. Safety and efficacy of azithromycin in the treatment of community-acquired pneumonia in children. *Pediatr Infect Dis J* **17**:865-71.
- Hedreyda, C. T., K. K. Lee, and D. C. Krause.** 1993. Transformation of *Mycoplasma pneumoniae* with Tn4001 by electroporation. *Plasmid* **30**:170-5.
- Hedreyda, C. T., and D. C. Krause.** 1995. Identification of a possible cytoadherence regulatory locus in *Mycoplasma pneumoniae*. *Infect Immun* **63**:3479-83.
- Heiskanen-Kosma, T., M. Korppi, C. Jokinen, S. Kurki, L. Heiskanen, H. Juvonen, S. Kallinen, M. Sten, A. Tarkiainen, P. R. Ronnberg, M. Kleemola, P. H. Makela, and M. Leinonen.** 1998. Etiology of childhood pneumonia: serologic results of a prospective, population-based study. *Pediatr Infect Dis J* **17**:986-91.
- Helms, C.** 1978. Legionnaires' disease. *J Iowa Med Soc* **68**:254-5.
- Helms, C. M., J. P. Viner, R. H. Sturm, E. D. Renner, and W. Johnson.** 1979. Comparative features of pneumococcal, mycoplasmal, and Legionnaires' disease pneumonias. *Ann Intern Med* **90**:543-7.

- Hermolin, J., and R. H. Fillingame.** 1995. Assembly of F0 sector of *Escherichia coli* H⁺ ATP synthase. Interdependence of subunit insertion into the membrane. *J Biol Chem* **270**:2815-7.
- Himmelreich, R., H. Hilbert, H. Plagens, E. Pirkl, B. C. Li, and R. Herrmann.** 1996. Complete sequence analysis of the genome of the bacterium *Mycoplasma pneumoniae*. *Nucleic Acids Res* **24**:4420-49.
- Hu, P. C., A. M. Collier, and J. B. Baseman.** 1975. Alterations in the metabolism of hamster tracheas in organ culture after infection by virulent *Mycoplasma pneumoniae*. *Infect Immun* **11**:704-10.
- Hu, P. C., A. M. Collier, and J. B. Baseman.** 1976. Interaction of virulent *Mycoplasma pneumoniae* with hamster tracheal organ cultures. *Infect Immun* **14**:217-24.
- Hu, P. C., A. M. Collier, and J. B. Baseman.** 1977. Surface parasitism by *Mycoplasma pneumoniae* of respiratory epithelium. *J Exp Med* **145**:1328-43.
- Hu, P. C., R. M. Cole, Y. S. Huang, J. A. Graham, D. E. Gardner, A. M. Collier, and W. A. Clyde, Jr.** 1982. *Mycoplasma pneumoniae* infection: role of a surface protein in the attachment organelle. *Science* **216**:313-5.
- Hu, P. C., C. H. Huang, A. M. Collier, and W. A. Clyde, Jr.** 1983. Demonstration of antibodies to *Mycoplasma pneumoniae* attachment protein in human sera and respiratory secretions. *Infect Immun* **41**:437-9.
- Hutchison, C. A., S. N. Peterson, S. R. Gill, R. T. Cline, O. White, C. M. Fraser, H. O. Smith, and J. C. Venter.** 1999. Global transposon mutagenesis and a minimal *Mycoplasma* genome. *Science* **286**:2165-9.
- Inamine, J. M., T. P. Denny, S. Loechel, U. Schaper, C. H. Huang, K. F. Bott, and P. C. Hu.** 1988. Nucleotide sequence of the P1 attachment-protein gene of *Mycoplasma pneumoniae*. *Gene* **64**:217-29.
- Jacobs, E., K. Schopperle, and W. Brecht.** 1985. Adherence inhibition assay: a specific serological test for detection of antibodies to *Mycoplasma pneumoniae*. *Eur J Clin Microbiol* **4**:113-8.
- Jacobs, E., A. Stuhlert, M. Drews, K. Pumpe, H. E. Schaefer, M. Kist, and W. Brecht.** 1988. Host reactions to *Mycoplasma pneumoniae* infections in guinea-pigs preimmunized systemically with the adhesin of this pathogen. *Microb Pathog* **5**:259-65.

- Jacobs, E., A. Pilatschek, B. Gerstenecker, K. Oberle, and W. Brecht.** 1990. Immunodominant epitopes of the adhesin of *Mycoplasma pneumoniae*. *J Clin Microbiol* **28**:1194-7.
- Jokinen, C., L. Heiskanen, H. Juvonen, S. Kallinen, K. Karkola, M. Korppi, S. Kurki, P. R. Ronnberg, A. Seppa, S. Soimakallio, and et al.** 1993. Incidence of community-acquired pneumonia in the population of four municipalities in eastern Finland. *Am J Epidemiol* **137**:977-88.
- Jordan, J. L., K. M. Berry, M. F. Balish, and D. C. Krause.** 2001. Stability and subcellular localization of cytoadherence-associated protein P65 in *Mycoplasma pneumoniae*. *J Bacteriol* **183**:7387-91.
- Jordan, J. L., and D. C. Krause.** submitted. Mutant Analysis reveals distinct requirements for protein P30 in *Mycoplasma pneumoniae* cytoadherence and gliding motility.
- Kenri, T., R. Taniguchi, Y. Sasaki, N. Okazaki, M. Narita, K. Izumikawa, M. Umetsu, and T. Sasaki.** 1999. Identification of a new variable sequence in the P1 cytoadhesin gene of *Mycoplasma pneumoniae*: evidence for the generation of antigenic variation by DNA recombination between repetitive sequences. *Infect Immun* **67**:4557-62.
- Kihara, A., Y. Akiyama, and K. Ito.** 1995. FtsH is required for proteolytic elimination of uncomplexed forms of SecY, an essential protein translocase subunit. *Proc Natl Acad Sci U S A* **92**:4532-6.
- Kirchhoff, H.** 1992. Motility, p. 289-306. *In* R. N. M. J. Maniloff, L. R. Finch & J. B. Baseman. (ed.), *In Mycoplasmas- Molecular Biology and Pathogenesis*. American Society for Microbiology, Washington, D.C.
- Kist, M., E. Jacobs, and W. Brecht.** 1982. Release of *Mycoplasma pneumoniae* substances after phagocytosis by guinea pig alveolar macrophages. *Infect Immun* **36**:357-62.
- Klein, J. O.** 1997. History of macrolide use in pediatrics. *Pediatr Infect Dis J* **16**:427-31.
- Knudtson, K. L., and F. C. Minion.** 1993. Construction of Tn400/lac derivatives to be used as promoter probe vectors in mycoplasmas. *Gene* **137**:217-22.
- Krause, D. C., D. K. Leith, R. M. Wilson, and J. B. Baseman.** 1982. Identification of *Mycoplasma pneumoniae* proteins associated with hemadsorption and virulence. *Infect Immun* **35**:809-17.
- Krause, D. C., D. K. Leith, and J. B. Baseman.** 1983. Reacquisition of specific proteins confers virulence in *Mycoplasma pneumoniae*. *Infect Immun* **39**:830-6.

- Krause, D. C., and K. K. Lee.** 1991. Juxtaposition of the genes encoding *Mycoplasma pneumoniae* cytoadherence-accessory proteins HMW1 and HMW3. *Gene* **107**:83-9.
- Krause, D. C., and D. Taylor-Robinson.** 1992. Mycoplasmas which infect humans, p. 417-415. In J. B. Baseman (ed.), *Mycoplasmas: molecular biology and pathogenesis*. American Society for Microbiology, Washington DC.
- Krause, D. C., T. Proft, C. T. Hedreyda, H. Hilbert, H. Plagens, and R. Herrmann.** 1997. Transposon mutagenesis reinforces the correlation between *Mycoplasma pneumoniae* cytoskeletal protein HMW2 and cytoadherence. *J Bacteriol* **179**:2668-77.
- Krause, D. C., and M. F. Balish.** 2001. Structure, function, and assembly of the terminal organelle of *Mycoplasma pneumoniae*. *FEMS Microbiol Lett* **198**:1-7.
- Krebes, K.A., L.B. Dirksen, and D.C. Krause.** 1995. Phosphorylation of *Mycoplasma pneumoniae* cytoadherence-accessory proteins in cell extracts. *J Bacteriol* **177**:4571-74.
- Krivan, H. C., L. D. Olson, M. F. Barile, V. Ginsburg, and D. D. Roberts.** 1989. Adhesion of *Mycoplasma pneumoniae* to sulfated glycolipids and inhibition by dextran sulfate. *J Biol Chem* **264**:9283-8.
- Ladefoged, S. A., and G. Christiansen.** 1992. Physical and genetic mapping of the genomes of five *Mycoplasma hominis* strains by pulsed-field gel electrophoresis. *J Bacteriol* **174**:2199-207.
- Layh-Schmitt, G., and R. Herrmann.** 1992. Localization and biochemical characterization of the ORF6 gene product of the *Mycoplasma pneumoniae* P1 operon. *Infect Immun* **60**:2906-13.
- Layh-Schmitt, G., and R. Herrmann.** 1994. Spatial arrangement of gene products of the P1 operon in the membrane of *Mycoplasma pneumoniae*. *Infect Immun* **62**:974-9.
- Layh-Schmitt, G., H. Hilbert, and E. Pirkl.** 1995. A spontaneous hemadsorption-negative mutant of *Mycoplasma pneumoniae* exhibits a truncated adhesin-related 30-kilodalton protein and lacks the cytoadherence-accessory protein HMW1. *J Bacteriol* **177**:843-6.
- Leffers, G. G., Jr., and S. Gottesman.** 1998. Lambda Xis degradation in vivo by Lon and FtsH. *J Bacteriol* **180**:1573-7.
- Lipman, R. P., W. A. Clyde, Jr., and F. W. Denny.** 1969. Characteristics of virulent, attenuated, and avirulent *Mycoplasma pneumoniae* strains. *J Bacteriol* **100**:1037-43.

- Lo, S. C., M. M. Hayes, H. Kotani, P. F. Pierce, D. J. Wear, P. B. Newton, 3rd, J. G. Tully, and J. W. Shih.** 1993. Adhesion onto and invasion into mammalian cells by mycoplasma penetrans: a newly isolated mycoplasma from patients with AIDS. *Mod Pathol* **6**:276-80.
- Lynch, R. E., and B. C. Cole.** 1980. *Mycoplasma pneumoniae*: a prokaryote which consumes oxygen and generates superoxide but which lacks superoxide dismutase. *Biochem Biophys Res Commun* **96**:98-105.
- Mahairas, G. G., and F. C. Minion.** 1989. Transformation of *Mycoplasma pulmonis*: demonstration of homologous recombination, introduction of cloned genes, and preliminary description of an integrating shuttle system. *J Bacteriol* **171**:1775-80.
- Maniloff, J.** 1992. Phylogeny of Mycoplasmas, p. 549-559. *In* J. B. Baseman (ed.), *Mycoplasmas: molecular biology and pathogenesis*. American Society for Microbiology, Washington DC.
- Mansel, J. K., E. C. Rosenow, 3rd, T. F. Smith, and J. W. Martin, Jr.** 1989. *Mycoplasma pneumoniae* pneumonia. *Chest* **95**:639-46.
- Marmion, B. P., and G. M. Goodburn.** 1961. Effect of an inorganic gold salt on Eaton's primary atypical pneumonia agent and other observations. *Nature* **189**:247-248.
- Matsuyama, S., J. Akimaru, and S. Mizushima.** 1990. SecE-dependent overproduction of SecY in *Escherichia coli*. Evidence for interaction between two components of the secretory machinery. *FEBS Lett* **269**:96-100.
- Meier, B., and G. G. Habermehl.** 1990. Evidence for superoxide dismutase and catalase in mollicutes and release of reactive oxygen species. *Arch Biochem Biophys* **277**:74-9.
- Meng, K. E., and R. M. Pfister.** 1980. Intracellular structures of *Mycoplasma pneumoniae* revealed after membrane removal. *J Bacteriol* **144**:390-9.
- Michel, G., S. Bleves, G. Ball, A. Lazdunski, and A. Filloux.** 1998. Mutual stabilization of the XcpZ and XcpY components of the secretory apparatus in *Pseudomonas aeruginosa*. *Microbiology* **144**:3379-86.
- Morowitz, H. J., and D. C. Wallace.** 1973. Genome size and life cycle of the mycoplasma. *Ann N Y Acad Sci* **225**:62-73.
- Morrison-Plummer, J., D. K. Leith, and J. B. Baseman.** 1986. Biological effects of anti-lipid and anti-protein monoclonal antibodies on *Mycoplasma pneumoniae*. *Infect Immun* **53**:398-403.

- Murphy, T. F., F. W. Henderson, W. A. Clyde, Jr., A. M. Collier, and F. W. Denny.** 1981. Pneumonia: an eleven-year study in a pediatric practice. *Am J Epidemiol* **113**:12-21.
- Murray, H. W., H. Masur, L. B. Senterfit, and R. B. Roberts.** 1975. The protean manifestations of *Mycoplasma pneumoniae* infection in adults. *Am J Med* **58**:229-42.
- Nascimento-Carvalho, C. M.** 2001. Etiology of childhood community acquired pneumonia and its implications for vaccination. *Braz J Infect Dis* **5**:87-97.
- Neimark, H., and M. C. Tung.** 1973. Properties of a fructose-1,6-diphosphate-activated lactate dehydrogenase from *Acholeplasma laidlawii* type A. *J Bacteriol* **114**:1025-33.
- Neimark, H.** 1979. Phylogenetic relationships between mycoplasmas and other prokaryotes, p. 43-61. *In* S. Razin (ed.), *The mycoplasmas*, vol. 1. Academic Press, Inc., New York.
- Neimark, H., and J. London.** 1982. Origins of the mycoplasmas: sterol-nonrequiring mycoplasmas evolved from streptococci. *J Bacteriol* **150**:1259-65.
- Nelson, C. T.** 2002. *Mycoplasma* and *Chlamydia pneumoniae* in pediatrics. *Semin Respir Infect* **17**:10-4.
- Ogle, K. F., K. K. Lee, and D. C. Krause.** 1992. Nucleotide sequence analysis reveals novel features of the phase-variable cytoadherence accessory protein HMW3 of *Mycoplasma pneumoniae*. *Infect Immun* **60**:1633-41.
- Pechere, J. C.** 1995. *Community-acquired pneumoniae in children*. Worthing, U K: Cambridge Medical Publications.
- Pietsch, K., S. Ehlers, and E. Jacobs.** 1994. Cytokine gene expression in the lungs of BALB/c mice during primary and secondary intranasal infection with *Mycoplasma pneumoniae*. *Microbiology* **140 (Pt 8)**:2043-8.
- Pollack, D. J.** 1992. Carbohydrate metabolism and energy conservation, p. 181-200. *In* J. B. Baseman (ed.), *The mycoplasmas: molecular biology and pathogenesis*. American Society for Microbiology, Washington DC.
- Popham, P. L., T. W. Hahn, K. A. Krebs, and D. C. Krause.** 1997. Loss of HMW1 and HMW3 in noncytoadhering mutants of *Mycoplasma pneumoniae* occurs post-translationally. *Proc Natl Acad Sci U S A* **94**:13979-84.

- Possot, O. M., G. Vignon, N. Bomchil, F. Ebel, and A. P. Pugsley.** 2000. Multiple interactions between pullulanase secretin components involved in stabilization and cytoplasmic membrane association of Pule. *J Bacteriol* **182**:2142-52.
- Pribnow, D.** 1975. Bacteriophage T7 early promoters: nucleotide sequences of two RNA polymerase binding sites. *J Mol Biol* **99**:419-43.
- Principi, N., and S. Esposito.** 2001. Emerging role of *Mycoplasma pneumoniae* and *Chlamydia pneumoniae* in paediatric respiratory-tract infections. *Lancet Infect Dis* **1**:334-44.
- Proft, T., and R. Herrmann.** 1994. Identification and characterization of hitherto unknown *Mycoplasma pneumoniae* proteins. *Mol Microbiol* **13**:337-48.
- Proft, T., H. Hilbert, G. Layh-Schmitt, and R. Herrmann.** 1995. The proline-rich P65 protein of *Mycoplasma pneumoniae* is a component of the Triton X-100-insoluble fraction and exhibits size polymorphism in the strains M129 and FH. *J Bacteriol* **177**:3370-8.
- Proft, T., H. Hilbert, H. Plagens, and R. Herrmann.** 1996. The P200 protein of *Mycoplasma pneumoniae* shows common features with the cytoadherence-associated proteins HMW1 and HMW3. *Gene* **171**:79-82.
- Py, B., L. Loiseau, and F. Barras.** 2001. An inner membrane platform in the type II secretion machinery of Gram-negative bacteria. *EMBO Rep* **2**:244-8.
- Pyle, L. E., and L. R. Finch.** 1988. A physical map of the genome of *Mycoplasma mycoides* subspecies *mycoides* Y with some functional loci. *Nucleic Acids Res* **16**:6027-39.
- Pyle, L. E., T. Taylor, and L. R. Finch.** 1990. Genomic maps of some strains within the *Mycoplasma mycoides* cluster. *J Bacteriol* **172**:7265-8.
- Radestock, U., and W. Brecht.** 1977. Motility of *Mycoplasma pneumoniae*. *J Bacteriol* **129**:1495-501.
- Razin, S., B. Prescott, and R. M. Chanock.** 1970. Immunogenicity of *Mycoplasma pneumoniae* glycolipids: a novel approach to the production of antisera to membrane lipids. *Proc Natl Acad Sci U S A* **67**:590-7.
- Razin, S.** 1985. Molecular biology and genetics of mycoplasmas (Mollicutes). *Microbiol Rev* **49**:419-55.
- Razin, S., and E. Jacobs.** 1992. *Mycoplasma* adhesion. *J Gen Microbiol* **138**:407-22.

- Razin, S., D. Yogev, and Y. Naot.** 1998. Molecular biology and pathogenicity of mycoplasmas. *Microbiol Mol Biol Rev* **62**:1094-156.
- Razin, S.** 1999. Adherence of pathogenic mycoplasmas to host cells. *Biosci Rep* **19**:367-72.
- Regula, J. T., G. Boguth, A. Gorg, J. Hegermann, F. Mayer, R. Frank, and R. Herrmann.** 2001. Defining the mycoplasma 'cytoskeleton': the protein composition of the Triton X-100 insoluble fraction of the bacterium *Mycoplasma pneumoniae* determined by 2-D gel electrophoresis and mass spectrometry. *Microbiology* **147**:1045-57.
- Riftkind, D., and R. M. Chanock.** 1962. Ear involvement (myringitis) and primary atypical pneumonia following inoculation of volunteers with Eaton agent. *Am Rev Respir Dis* **85**:479-489.
- Roberts, D. D., L. D. Olson, M. F. Barile, V. Ginsburg, and H. C. Krivan.** 1989. Sialic acid-dependent adhesion of *Mycoplasma pneumoniae* to purified glycoproteins. *J Biol Chem* **264**:9289-93.
- Rodwell, A. W., and A. Mitchell.** 1979. Nutrition, Growth and Reproduction, p. 103-139. *In* S. Razin (ed.), *The Mycoplasmas. Cell Biology*, vol. 1. Academic Press, Inc, New York.
- Romero-Arroyo, C. E., J. Jordan, S. J. Peacock, M. J. Willby, M. A. Farmer, and D. C. Krause.** 1999. *Mycoplasma pneumoniae* protein P30 is required for cytoadherence and associated with proper cell development. *J Bacteriol* **181**:1079-87.
- Rosenbusch, J., M. Fischer, and H. Kirchhoff.** 1990. An experimental system for the detection of chemotaxis of mycoplasmas. *Zentralbl Bakteriol Suppl* **20**:645-646.
- Ruland, K., R. Wenzel, and R. Herrmann.** 1990. Analysis of three different repeated DNA elements present in the P1 operon of *Mycoplasma pneumoniae*: size, number and distribution on the genome. *Nucleic Acids Res* **18**:6311-7.
- Sambrook, J., E. F. Fritsch, and T. Maniatis.** 1989. *Molecular Cloning: A Laboratory Manual*, 2nd ed. Cold Spring Harbor Laboratory Press, Cold Spring Harbor, NY.
- Sandkvist, M., M. Bagdasarian, S. P. Howard, and V. J. DiRita.** 1995. Interaction between the autokinase EpsE and EpsL in the cytoplasmic membrane is required for extracellular secretion in *Vibrio cholerae*. *Embo J* **14**:1664-73.
- Sandkvist, M., L. P. Hough, M. M. Bagdasarian, and M. Bagdasarian.** 1999. Direct interaction of the EpsL and EpsM proteins of the general secretion apparatus in *Vibrio cholerae*. *J Bacteriol* **181**:3129-35.

- Scully, R.E., E.J. Mark, and B.U. McNeely.** 1983. Case records of the Massachusetts General Hospital: Weekly clinicopathological exercises. Case 39-1983. (Pulmonary consolidation associated with hemolytic anemia.). *N Engl J Med* **309**:782-789.
- Seto, S., G. Layh-Schmitt, T. Kenri, and M. Miyata.** 2001. Visualization of the attachment organelle and cytoadherence proteins of *Mycoplasma pneumoniae* by immunofluorescence microscopy. *J Bacteriol* **183**:1621-30.
- Smith, C. K., T. A. Baker, and R. T. Sauer.** 1999. Lon and Clp family proteases and chaperones share homologous substrate-recognition domains. *Proc Natl Acad Sci U S A* **96**:6678-6682.
- Smith, P. F.** 1967. The physiology of mycoplasma. In C. Panos (ed.), *Mycoplasma and bacterial L-forms*. World Publishing Company, New York.
- Sobeslavsky, O., B. Prescott, and R. M. Chanock.** 1968. Adsorption of *Mycoplasma pneumoniae* to neuraminic acid receptors of various cells and possible role in virulence. *J Bacteriol* **96**:695-705.
- Sperker, B., P. Hu, and R. Herrmann.** 1991. Identification of gene products of the P1 operon of *Mycoplasma pneumoniae*. *Mol Microbiol* **5**:299-306.
- Stevens, M. K., and D. C. Krause.** 1990. Disulfide-linked protein associated with *Mycoplasma pneumoniae* cytoadherence phase variation. *Infect Immun* **58**:3430-3433.
- Stevens, M. K., and D. C. Krause.** 1991. Localization of the *Mycoplasma pneumoniae* cytoadherence-accessory proteins HMW1 and HMW4 in the cytoskeletonlike Triton shell. *J Bacteriol* **173**:1041-50.
- Stevens, M. K., and D. C. Krause.** 1992. *Mycoplasma pneumoniae* cytoadherence phase-variable protein HMW3 is a component of the attachment organelle. *J Bacteriol* **174**:4265-74.
- Su, C. J., V. V. Tryon, and J. B. Baseman.** 1987. Cloning and sequence analysis of cytoadhesin P1 gene from *Mycoplasma pneumoniae*. *Infect Immun* **55**:3023-9.
- Su, C. J., A. Chavoya, and J. B. Baseman.** 1988. Regions of *Mycoplasma pneumoniae* cytoadhesin P1 structural gene exist as multiple copies. *Infect Immun* **56**:3157-61.
- Su, C. J., A. Chavoya, and J. B. Baseman.** 1989. Spontaneous mutation results in loss of the cytoadhesin (P1) of *Mycoplasma pneumoniae*. *Infect Immun* **57**:3237-9.
- Su, C. J., A. Chavoya, S. F. Dallo, and J. B. Baseman.** 1990. Sequence divergency of the cytoadhesin gene of *Mycoplasma pneumoniae*. *Infect Immun* **58**:2669-74.

- Taura, T., T. Baba, Y. Akiyama, and K. Ito.** 1993. Determinants of the quantity of the stable SecY complex in the *Escherichia coli* cell. *J Bacteriol* **175**:7771-5.
- Tryon, V. V., and J. B. Baseman.** 1992. Pathogenic determinants and mechanisms, p. 457-471. *In* J. B. Baseman (ed.), *Mycoplasmas: molecular biology and pathogenesis*. American Society for Microbiology, Washington, DC.
- Tully, J. G.** 1983. Cloning and filtration techniques for mycoplasmas. *In* J. G. Tully (ed.), *Methods in Mycoplasmaology*, vol. 1. Academic Press Inc., New York.
- Upchurch, S., and M. G. Gabridge.** 1981. Role of host cell metabolism in the pathogenesis of *Mycoplasma pneumoniae* infection. *Infect Immun* **31**:174-81.
- von Meyenburg, K., B. B. Jorgensen, O. Michelsen, L. Sorensen, and J. E. McCarthy.** 1985. Proton conduction by subunit a of the membrane-bound ATP synthase of *Escherichia coli* revealed after induced overproduction. *Embo J* **4**:2357-63.
- Waldo, R. H., 3rd, P. L. Popham, C. E. Romero-Arroyo, E. A. Mothershed, K. K. Lee, and D. C. Krause.** 1999. Transcriptional analysis of the *hmw* gene cluster of *Mycoplasma pneumoniae*. *J Bacteriol* **181**:4978-85.
- Wallace, D. C., and H. J. Morowitz.** 1973. Genome size and evolution. *Chromosoma* **40**:121-6.
- Wenzel, R., and R. Herrmann.** 1988. Physical mapping of the *Mycoplasma pneumoniae* genome. *Nucleic Acids Res* **16**:8323-36.
- Wenzel, R., E. Pirkl, and R. Herrmann.** 1992. Construction of an *EcoRI* restriction map of *Mycoplasma pneumoniae* and localization of selected genes. *J Bacteriol* **174**:7289-96.
- White, R. J., A. D. Blainey, K. J. Harrison, and S. K. Clarke.** 1981. Causes of pneumonia presenting to a district general hospital. *Thorax* **36**:566-70.
- Willby, M. J., and D. C. Krause.** 2002. Characterization of a *Mycoplasma pneumoniae hmw3* mutant: implications for attachment organelle assembly. *J Bacteriol* **184**:3061-8.
- Wilson, M. H., and A. M. Collier.** 1976. Ultrastructural study of *Mycoplasma pneumoniae* in organ culture. *J Bacteriol* **125**:332-9.
- Woese, C. R., J. Maniloff, and L. B. Zablen.** 1980. Phylogenetic analysis of the mycoplasmas. *Proc Natl Acad Sci U S A* **77**:494-8.

- Wolffing, B. K., and M. G. Gabridge.** 1979. Effect of in vitro cultivation and *Mycoplasma pneumoniae* infection on intracellular cyclic AMP levels in hamster tracheal organ cultures. *In Vitro* **15**:308-14.
- Wubbel, L., L. Muniz, A. Ahmed, M. Trujillo, C. Carubelli, C. McCoig, T. Abramo, M. Leinonen, and G. H. McCracken, Jr.** 1999. Etiology and treatment of community-acquired pneumonia in ambulatory children. *Pediatr Infect Dis J* **18**:98-104.